NASA Contractor Report 201623

Conflict Probe Concepts Analysis in Support of Free Flight

Anthony W. Warren
Robert W. Schwab
Timothy J. Geels
Arek Shakarian

Boeing Commercial Airplane Group
Seattle, Washington

Contract NAS1 - 20267

January 1997

National Aeronautics and
Space Administration
Langley Research Center
Hampton, Virginia 23681 - 0001

ABSTRACT

This study develops an operational concept and requirements for en route Free Flight using a simulation of the Cleveland Air Route Traffic Control Center, and develops requirements for an automated conflict probe for use in the Air Traffic Control Centers. In this paper we present the results of simulation studies and summarize concepts and infrastructure requirements to transition from the current air traffic control system to mature Free Flight. The transition path to Free Flight envisioned in this paper assumes an orderly development of Communication /Navigation /Surveillance technologies based on results from our simulation studies. The main purpose of this study is to provide an overall context and methodology for evaluating airborne and ground-based requirements for cooperative development of the future Air Traffic Control system.

This study is limited to Free Flight implementation concepts which enable en route User Preferred Trajectories (UPT). Inherent in these concepts is the notion of intent. We assume an aircraft is flying a strategic flight plan, or will provide to air traffic control some level of intent whenever an aircraft deviates from its intended flight plan. Those concepts of Free Flight operation that do not require any knowledge of aircraft intent (other than that provided by radar surveillance) may tend to increase controller workload. This study assumes that controller workload is the primary limiting factor in managing airspace, and that any concept for removing flight restrictions must also address controller workload. Aircraft intent is essential in this study for enabling more efficient use of Center resources, off-loading controller workload through automation concepts such as medium term (10-30 min) conflict probe and conflict resolution across sector boundaries.

TABLE OF CONTENTS

TABLE OF CONTENTS

TABLE OF CONTENTS

SECTION **PAGE**

EXECUTIVE SUMMARY

A number of concepts and methodologies have been proposed for moving towards a more user oriented air traffic control (ATC) system. The great challenge is to find a transition strategy for both users and service providers which will provide economic benefits to justify infrastructure investments, while still accommodating the great diversity of existing airspace users and their need for ATC services. In this report we examine several operational concepts for separation assurance which require the development of new airborne or ground based infrastructure, i.e. conflict probe, alert zone separation assurance, and use of advanced CNS (Communications/ Navigation/ Surveillance) technologies. The central focus of our study is to specify requirements for conflict probe development and to illustrate its role in transitioning to Free Flight. The major results of this study are preliminary operational requirements for separation assurance during the transition to Free Flight, and specification of CNS technical requirements for infrastructure development in the initial transition toward Free Flight.

The transition path to Free Flight envisioned in this report is based on augmenting the way that separation between aircraft is achieved in the current ATC system. The concept utilized in this report is to partition separation assurance into several time scales, and develop distinct methods for managing separation at each time scale. In the current system, the sector controller has prime responsibility for separation. System capacity is limited by the capability of sector controllers to manage separation. The task of performing separation assurance can be conceptually divided into four primary time scales: strategic planning, medium term (10 - 30 min) separation assurance, short term separation, and immediate separation and conflict avoidance. (See Table I, below.) In our concept, a medium term conflict probe is used to detect and resolve potential path conflicts prior to the application of short term separation. Similarly, immediate separation is a function which would be provided by an appropriately equipped air-crew prior to and during a close encounter between two aircraft.

Table I : Separation Assurance Time Partitioning

Time Scale	Current Separation Method	Future Separation Method
Strategic Planning	Central Flow Management	Central Flow Management
Medium Term Planning & Separation	Center Traffic Management Unit (TMU)	Center TMU + Conflict Probe
Short Term Separation	Sector Controller + Conflict Alert	Sector Controller + Conflict Alert
Immediate Separation	Air Crew + Traffic Collision Avoidance	Air Crew + TCAS + Alert Zone Monitoring

	System (TCAS)	

A conflict probe is vital for Free Flight operations since traffic conflicts can occur anywhere in a sector with Free Flight, whereas the high workload conflicts today primarily occur at high density route crossings or merge points. The conflict probe will identify and alert traffic managers and controllers to conflicts well in advance of a potential problem, allowing most conflicts to be resolved before the sector controller needs to become involved. This operational concept has several advantages: (1) we believe that conflicts can be resolved with smaller perturbations to the flight plan than with current methods, since more time is available to achieve the needed separation, (2) the sector controller will be less impacted by high density traffic, allowing the controller more time to apply separation aids such as future intent displays, and to respond to airspace user requests, and (3) controllers are less likely to intervene tactically, allowing users greater benefit from user preferred trajectories.

The advantage of having several redundant systems responsible for separation assurance is less dependence on one critical subsystem. For example, the conflict probe does not have to detect all potential conflicts since the sector controller can easily manage short term conflicts, provided that the number of such conflicts is reasonably contained. Similarly, airborne based (alert zone) guidance can provide a high integrity system for managing opposing encounters which are difficult for current ground based ATC systems.

The methodology employed in our study was to simulate various Free Flight transition options and evaluate en route encounters parametrically as a function of traffic load. We developed a simulation of aircraft operations in the Cleveland Air Route Traffic Control Center over a one day period and benchmarked close encounter statistics for 1995 operations. We then studied the effect of traffic growth over time, and the effect of implementing various transition options to Free Flight. Figure I summarizes the methodology that was used to translate the en route encounters obtained for each transition option into nominal separation parameters. The basis of this process is to limit the number of encounters at each transition stage to that of the 1995 benchmark.

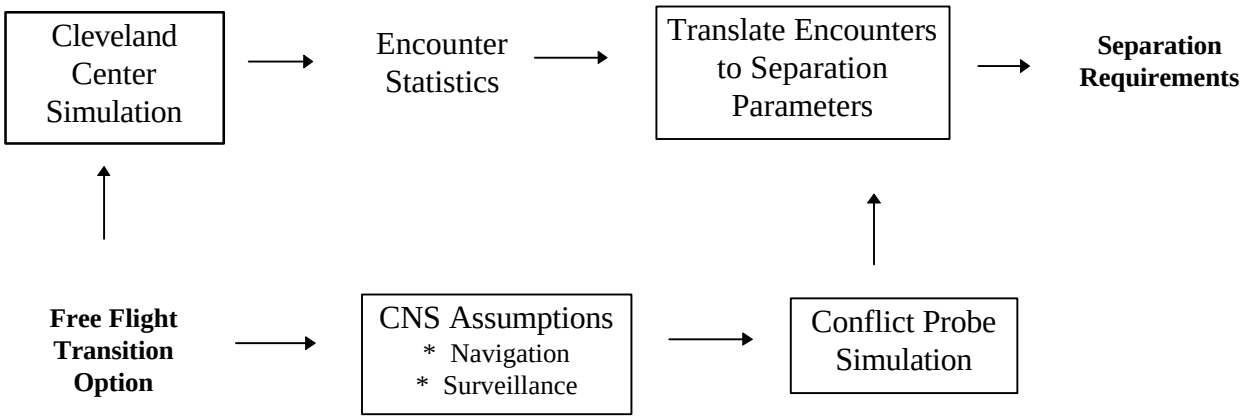

Figure I : Methodology to Obtain Requirements for Free Flight Transitions

For each transition option we assume either radar or Automatic Dependent Surveillance (ADS), and a Required Navigation Performance (RNP) level. The uncertainty in estimating closest approach point of proximate traffic is evaluated with a detailed conflict probe simulation. Then, separation parameters are derived for each option and transition time phase, consistent with the CNS infrastructure assumed.

There are four routing / altitude options for transitioning to Free Flight analyzed in our studies. The first option, denoted **Baseline** constrains the trajectories by terminal exit and entry conditions to efficiently manage terminal flows, and constrains cruise altitudes to 1000 or 2000 foot steps, segregated by east or west flying routes. This option permits the users freedom in selection of lateral routes and cruise airspeeds, and requires the least amount of ground and air infrastructure for implementation. The second option, **Baseline Plus RVSM** (Reduced Vertical Separation Minimum) reduces the vertical separation minimum and the vertical steps in cruise altitude above FL290 to 1000 feet. This option permits Baseline flight operations and more efficient use of cruise flight levels. The third option, **En Route UPT** (User Preferred Trajectories) removes the constraints on user preferred cruise altitudes, i.e. the user is free to select preferred altitude and speed cruise parameters as well as lateral path routing. This option permits greater freedom in route selection at the cost of greater ground and air infrastructure to achieve greatly reduced separations. The fourth option, **En Route UPT Plus RVSM** permits En route UPT flight operations with reduced vertical separations. This option represents a possible end state for mature Free Flight.

The initial results of our studies are summarized in Table II. The separation standard is the horizontal separation minimum for en route operations, and the intervention standard is the threshold value used by a controller or conflict automation to avoid intervening in a close aircraft encounter.

Table II : Initial Separation Requirements for Free Flight Transitions

Free Flight Transition Stages	IOC Date	Separation Standard	Intervention Standard
1995 Benchmark	Today	5 nm	10 nm
Initial Free Flight: * Baseline	2002	4 nm	7.5 nm
Mature Free Flight: * Baseline Plus RVSM	2006	3 nm	5 nm
Mature Free Flight: *En Route UPT Plus RVSM	2010	2 nm	4 nm

For the initial Free Flight implementation, the Baseline option is assumed since this option minimizes the requirements for additional infrastructure. The Baseline option can be implemented using existing radar technology for surveillance, whereas we will need data-link and probably some form of ADS reporting for implementing the other options. The Baseline option will require precision navigation (RNP-1) equipage in order to accommodate opposing traffic conflicts. The ground based system will require substantial improvements to the radar tracking system, and implementation of several Center automation functions in order to accommodate a 4 nm separation standard and to shrink the intervention standard to 7.5 nm. However, there is not a high risk in implementing these improvements since all the basic technologies are currently in place. Consequently, we have selected the Baseline flight concept with the above horizontal separation parameters for the Initial Free Flight transition.

The next step to Free Flight assumed in Table II is the Baseline Plus RVSM concept, since it has the greatest economic value for users, with the least reduction in separation parameters to accommodate future traffic growth. However, the Baseline plus RVSM concept requires that all airspace users flying at or above FL290, including those not flying Free Flight paths, be equipped for RVSM.

The transition to Mature Free Flight is completed using the En route UPT plus RVSM concept, which again requires reduced separation standards compared with the Baseline plus RVSM concept. However, the horizontal separation standards are much less severe than those for the En route UPT concept without RVSM, i.e. our studies show that RVSM should precede the transition to En route UPT. This concept will require Alert Zone monitoring to manage same altitude opposing encounters. Thus, this option is implemented last in our transition plan to Mature Free Flight.

The emphasis of this report is in developing requirements for the proposed initial step to Free Flight routing, i.e. the ability to fly direct, unconstrained lateral routes while en-route between terminal areas. The main requirement specified for airborne users is an RNAV system with RNP-1 navigation and path following capability. Some form of medium term conflict probe will probably be required at the Air Route Traffic Control Centers in order to accommodate the increased diversity in path routings. The analysis studies show that substantial infrastructure changes will be needed at the Centers in order to support a nominal 20 minute conflict probe. These include development of enhanced multi-sensor aircraft tracking algorithms, enhanced weather forecasting with reduced data latency, and implementation of Center automation tools to support medium term separation assurance. The medium term conflict probe will require current path intent for performing trajectory predictions. Consequently, flight path intent must be updated when path deviations occur, and intent must be validated by real time conformance monitoring in order to use medium term conflict probe and separation assurance. The process of updating path intent can be greatly aided by use of air-ground data-link, i.e. the use of Controller-Pilot Data Link Communications (CPDLC) for path deviation clearances and the use of ADS for verifying current path intent.

LIST OF ACRONYMS

3-D	Three Dimensional (lat., long., vertical)
4-D	Four Dimensional (lat., long., vertical, time)
ADS	Automatic Dependent Surveillance
ADS -B	Broadcast ADS
AEEC	Airline Electronic Engineering Committee
AERA	Automated En Route ATC
ARTCC	Air Route Traffic Control Center
ASR	Airport Surveillance Radar
ATC	Air Traffic Control
ATM	Air Traffic Management
AVPAC	Aviation VHF Packet Communications
CDTI	Cockpit Display of Traffic Information
CNS	Communications / Navigation / Surveillance
CPA	Closest Point of Approach
CPDLC	Controller-Pilot Data Link Communications
CTAS	Center- TRACON Automation System
DME	Distance Measuring Equipment
ETMS	Enhanced Traffic Management System
FAA	Federal Aviation Administration
FMS	Flight Management System
FP	Flight Plan
FTE	Flight Technical Error
GA	General Aviation
GICB	Ground Initiated Comm-B (for Mode-S)
GPS	Global Positioning System
Host	The computer used in the ARTCCs for radar and data processing
ICAO	International Civil Aviation Organization
IMM	Interacting Multiple Model (Tracker)
IOC	Initial Operating Capability
ITWS	Integrated Terminal Weather System
LORAN	Long Range Navigation
MAPS	Mesoscale Analysis and Prediction System
MASPS	Minimum Aviation System Performance Standard
Mode-S	Mode Select of Secondary Radar
NAS	National Airspace System
OAG	Official Airline Guide
RGCS	Review of General Concept of Separation (ICAO Panel)
RNAV	Area Navigation
RNP	Required Navigation Performance
RTA	Required Time of Arrival
RTCA	Requirements and Technical Concepts for Aviation
RVSM	Reduced Vertical Separation Minimums

RUC	Rapid Update Cycle (Wind & Temperature Forecasting)
SARP	Standards and Recommended Practices
SSR	Secondary Surveillance Radar
STCA	Short Term Conflict Alert
TAAM	Total Airspace and Airport Modeler
TCAS	Traffic Alert and Collision Avoidance System
TRACON	Terminal Radar Approach Control
TWDL	Two Way Data Link
UPT	User Preferred Trajectories
VHF	Very High Frequency
WAAS	Wide Area Augmentation System (for GPS)

1.0 Introduction and Requirements Summary

In today's air traffic control system the freedom to fly user preferred trajectories is severely limited, given the automation support systems available to controllers. In fact, as demand has grown in NAS airspace, more constraining procedures and flow control techniques have been implemented in order to keep pace with traffic growth. Procedural restrictions such as en-route spacing and arrival fix spacing, along with flow restrictions on departure and at critical waypoints are increasingly used today to safely manage peak traffic flows. However, there are two undesirable effects of this traffic management system. The first is that the users ability to fly economically optimized trajectories, and the timing of the user's flights are greatly constrained by the traffic management system. The second is that without additional technology for managing traffic and increased controller productivity, additional airspace limitations will be needed in the future to restrain the growing traffic demand.

The Free Flight initiative is aimed at evolving airspace management to support traffic growth and efficiency of operations, i.e. developing procedures and traffic management methods which give airline dispatchers and airspace users greater freedom in selecting and modifying flight plans, and some relaxation of flight path constraints when operating under airspace flow constraints. The critical element in achieving this goal is controller productivity. In today's ATC system, the flexibility of the system is determined by the workload of the sector controllers, i.e. when workload is light, the controllers can more easily accommodate user's requests for height and path adjustments, and when workload is heavy, the controllers can only accommodate basic services for traffic separation. This report focuses on methodologies for separation assurance which can off-load the controllers workload or increase controller productivity, and on methods for implementing Free Flight which are workload efficient for both airspace users and sector controllers. Our study focuses primarily on en route ATC, and the role that automated conflict probe can play in transitioning to Free Flight.

A number of concepts and methodologies have been proposed for moving towards a more user oriented ATC system. The great challenge is to develop a transition strategy for both users and service providers which will enable economic benefits to justify infrastructure investments, while still accommodating the great diversity of existing airspace users and their need for ATC services. In this report we examine several operational concepts for separation assurance which require the development of new airborne or ground based infrastructure, i.e. conflict probe, alert zone separation assurance, and use of advanced CNS (Communications/ Navigation/ Surveillance) technologies. The central focus of our study is to specify requirements for conflict probe development and to illustrate the probe's role in transitioning to Free Flight. The major results of this study are preliminary operational requirements for separation assurance during the transition to Free Flight, and specification of CNS technical requirements for infrastructure development during an initial transition stage to Free Flight.

1.1 Separation Assurance for Free Flight

Although the critical link for en route separation assurance today is the sector controller, several independent and partially redundant systems will be needed for future traffic separation, each of which have responsibility for some distinct aspect of separation assurance. Traffic separation is here partitioned into four distinct functions, each of which operates in a different time scale and with a distinct charter. Table 2 shows such a partitioning involving four time scales:

* Strategic Planning - flow management to avoid traffic saturation at critical waypoints and high density traffic sectors,

* Medium Term Separation - center wide conflict probe (using flight plan intent) and flight path changes to avoid future conflicts,

* Short Term Separation - controller based separation with automated Conflict Alert augmentation to resolve airspace conflicts

* Immediate Separation - onboard collision avoidance, separation monitoring and flight path guidance.

Table 1 shows the relationship between the current and proposed future separation methods. In the current ATM (Air Traffic Management) system, strategic planning is performed with flow control and en route spacing restrictions, medium term planning is performed by the center Traffic Management Unit (TMU) to assure efficient traffic flows, short term separation is performed by the sector controller aided by the Conflict Alert function, and collision avoidance is performed by the air-crew using visual monitoring and the TCAS system.

Table 1: Separation Assurance Time Partitioning

Time Scale	Current Separation Method	Future Separation Method
Strategic Planning	Central Flow Management	Central Flow Management
Medium Term Planning & Separation	Center TMU	Center TMU + Conflict Probe
Short Term Separation	Sector Controller + Conflict Alert	Sector Controller + Conflict Alert
Immediate Separation & Collision Avoidance	Air Crew + TCAS	Air Crew + TCAS + Alert Zone Monitoring

Table 2: Mature Free Flight Separation Assurance Concepts

Lookahead Interval	Separation Assurance Concepts	Infrastructure Required
* Strategic Planning (> 30 min)	* Flow Management - Coarse (15 min) - Fine (5 min)	* Enhanced Wind Forecasts * Software Upgrades to Existing Systems
* Medium Term Separation (10 - 30 min)	* Conflict Probe * Path Conformance * Dynamic Density Display * Free Flight Restrictions	* Enhanced Wind Forecasts * Enhanced Surveillance * Center Automation Tools
* Short Term Separation Aids (< 5 min)	* Short Term Conflict Alert - Protection Zone Monitor * Future Intent Display Aids	* Enhanced Surveillance * Center Automation Tools
* Immediate Separation Aids (< 2 min)	* Collision Avoidance System * Alert Zone Monitoring - Free Flight Restrictions	* Precision RNAV * Mode-S Data Link with ADS, ADS-B * TCAS / Alert Zone CDTI

For Free Flight operations, changes and augmentations are needed in all four functional areas as summarized in Table 2 :

* Improved flow management methods will be needed to prevent traffic congestion at critical arrival sectors and during severe weather conditions. Augmentations may also be needed to prevent local saturation of sectors and critical juncture points where traffic arrives from several directions in a short time interval. One method to achieve this would be to use fine time scale flow restrictions, as well as the current 15 minute coarse flow restrictions. This may be necessary since en route spacing or arrival time spacing, typically applied in the current system to prevent saturation at crossing and arrival fixes, will not be available for non-traditional routes.

* Perhaps the most important addition to the current system for implementing Free Flight is the use of a medium term (10-30 min) conflict probe to detect and eliminate potential conflicts prior to the application of short term (tactical) separation. This concept is vital for Free Flight operations since traffic conflicts can occur anywhere in a

sector with Free Flight, whereas the high workload conflicts today primarily occur at known route crossing or merge points. The conflict probe will identify and alert traffic managers and area controllers to conflicts well in advance of a potential problem, allowing most conflicts to be resolved before the sector controller needs to become involved. Thus, much of the extra workload during peak traffic can be transferred to the controller working the conflict probe, provided that he can directly intervene to resolve potential conflicts. This operational concept has several advantages: (1) we believe that conflicts can be resolved with smaller perturbations to the flight plan than currently, since more time is available to achieve the needed separation, and (2) the sector controller will be less impacted by high density traffic, allowing the controller more time to apply separation aids such as future intent displays, and to respond to user requests.

Another function which may be implemented for medium term planning is display of the traffic load density as a plan view mapping of Center airspace over specified lookahead intervals. This function may have several applications for mature Free Flight. One application is dynamic resectorization of Center airspace to prevent workload saturation at heavily congested traffic areas, i.e. reassignment of controllers to airspace sectors optimized for working high traffic loads. Another function may be to apply Free Flight restrictions such as mandatory waypoint fixes when entering or exiting sectors with high traffic density.

***** Several enhancements to the current system of short-term, tactical separation will probably be needed for Free Flight operations. One is that decision support tools such as a future intent display will be needed to implement reduced separation standards. Reduced separations, in turn, will be needed to keep workload from growing substantially as Free Flight is successively implemented, and as traffic grows over time. Eventually, the process of reducing separations will be limited by inherent time lags in the control loop, i.e. detecting traffic problems, communicating resolutions to the pilot, and pilot and airplane response times to resolve the problem. This situation is most critical with opposing conflicts, where the time scales for problem resolution are compressed. Consequently, the evolution to mature Free Flight will require additional system augmentation to manage opposing conflicts and reduced separation encounters.

* The assumed separation systems above are all ground based. In order to manage close encounters safely, an airborne system may be needed which will allow the aircrews in close encounter situations to assume responsibility for separation assurance, and to provide guidance restrictions immediately preceding and following a close encounter between two suitably equipped aircraft. Operationally, this means there would be a handoff of responsibility between the ground controller and the aircrews prior to a close encounter between two aircraft, which would persist until the encounter was over. The ground controller would then resume responsibility for separation assurance. This function has been described somewhat differently by the Free Flight task force, using the concept of an Alert Zone, which defines a region in

space encompassing a Free Flight aircraft where flight guidance restrictions are imposed whenever an intruder enters the Alert Zone. This function could include an enhanced TCAS, which would operate somewhat differently than current TCAS systems, since the system would function to maintain separation standards during an encounter, while current TCAS functions as a backup collision avoidance system.

The implementation of these concepts is dependent on the maturity of the technologies involved, and availability of supporting infrastructure. Initial Free Flight will probably include medium term conflict probe and separation functions, and various hardware and software enhancements in the ARTCC's to support this function, most notably a new host computer system and surveillance system tracker, and enhancements in wind forecasting for accurate path predictions. The Alert Zone concept is new, and will require substantial research and development before it is mature enough for application as a means of separation assurance. It is clear however, that the full benefits of Mature Free Flight will require new CNS technologies onboard, such as precision RNAV or Flight Management Systems, and an ADS[1] data link for transferring aircraft position, velocity, and intent information to ground based ATC centers, and to nearby aircraft.

1.2 Operational Requirements and Concepts Summary

An initial simulation study was undertaken to evaluate operational requirements for separation assurance, based on modeling en route flight operations in a high density Center in the current NAS system, and with various Free Flight implementation concepts. In the simulation studies we evaluated aircraft close encounter statistics for 1995 benchmark traffic and for traffic growth to 200% of the 1995 benchmark. Assuming a nominal 5% per year growth in traffic, then by 2002, the year assumed for initial Free Flight implementation, traffic will have grown by 140%. By 2010, the year assumed for mature Free Flight Initial Operating Capability (IOC), aircraft traffic will have doubled. Thus, we have chosen to evaluate the operational requirements needed for initial Free Flight using 140% traffic statistics, and the operational requirements for mature Free Flight using 200% traffic statistics. The methodology in these studies is to determine separation parameters such that the number of tactical interventions for initial and mature Free Flight operations does not substantially exceed that for the 1995 benchmark.

In the current NAS system, the horizontal separation standard for en route radar control is 5 nm. Controllers will typically not intervene when the predicted Closest Point of Approach (CPA) distance of an aircraft pair is more than 10 nm, but will intervene when the predicted CPA distance is less than 10 nm to assure safe separation considering path prediction errors such as radar errors and uncertainty in aircraft intent. The effective threshold above which a controller (or conflict alerting process) will not

[1] In this report we refer to ADS in a generic sense rather than as a specific implementation, i.e. we include Mode-S Specific Services and Mode-S extended squitters as well as VHF based implementations of ADS.

intervene is very important for Free Flight operations and is here called the intervention standard, in contrast with the separation standard. For the benchmark study, the assumed intervention standard is 10 nm.

In the detailed simulation studies described in Section 3.0, the initial implementation step for Free Flight, as described above is denoted the **Baseline** concept, the next step is denoted **Baseline Plus RVSM**, and the final step to mature Free Flight is denoted **En Route UPT Plus RVSM**. (The vertical separation standard changes when RVSM is implemented.) The operational requirements for these system concepts, including the effect of assumed traffic growth is shown in Table 3. Although these requirements are preliminary, and must be validated with in-depth simulation studies and prototype demonstrations, they provide an initial quantitative basis for specifying airborne and ground system requirements for each transition step toward Free Flight.

Table 3: Selected Operational Requirements for Transition to Free Flight

Free Flight Transition Stages	IOC Date	Assumed Traffic Level	Separation Standard	Intervention Standard
1995 Benchmark	Today	100 %	5 nm	10 nm
Initial Free Flight: (Baseline)	2002	140 %	4 nm	7.5 nm
Intermediate Free Flight: (Baseline Plus RVSM)	2006	170 %	3 nm / RVSM	5 nm
Mature Free Flight: (En Route UPT Plus RVSM)	2010	200 %	2 nm / RVSM	4 nm

The proposed transition path to mature Free Flight is based on the simulation studies in section 3. These studies show that the first two transition steps, which focus on reduced horizontal and vertical separations, are very effective means of reducing tactical interventions. Consequently, these steps are recommended for increased efficiency in Center operations, both to support Free Flight operations and to manage controller workload in high density traffic. Implementing En Route UPT is more difficult, since it allows same altitude, opposing traffic conflicts. The simulation results for this concept show that opposing conflicts increase dramatically when users are able to fly unconstrained cruise altitudes. Moreover, even if users are only allowed to fly unconstrained altitudes in sparse traffic, opposing conflicts are difficult for controllers to manage because of the short time intervals for resolving such conflicts. This option may require that the sector controller transfer separation assurance to an air-air based

function prior to the occurrence of a close converging encounter, and until such an encounter is completed. (See Section 2.2.2.) This is the purpose of Alert Zone[2] monitoring and path guidance, i.e. to provide immediate closed loop guidance for separation assurance to prevent an intruder from penetrating a protection zone around the ownship. The protection zone, as used here, consists of a disk shaped zone with horizontal radius equal to the horizontal separation standard, and vertical extent (up or down) equal to the vertical separation standard.

1.3 Free Flight Transitions and Mixed Fleet ATM

From an airspace user's point of view, the most important aspect of Free Flight is the investment necessary to obtain benefits in terms of increased capacity and flight efficiency. Different users have greatly different needs, which will influence infrastructure decisions on airborne equipage. Consequently, the transition path to Free Flight must have several intermediate stages, in terms of both system implementation and user required infrastructure. Table 4 is a transition path to Free Flight based on the operational requirements in the previous section, which successively build on earlier steps to incrementally move towards Free Flight, while allowing users freedom of choice in infrastructure upgrades. (The names of the incremental stages are shown boldface, underlined in the table.) There are basically four classes of users in positive control airspace and three incremental stages to achieve mature Free Flight in this transition concept:

* Classic, non-FMS aircraft - These aircraft would fly on fixed airways and operate using ground-based navigation aids, exactly as in today's NAS system. The ATC services and separation standards would also be maintained as currently, until such services are discontinued as the older navigation aids are decommissioned.

* Precision RNAV / FMS aircraft - In the initial stage of Free Flight, these aircraft would be allowed to fly direct routings and optimal wind routings en-route between a departure exit point and an arrival entry point. (Precision RNAV capability would include aircraft certified for RNP-1 operations, i.e. GPS, LORAN, and Dual DME based systems.) Aircraft in this class would be constrained to fly their ground cleared flight plan (or change their flight plan with ATC approval), and would fly discrete cruise altitude levels as in the current ATM system. This capability will require integration and fusion of flight plan and surveillance data to perform medium term (~20 minute) flight path predictions and conflict detection. Aircraft will be monitored in real time for flight plan conformance, i.e. accurately following the lateral and height profiles in the flight plan. Those aircraft which conform to their intended flight plan will be given reduced separation minima, and will be subject to less ATC interventions. Those aircraft which temporarily deviate from the flight plan and are thus not easily predictable for conflict detection, will be subject to separation minima as in the current system.

[2] The Alert Zone concept in this report is somewhat different than that assumed by the RTCA Free Flight Task Force. Our concept uses the intervention standard to define the Alert Zone boundary.

Table 4: Airborne Categories for Free Flight Transition Stages

Airplane Equipage	Operational Concept (Ground Operations)	IOC	Benefits
* Classic, Non-FMS	**1995 Benchmark** * 1995 NAS Operations	1995	* Fixed Flight Routes * Radar Separation
* Precision RNAV / FMS (RNP -1)	**Baseline Free Flight** * Integrated Flight Path & Radar Data Processing - Conflict Probe - Path Conformance	2002[1]	* Reduced Workload * Increased Capacity * Partial Free Flight
* GPS RNAV / ADS / RVSM	**Baseline Plus RVSM** * Integrated Flight Path & Radar / ADS Surveillance - RVSM above FL290	2006[1]	* Partial Free Flight * Dynamic Rerouting * Reduced Separations * More Efficient Cruise
* 4-D RNAV / Cooperative Separation (Alert Zone)	**En Route UPT Plus RVSM** * Integrated 4-D Flight Path +Air / Ground Surveillance	2010[1]	* Free Flight Clearances - User Preferred Profiles * Reduced Separations * Priority Scheduling

[1] Assumes 1996 Consensus on Transition Path for Free Flight

* GPS RNAV / ADS / RVSM aircraft - In the transition stage after initial Free Flight , an ADS capable air-ground data link will be integrated into the Center operations, and ADS equipped aircraft will be given additional en-route flight options. These may include dynamic path routing and automated flight adjustment options such as flight plan offsets and step-climbs. Integration of radar, ADS, and flight plan data will enable the intended flight path of the aircraft to be automatically updated for conflict probe and separation services. The benefits of this transition stage include dynamic flight adjustments and reduced separation minimums including RVSM (Reduced Vertical Separation Minimum) above FL 290, enabling additional cruise flight levels. Eventually, all aircraft flying in high altitude airspace may be required to upgrade to ADS capability, in order to support reduced separations for airspace capacity and Free Flight compatibility.

* 4-D RNAV / Cooperative Separation Aircraft - The final transition stage to Mature Free Flight will allow specially equipped aircraft to fly User Preferred Trajectories in both space and time, based on cooperative separation procedures involving the

airborne user and ground based air traffic services. The needed infrastructure will include an advanced FMS system capable of flying one or more Required Time of Arrival (RTA) points and of monitoring lateral, height, and time-at-waypoint path conformance to an intended 4-D flight plan. In addition to the ADS capability of the previous stage, such aircraft will also have Alert Zone monitoring and Free Flight guidance capability, possibly contained in a TCAS processor or in a CDTI processor. Equipage at this level may depend on regional implementation of Free Flight initiatives, i.e. some users may obtain benefits by implementing 4-D RNAV capability, while others may opt for Alert Zone monitoring. The assumed benefits of time-conformance and RTA capability are priority scheduling at arrival fixes and high capacity crossing fixes, i.e. RTA equipped aircraft may be allowed schedule priority over non-equipped aircraft. The benefits of Alert Zone monitoring and cooperative separation are increased ability to fly user preferred routings including optimal cruise-climb and speed, reduced separation minimums, and increased ability to dynamically modify their flight plan.

This vision of the path to Free Flight reflects the need to reconcile many diverse interests, including the needs of airspace users, and the need to grow airspace capacity to satisfy future demands for air traffic services. The needs of users with existing FMS systems and modern RNAV systems to fly direct routings and wind efficient flight paths, independent of ground based navigation aids is first addressed in the Initial Free Flight stage. This can be achieved efficiently by integrating medium term conflict detection into the existing system, while simultaneously improving the tracking and wind forecasting capabilities in the traffic control Centers. This transition is the primary focus of this study. Next, the need to expand airspace capacity and to fly more efficient vertical paths is addressed by integrating ADS air /ground data link and RVSM into high-altitude airspace management. This step can be achieved at relatively low cost to airspace users, with near term technology by integrating FMS or RNAV systems with a data-link enhanced mode-S transponder. (Other options are also available, but are either longer term technology solutions, or require larger retrofit investments.) Initially, ADS capability in the Centers may be used to obtain more accurate and responsive velocity for flight path predictions, to dynamically update the flight plan for traffic planning, and for GPS equipped aircraft, as an independent source of altitude data for RVSM separation assurance.

The final step to mature Free Flight will require extensive research and technology development to validate and implement Alert Zone monitoring and cooperative separation as envisioned here. However, this step would permit equipped users much greater freedom in selecting user preferred trajectories and flight schedules, based on increased situation awareness and shared responsibility for separation assurance.

1.4 Conflict Probe Concepts Analysis

In the initial study phase we examined several different concepts for implementing medium term conflict detection. These are denoted below Fixed Threshold,

Covariance, and Conformance Bound methods. Each of the concepts examined uses the same data sources to perform flight predictions, i.e. flight plan intent, radar or ADS surveillance data, and vector wind forecasts. The concepts differ in the way that the data is fused into path predictions, and in the way that conformance to the predicted flight path is monitored.

Conventional, strategic flight path predictions use flight plan waypoints and air data based parameters such as cruise Mach number, together with forecast winds to build a 4-dimensional flight path prior to aircraft departure. This flight path is then updated periodically by removing past waypoints and modifying waypoint times such that the latest observed aircraft position agrees with the latest observation time. This method of data fusion and reestablishing conformance of the flight plan may be inaccurate for medium term predictions since it does not use current ground velocity from the surveillance tracker to perform the flight predictions.

The conflict probes examined in this report use a more accurate methodology to fuse surveillance, wind forecasting, and flight plan waypoints into 4-D flight predictions. We use flight plan data to determine ground track and altitude profiles for flight predictions, and longitudinal along-track position is determined by projecting the tracker state vector longitudinally from the current radar position. The forecast along-track wind is differenced at intervals along the path to provide an estimate of along-track wind shear for track segment velocity corrections. This data fusion concept was assumed for all the medium term conflict probes analyzed in this report. (The Short Term Conflict Alert (STCA) algorithms do not currently use flight plan or wind forecast data, and only use the tracker state vector to project the flight path forward.)

Three concepts for horizontal plane conflict probe were selected for detailed analysis and study:

* Fixed Threshold Conflict Detection - In this concept, the CPA time and distance of closest approach are first obtained for each potential path conflict pair. Two thresholds are used to declare conflicts and non-conflicts, respectively. If the CPA time is outside a fixed lookahead interval, or if the CPA distance is larger than an outer threshold (nominally 8 nm for an advanced radar tracker) then the aircraft pair is declared non-conflicting, and is removed from the list of potential conflict pairs. If the CPA time is inside the probe lookahead interval (nominally 5 min to 25 min) and if the CPA distance is less than an inner threshold (nominally 5 nm) then the aircraft pair is declared conflicting. In order to make the detection process more robust to tracker noise errors, conflicts must be detected two times in a row on two successive probe updates for a conflict alert to be issued for path resolution. (Once a given aircraft has been checked for path conflicts and found non-conflicting with all other pairs, it is cleared by the system for unconstrained flight until the next sector exit point is reached, or the aircraft path is detected out of conformance with the predicted flight path.)
* Covariance Method Conflict Detection - In this concept, error ellipse path uncertainty regions are computed at the closest approach time together with CPA distance for each potential path conflict pair. These error ellipses are based on covariance matrix

calculations obtained by modeling tracker surveillance errors, wind forecasting errors, and aircraft path following errors (Ref. 1). The thresholds for declaring conflicts and non-conflicts are based on the horizontal separation standard and the estimated CPA uncertainty obtained from the error ellipses. The thresholds with this method are dynamic and depend on the geometry of the conflict and the time to closest approach. The detection logic for declaring conflicts and non-conflicts is similar to that above, once the inner and outer thresholds are computed.

* Conformance Bound Conflict Detection - This concept is a generic version of the conflict detection method proposed for the AERA-2 program (Ref. 2, 3). As originally proposed, each Center maintains a strategic, 4-D flight plan for all aircraft entering into Center controlled airspace. This flight plan reflects the current aircraft intent and is kept updated by path conformance monitoring and surveillance based reconformance if the actual position drifts too far from the predicted flight plan. Conflict detection with this concept is performed periodically on each aircraft between entry and exit from Center airspace, and whenever aircraft paths are out of conformance with the intended plan. As applied here, flight predictions are performed using the data fusion method described above. Fixed size error ellipses are used to model horizontal conformance bounds for trajectory path following (nominally, 1 nm lateral semi-axis by 2 nm longitudinal semi-axis). The detection thresholds for this concept are determined by the horizontal separation standard and the estimated CPA uncertainty obtained from the conformance ellipses. (For details see section 4.1.) Again, the detection logic for declaring conflicts and non-conflicts is similar to that above, once the detection thresholds are computed.

The overall performance of these three methods in detecting horizontal plane conflicts was evaluated in Monte-Carlo simulations of in-trail, crossing, and opposing path conflicts. The simulation included the major sources of prediction error including tracker noise, wind forecasting error, and lateral FTE path following error. All three conflict probe methods were evaluated with the same error sources and geometry, and common parameters reflecting a 2002 initial operating capability, i.e. a lookahead interval of 20 minutes, separation standard = 4 nm, and intervention standard = 7.5 nm. The thresholds were tuned as needed to attain a missed detection probability (where no alert is issued for a true conflict) of less than 2 %, and the probability of conflict detection was evaluated for encounters with approach distance less than 10 nm. The results were then aggregated to count the expected number of interventions for each conflict probe method, and compared to the Benchmark simulation results for 1995 encounters. The results of this study are summarized in Figure 1.

This figure shows expected number of conflict alerts over a one day period. The results show that the Covariance method has the best performance, and results in only 9% more interventions than the benchmark, even though the simulated traffic load has grown by 40 % from the 1995 benchmark. The Fixed threshold method also performs well, compared to Covariance based conflict detection. Of these two, the Covariance method is preferred since it is more easily adapted to changes in CNS system performance, and parameter tuning is easier than with the Fixed threshold method.

The Conformance method is not competitive with the other concepts. It is simply too conservative in choosing detection thresholds, which results in very few missed detections, but excessive false alerts. (A false alert is generated whenever a conflict is declared even though the true CPA distance is greater than the intervention standard.)

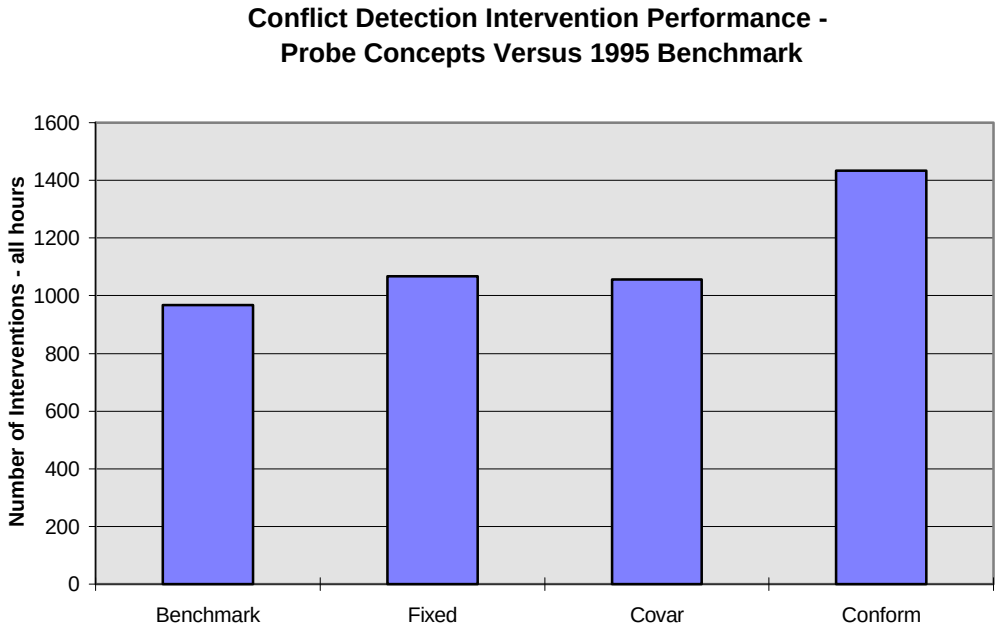

Figure 1: Conflict Probe Concepts Performance Summary

1.5 Technical Requirements for Initial Free Flight

In the initial study phase reported here, we examined requirements to obtain a desired level of performance for the medium term conflict probe, and for associated CNS functions to implement the envisioned initial transition to Free Flight. The performance requirements for the conflict probe are first summarized, and then derived technical requirements for Navigation, Surveillance, Communications, and Wind Forecasting, are summarized, based on initial studies to date.

Conflict Probe Requirements

The main requirements for the conflict probe relate to probability of correct conflict detection, and to detection time parameters. Key design variables are the probability of missed detection, i.e. the probability of not detecting an aircraft pair during the allowed lookahead interval, where CPA < separation standard (nominally 4 nm for Initial Free Flight), and the probability of false alert, i.e. the probability of declaring a conflict alert on an aircraft pair where CPA distance > intervention standard (nominally 7.5 nm). We have used the following initial requirements for our study:

* Missed Detection Probability < 2 %

* False Alert Probability < 6 %

We have initially selected a 2 % rate on missed detection under the assumption that low rates are not necessary due to redundancy in separation assurance, i.e. if the conflict probe misses some potential violations, then either the sector controller or Conflict Alert automation will detect the violation. The false alert rate is a nominal value which primarily affects the intervention rate for traffic conflicts. Figure 2 shows nominal conflict probe detection performance for Initial Free Flight. The detection probability is the observed ratio of conflict detections given 2000 simulated encounters.

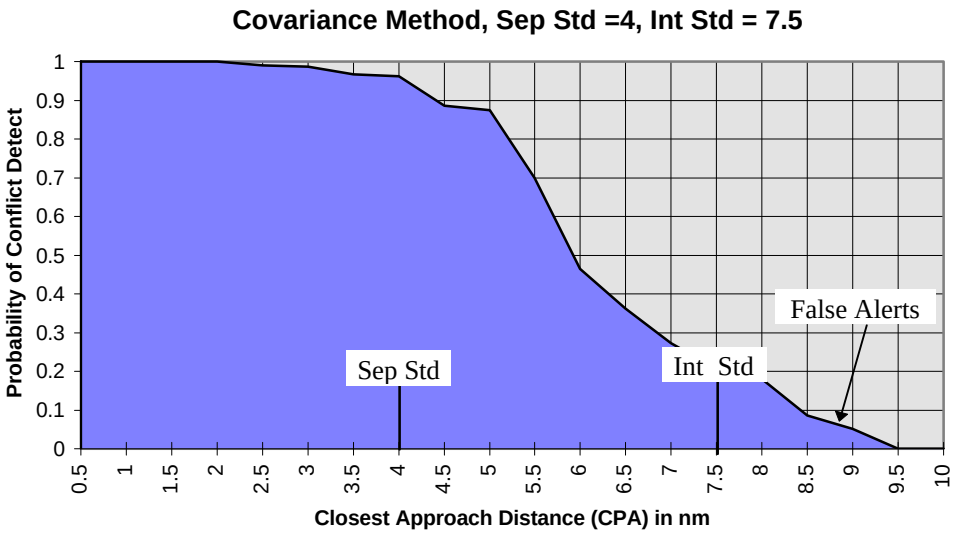

Figure 2: Nominal Conflict Probe Performance (Crossing Angle = 90 deg)

The most important time related requirements for conflict probe are the extent of the lookahead interval, the update period between probes, and the mean warning time between conflict detection and the predicted conflict. A lookahead interval of at least 20 minutes prior to CPA time is desired in order to clear an aircraft path through a sector, prior to sector handover. Since the typical time to fly through a sector is on the order of 10 - 15 min (for the simulation described in Section 3), and clearance is desired at least 5 min before sector entry, a 20 min lookahead will generally meet this need. However, 25 min lookahead is desirable and is supported by the covariance method for conflict probe. The covariance method begins conflict detection when the quality of the CPA predictions are sufficiently good, i.e. this method will typically begin detecting conflicts with 12 min to 24 min prediction times, depending on geometry and path uncertainty. The minimum lookahead time for the conflict probe should coincide with or overlap the lookahead interval for short term Conflict Alert, i.e. nominally 5 minutes lookahead.

The other conflict probe detection time requirements are:

* conflict probe update period < = 1 min

* mean conflict warning time > = 10 min.

Although most of the conflict probe studies utilized a 2 min update interval, a sensitivity study described in section 4.3 revealed that conflict probe detection performance is more reliable with one minute probe updates, and that mean warning time is somewhat larger with one minute updates. The conflict warning time is important for conflict resolutions and at least 10 minutes warning time is assumed in order to minimize path deviations to achieve safe separation, and to off-load the workload of the affected sector controller during peak traffic periods. In practice, one of the goals for the conflict probe is to achieve 15 minutes warning time, whenever possible. This allows more options for conflict resolution, such as the use of moderate speed and heading deviations to achieve safe separation during close encounters.

Navigation Requirements

One of the requirements for implementing medium term separation and reduced separation standards is the necessity to accurately follow the intended flight plan, or to dynamically change the flight plan as events require. In order to allow crossing or opposing encounters with predicted CPA distances less than 10 nm, it will be necessary for the airplanes involved to fly precise, predictable RNAV paths. In particular, the navigation systems for initial free flight aircraft should be capable of precision RNAV operation equivalent to RNP-1. Precision RNAV capability will be required to meet collision risk safety requirements for flight path deviations.

Users may be allowed to fly basic RNAV / FMS certified aircraft on free flight trajectories for some grand-fathered time period, in order to encourage adoption of Free Flight. However, such aircraft will not qualify for the reduced separation standards proposed above, and as a result will tend to increase controller workload in the Centers, compared with current jet route operations. The transition to precision RNAV standards should be achievable by many modern FMS and RNAV systems, since this level of accuracy and integrity should be attainable with dual DME and other multi-sensor navigation systems, as well as with GPS systems.

Surveillance Requirements

The implementation of a medium term conflict probe will require significant changes to the current surveillance system. The current mode-S Secondary Surveillance Sensors (SSR) and Airport Surveillance Radar (ASR) sensors are state-of-the-art systems and will be adequate for ground-based aircraft tracking for the initial phase of Free Flight.

However, the current aircraft trackers embedded in the Host computer system are obsolete, based on legacy software which is difficult to change, and will need to be redeveloped for the conflict probe and other ATC applications (such as the CTAS terminal approach system). There are two primary problems with these trackers. First, the en route tracking systems use sensor mosaics which determines the single best radar system to use for aircraft tracking in each mosaic subsector of airspace. Secondly, most U.S. Centers use 30 year old adaptive, alpha-beta-gamma tracker algorithms which are sub-optimal compared to current state-of-the-art algorithms, and which are incapable of fusing multiple site, multiple sensor data inputs (Ref. 4) . The problem with sensor mosaics is that aircraft track positions and velocities may jump unacceptably as the aircraft transits from one mosaic region to the next. This problem is compounded by the use of legacy trackers which cannot easily differentiate between false reports, mosaic jumping of position reports, and aircraft maneuvering.

The use of a state-of-the-art Kalman filter tracker supported by modern computing hardware has been proposed to overcome these tracker problems. Such a tracker will have multi-sensor radar fusion capability for smooth target tracking, and will support fusion of multi-sensor radar and ADS data for future ATM applications. The following specific requirements have emerged from the conflict probe studies in section 4, and from an analysis of state-of-the-art tracker capabilities:

* Radar position report accuracy - 0.15 - 0.20 nm relative rms error,

* Tracker horizontal velocity accuracy - 5 knots rms error (steady state)

* Tracker maneuver convergence time - 20 seconds following maneuver end.

The first requirement is necessary for adequate conformance monitoring and to develop accurate velocity estimates for medium term flight predictions. This requirement should be easily met with modern monopulse radars with rms azimuth errors on the order of one milliradian or less, since a one milliradian error results in a 0.15 nm crossrange error at 150 nm range. However, the older primary radars have rms azimuth errors on the order of two to three milliradians, and accurate fusion of multiple radars may be required to meet this requirement. (Ref. 5 discusses multilateration techniques for fusing sensor inputs and test results which illustrate that this capability can be achieved with older en route radars using multi-site data fusion.)

The requirement on velocity accuracy is necessary to obtain accurate estimates of closest approach parameters with up to 20 minute path lookahead. This can be achieved using a heavily damped tracking filter with long data latency time. However, the tracking filter must also be able to adapt rapidly to turning maneuvers, i.e. to switch between steady state and adaptive maneuver tracking. Both steady state and maneuver response requirements can be achieved by using modern tracking logic such as an Interacting Multiple Model (IMM) tracker (Ref. 6). During vertical transitions, higher accuracy is required even for 10 minute path lookahead, since the tracker must estimate ground speed and acceleration states for path predictions.

The requirement on tracker maneuver response time is a ‘placeholder’ requirement based on the performance achievable by modern tracking filters in simulation studies. (Convergence time can be defined various ways, e.g. as the time needed to obtain less than a 10 deg heading error after a maneuver is completed.) Fast maneuver adaptation is needed to support short term separation, and for flight plan conformance monitoring. It is important to achieve fast adaptation without over responding to false reports and large sensor errors. Further studies may be needed to validate this requirement in terms of improved short term conflict resolution. Good results have been reported in meeting this requirement by using either multilateration methods or the IMM tracker. Another method is to upgrade the SSR hardware, using back-to-back antennas which halve the (en route) radar report interval from 10-12 seconds to 5-6 seconds.

Communication Requirements

We do not assume any special voice or data-link communications for Initial Free Flight. In this phase the primary communication between ATC and the aircraft crew will be performed by VHF voice between the controller responsible for sector separation and the aircrew. It is assumed that the controller working the conflict probe position has some direct, but non-obtrusive method of communicating a recommended conflict resolution to the sector controller team responsible for separation assurance. The sector controller (or assistant) will assess the viability of the recommended resolution and communicate it to the aircrew. However, this process of implementing medium term conflict resolutions is indirect, subject to human error, and not ideal for tactical control. Consequently, some means of direct data-link communications will be needed for conflict resolutions in a later transition phase. Further studies are needed to analyze conflict resolution operational concepts and to derive technical requirements for more efficient means of implementing conflict resolutions.

Although not required for Initial Free Flight operations, the capability to dynamically update the flight plan and to communicate path intent will eventually be needed since medium term separation assurance depends on valid path intent. Thus, capability for domestic ADS communications will also be needed for later Free Flight transitions.

Wind & Weather Forecasting Requirements

The National Weather Service is currently developing an advanced weather prediction system for the continental U.S., which is called the Rapid Update Cycle (RUC). The RUC forecasts will use both ground based Doppler radars and airborne observations to perform detailed 3 hour forecasts for use in aircraft flight predictions. This system will use 60 km or finer grids and 19 flight levels to perform detailed, mesoscale level weather predictions throughout continental U.S. airspace. If current implementation schedules are satisfied, the RUC will become available in the en route Centers before

the turn of the century. Thus, we have assumed that the current 12 hour, coarse grid forecasting system will be replaced by the RUC prior to implementation of Initial Free Flight. The accuracy of the RUC in forecasting winds aloft can be estimated from the Mesoscale Analysis and Prediction System (MAPS) prototype which has been field tested at Orlando, Fl. and Memphis, Tenn. The field tests show that the RUC will have an along-track rms mean wind error of about 6 - 9 knots[3] (Ref. 7). Our conflict probe studies show that this level of forecast error will probably be adequate to support medium term flight predictions and conflict detection. Consequently, we have assumed this level of capability as the technical requirement for Initial Free Flight.

[3] More recent studies have shown that the along track errors associated with 3 hour forecasts may be closer to 10 knots rms (Ref. 11). However, the RUC forecasts may be improved by using 1 hour forecasts and finer grids to achieve the desired forecast accuracy.

2.0 Separation Assurance and Conflict Alerting Operational Concepts

The first step in analyzing advanced concepts for Free Flight such as conflict probe and alert zone monitoring is to specify the operational concept, i.e. how will these systems operate, and how will they interface to controllers and pilots to provide separation assurance. In succeeding sections we will analyze these concepts in greater detail with modeling and simulation tools, to derive requirements for system implementation. This discussion is necessary for understanding the context of the analysis. In this section we first discuss operational concepts for Initial Free Flight and then for Mature Free Flight.

2.1 Operational Concepts for Initial Free Flight

2.1.1 Regional Path Prediction and Load Demand Processing

Restructuring of the hardware and software architecture for Center operations will be needed to support automation functions such as local flow management, dynamic density display of load demand, and automated conflict probe. These operations will require systematic development of structured databases to support operational changes in Center operations. In this section we briefly describe some core software structures and databases needed to support medium term traffic planning and conflict probe automation for Initial Free Flight. The description below is not an operational concept, but is a conceptual description of software infrastructure for Conflict Probe and other medium term planning functions.

Figure 3 shows a top level flow diagram of the processing functions to support medium term flight planning and automated conflict probe. (The cylinder shapes represent databases stored on hard disk, and the rectangles represent processor functions.) Three dynamic data-bases are needed to perform medium term path predictions: (1) a central track table containing all of the aircraft tracks operating in or close to Center airspace, appropriately merged so that each aircraft is represented by one central track file, (2) a regional weather database containing forecast winds and temperatures over a 3-D grid, and (3) a regional flight planning database containing the intended 3-D waypoints and airspeeds of aircraft flying in Center airspace or which are anticipated to arrive or depart Center airspace in the next (~ 30 min) prediction cycle. Each aircraft track in the central track file which has a validated flight plan (in the sense that the aircraft track is in conformance with its flight plan) is predicted forward over a nominal 30 min lookahead using the data fusion concept described in section 1.4, and stored in a flight path intent database. The path intent files are subdivided into straight line segments which represent subsequent short intervals of flight, e.g. 1-2 minute flight segments. In addition to the internal path predictions, similar path intent files are communicated from nearby en route Centers whenever an aircraft path is predicted to

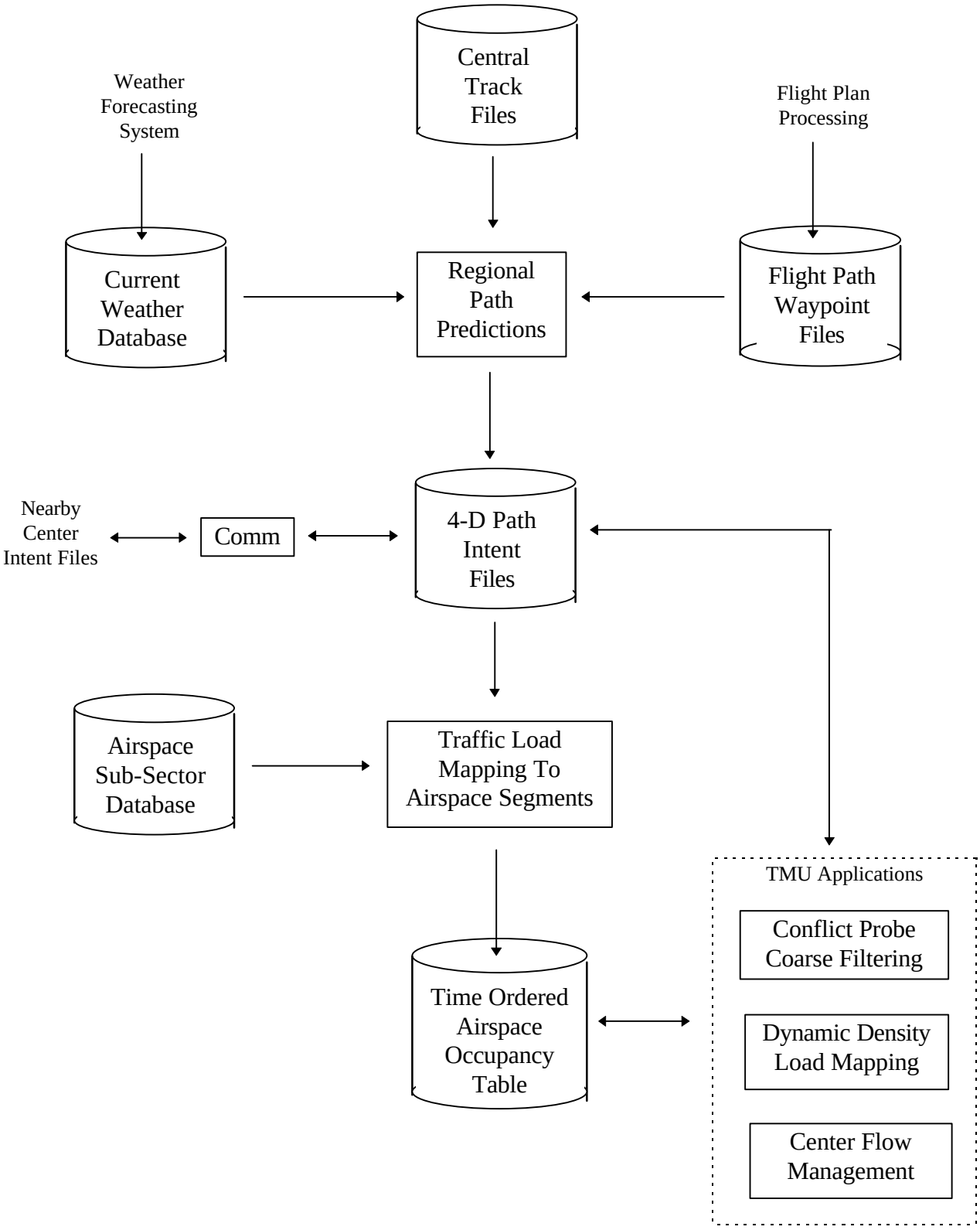

Figure 3: Medium Term Path Prediction and Traffic Load Processing

arrive in Center airspace during the prediction period. These path predictions are repeated at regular intervals, i.e. at nominal one minute update cycles.

In addition to the path prediction files, a systematic means of mapping the predicted trajectory paths into dynamic airspace traffic loading will be needed to support more complex Free Flight routings. Conceptually, for each intent path and time segment we first establish a mapping $P_{T,I}$ --> $A_{J,K,L}$ where $P_{T,I}$ denotes the path predictions for the T'th time segment and the I'th aircraft track, and $A_{J,K,L}$ denotes a 3-D airspace sub-sector occupied by the aircraft during the T'th time interval. When the mapping process is completed, then the results are stored in a database ordered by time and airspace sub-sector, i.e. for each time interval T and sub-sector $A_{J,K,L}$ a list of path prediction segments $\{ P_{T,I} \}$ which occupy that sub-sector is identified and the total number of aircraft transiting that sub-sector is counted.

The value of the airspace occupancy table is that it provides an underlying infrastructure for detecting and resolving medium term traffic load problems and for coarse identification of potential aircraft conflict pairs. One method for detecting load problems is to display dynamic density maps of regional airspace, where the number of aircraft transiting through each sub-sector over time intervals on the order of 5 - 15 min. are obtained and displayed graphically to traffic managers. The idea is to manage predicted traffic loads to better utilize Center resources. For example, if an arrival sub-sector near a terminal area is predicted to overload, then the traffic manager can divert some of the transiting aircraft in time (via en route holding or airspeed changes), or in space (via re-routing through adjacent, less congested sub-sectors). The conflict probe may be used to test the validity of trial flight plan diversions, in such cases, prior to issuing a tactical resolution. A traffic supervisor may also elect to resectorize Center airspace to concentrate one or several controllers on the congested areas.

There are several alternative methods to perform coarse conflict filtering prior to the application of fine resolution conflict detection and alert. One method is to use the airspace occupancy table to identify potential conflict pairs. Suppose that it is desired to clear a reference aircraft over a fixed lookahead interval, e.g. 20 minutes lookahead. Then the coarse filter would successively find the sub-sector $A_{J,K,L}$ transited by the reference aircraft in each subinterval with lookahead less than 20 min, and then poll all the aircraft occupying that sub-sector or an adjacent sub-sector to find potential conflict pairs. This method is much more efficient, for example, than polling all of the other aircraft in the path intent database to find potential conflict pairs.

It should be noted that the critical step in the above flow diagram is the path prediction process. It is important that the accuracy of all the databases supporting this function be examined and allocated an error budget which will support time critical applications such as fix metering and conflict probe. The primary issues here are the accuracy requirements on wind forecasting, surveillance error, and open loop trajectory synthesis (for climb and descent trajectory segments). Whether an advanced trajectory synthesis system such as CTAS, or an advanced ITWAS forecasting system are required

depends on the overall error budget allocation, and the quality of the other subsystems at the time of deployment.

2.1.2 Conflict Probe Operational Concepts

The basic idea for Initial Free Flight is to use medium term path predictions to identify and resolve most potential conflicts before they become short term conflicts. Whether used on a sector basis to clear aircraft paths through a sector, or on a regional basis to provide more strategic planning, the conflict probe will enable airspace problems to be identified earlier and solved more efficiently than with the current system. In the AERA concept (Ref. 3), once an aircraft path has been cleared for flight across a sector or over some lookahead period, the conflict probe and the path prediction does not need to be repeated again until the end condition is reached or the aircraft strays from the predicted path. We have also adopted this concept, except that the time interval for repeating the conflict probe should be some fraction of the lookahead interval for conflict detection, i.e. the conflict probe should be repeated at least twice over a 20 minute period, since the accuracy of path prediction increases significantly as the prediction time is decreased from 20 to 10 minutes.

The flight plan, which describes aircraft path intent and anticipated waypoint times, is essential for medium term flight predictions. However, short term deviations such as path offsets, heading vectors from the nominal path, and temporary altitude transitions need to be integrated into the planning and monitoring process whenever possible for the conflict probe to be effective. (Without a currently valid flight plan, flight predictions are not possible and only short term monitoring and control based on radar surveillance is feasible.) We shall designate the original, unmodified flight plan as the primary flight plan, and deviations from this plan as an alternative flight plan if this plan is currently active, or as a trial flight plan if this is a requested option by the air-crew or by a ground controller for solving an airspace problem. We here designate the position which monitors medium term conflicts as the planning controller. (It is assumed that the planning controller and the sector / radar controller are different positions.) The planning controller will have responsibility for medium term flight planning and identifying path resolutions to solve potential airspace conflicts. The planning controller will need considerable automation support in addition to the conflict probe, in order to assure that the aircraft is following the active flight plan (conformance monitoring), to aid the controller in validating separation with a proposed trial plan, and in activating an alternative flight plan when a dynamic path change is needed.

However constructed, the active flight plan is monitored at each radar scan for conformance with the predicted flight path established by the conflict probe, i.e. the predicted lateral and ground track are determined by the active flight plan and the predicted longitudinal position is determined from the aircraft state vector at the last probe time. The horizontal conformance bounds on the trajectory can be viewed as either uncertainty ellipses or as lateral and longitudinal parallelograms centered on the predicted path. In this report we assume that the conformance bounds are elliptical

regions, since this simplifies the analysis for detecting aircraft conflicts, and is compatible with our covariance analysis for modeling trajectory prediction uncertainty.

The use of medium term conflict detection extends separation assurance beyond the limits of current sector boundaries, i.e. this concept is area wide rather than sector wide. As an example, Figure 4 shows a typical case in which two aircraft cross near a sector boundary, and a potential conflict can be solved by a current sector controller before the aircraft enters into the sector where the conflict occurs. In this case, the planning controller could request Sector A controller to vector or slow AC1 in order to resolve the potential crossing conflict in Sector C.

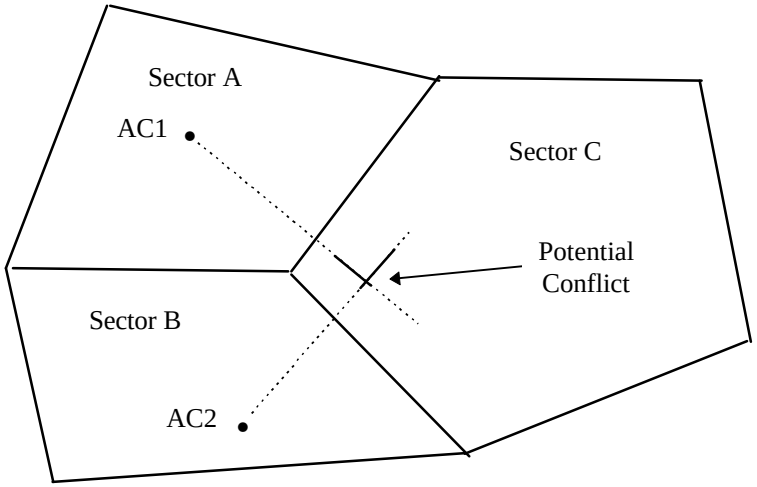

Figure 4 Example Medium Term Conflict Resolution Concept

The threshold settings and intervention rate for medium term separation must be designed consistent with that for short term separation to minimize total system interventions and controller workload. This can be accomplished in several ways. One method is to choose the thresholds and time interval for short term conflict alert (STCA) compatible with that for the conflict probe. Figure 5 illustrates this concept. This figure shows the detection thresholds for the preferred conflict probe concept, and system matched parameters for the STCA automation supporting the sector controller. The conflict probe selects its detection parameters dynamically based on conflict geometry and warning time to closest approach. However, fixed thresholds are adequate for the short 5 min lookahead shown for the STCA system, and there is no need for explicitly declaring non-conflict pairs since the Conflict Alert calculations are repeated on each radar scan update. Both systems are tuned for detecting conflicts whenever the observed CPA is less than the intervention standard (4 nm).

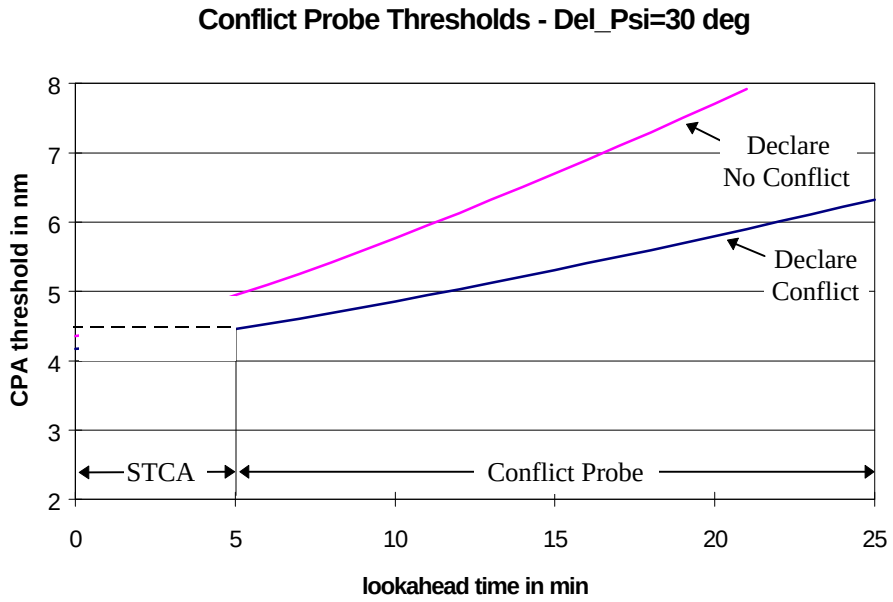

Figure 5 Conflict Probe and STCA Thresholds versus Lookahead Time

Of greater concern is the capability of controllers to provide oversight on the separations provided by the conflict probe. Additional automation tools will be needed to support reduced separation standards. Figure 6 shows a concept which uses predicted conflict uncertainty as a decision aid for the planning and sector controllers. In the event that the predicted separation between two aircraft is questionable, a controller will be able to call up an overlay display which shows the predicted intruder path relative to a reference aircraft. The reference aircraft in the figure has displayed the radial separation standard and the intervention standard for comparison with the predicted intruder path. The predicted intruder path relative to the reference aircraft and the path uncertainty are displayed by the dotted line overlays. In this figure, the intruder is climbing through the reference aircraft flight level. The time interval when vertical separation is lost is shown in heavy double lines. For medium term separation, the bounding lines for intruder containment can be at the 95% probability level or lower, since a reasonable level of missed detections is allowed, whereas the bounding lines for short term separation may be at the 99.9 % level or higher, since the sector controller is responsible for assuring separation greater than the minimum. The controllers should intervene if any portion of the heavy line containment boundary intersects with the reference aircraft inner circle (protection zone), and should not intervene if the intruder containment region lies outside the intervention ring. In the figure below, the decision to intervene or not is up to the controller, since the predicted CPA lies between the separation and intervention standards.

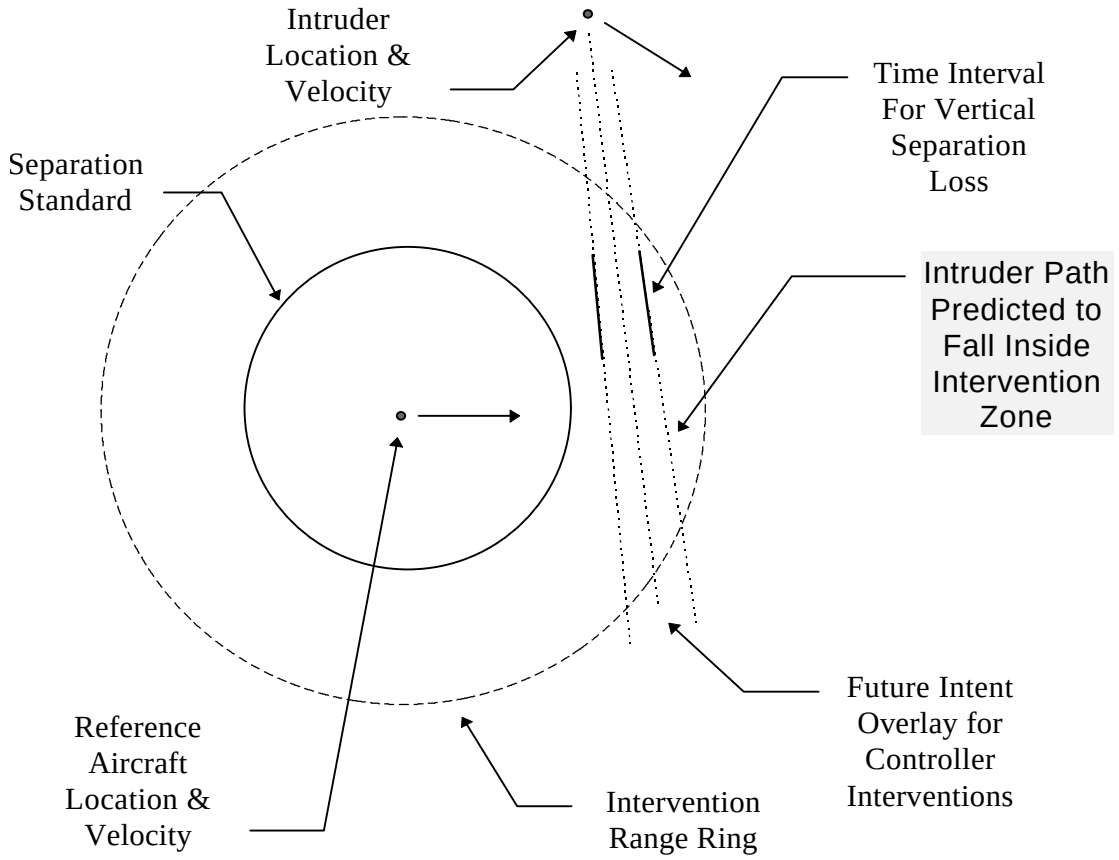

Figure 6: Future Intent Display Aid for Interventions

2.2 Operational Concepts for Mature Free Flight

There are two main themes which dominate the growth to mature Free Flight in our report: (1) the introduction and application of ADS air-ground data link for reduced separations, and (2) the concept of Alert Zone monitoring. In this section we first briefly discuss the applications and implementation of ADS for Free Flight, and then discuss an operational concept for Alert Zone monitoring.

2.2.1 ADS Implementation and Applications for Free Flight

It is here assumed that the primary air-ground data-link for ADS surveillance will be mode-S based. The reasons for this assumption are two-fold:

* The only other proposed medium for domestic ADS data-link in the 2002 time frame is VHF. However, the currently proposed VHF data links for this time period, i.e. the

AVPAC radio and the multiplexed digital voice / data-link radio will not have sufficient bandwidth for routine ADS surveillance, where report intervals of ten seconds or less must be sustained. By contrast, report intervals of one second or less are sustainable using mode-S squitter (Ref. 8) broadcasts (ADS-B).

* Most of the infrastructure for mode-S data-link currently exists, i.e. there are over 140 deployed mode-S ground sensors, and thousands of installed mode-S transponders, since all of the TCAS-II equipped planes carry a mode-S transponder. Moreover, low cost ($4000) mode-S transponders are currently available for GA aircraft. Since data-link capability is built into the mode-S system, the current generation of mode-S transponders can be upgraded to support ADS-B and TWDL capability.

The design and formatting of mode-S message formats for ADS is currently under definition in various ICAO, AEEC and RTCA standards committees. However, we can anticipate several capabilities based on current draft SARP and MASPS documents. The first is that all equipped aircraft will broadcast GPS 'squitters' containing their position and velocity states for air-air and terminal area air-ground applications. However, the GPS squitters may have limited range, and will not be directly applicable for en route air-ground applications. Consequently, ADS for en route applications will probably be based on the mode-S radars and on Ground Initiated Comm-B (GICB) requests for information as an aircraft comes within the current scan radar beam. (It is also possible to transmit unsolicited air-ground messages after the standard SSR reply on each scan, in order to transmit ADS broadcast messages at longer ranges.)

The following types of messages useful for Free Flight applications can be requested from ground sensors using mode-S special services message formats (Ref. 9):

* ground and air referenced position and velocity states

* pressure altitude and altitude rate

* geometric altitude and altitude rate

* aircraft wind and temperature states

* aircraft future intent
    - 4-D waypoints including waypoint times

* aircraft short term intent
    - vertical intent parameters including altitude target and time-to-level-off
    - horizontal turn parameters including selected ground track and time-to-turn.

There are many potential applications for ADS to improve future ATC Center operations. The most significant for transition to mature Free Flight are:

* Monitoring of ADS velocity vector and ADS / Radar data fusion :

One of the limiting factors in controlling aircraft tactically today is the uncertainty in short term aircraft intent, since the aircraft velocity state is not monitored, but derived indirectly by filtering noisy radar position measurements. When an aircraft deviates from its intended flight plan, it can take many scans to detect the deviation from radar measurements. ADS velocity monitoring will enable immediate detection of flight plan deviations, and immediate confirmation of tactical vectoring for separation assurance. This capability will be needed in mature Free Flight to support reduced separation standards.

The other area where ADS monitoring may be needed is to support medium term path predictions in climb and descent flight phases. The sensitivity studies in Section 4 show that conventional radar tracking during periods of non-constant velocity flight (such as climb and descent phases) may not support adequate lookahead periods for efficient resolution of potential conflicts. Aircraft path observability is greatly improved with ADS monitoring and its use in climb and descent predictions may be essential for reducing separation conflicts during vertical flight. Since the vast majority of close encounters in Initial Free Flight will involve climbing and descending aircraft, this is an area that needs close attention in future research studies.

* Monitoring of Geometric Altitude for RVSM :

One of the primary goals for efficient high altitude flight is the ability to fly at 1000 foot flight levels above FL290, rather than the current 2000 foot flight levels. The ability to fly 1000 foot flight levels will become a reality in 1997 for North-Atlantic flights in oceanic airspace. However, the methods used to support RVSM in the Atlantic are expensive for both airborne users and ATC service providers. The problem is that in the current system there is no independent cross-check on baro-altimeter accuracy. A special uplooking radar sensor is being developed for North-Atlantic flights that will check the altimeter accuracy as aircraft exit into the oceanic track system. However, by the year 2000, the Wide Area Augmentation System (WAAS) will be implemented over NAS airspace, and GPS based geometric altitude will be available with sufficiently high accuracy, integrity and availability for use in vertical separation assurance. Whether geometric altitude is used directly for vertical separation above FL290, or simply as an independent cross-check of baro-altimeter accuracy will be decided in the future. However, it appears to be a cost effective method of implementing RVSM for lower capability GA aircraft and for altimeter cross-checks at the ATC Centers. We assume that ADS broadcast of GPS altitude and altitude rate will become a required capability for aircraft flying above FL290 during the transition to mature Free Flight.

* Updating and Validation of Flight Plan Intent :

One of the operational problems which arises with medium term separation methods is that of updating the flight plan to reflect current conditions. If a pilot in an RNAV or FMS airplane, for example needs to make a weather based adjustment to the flight plan in concurrence with the sector controller, then the pilot will add or change waypoints to

implement the new flight plan. Without data link capability, the ground based flight plan is then invalid until either updated manually or until the aircraft returns to the previous flight plan. With ADS data link capability, the ground can update or validate the flight plan periodically by requesting future aircraft waypoints and checking them against the current flight plan. This process will assure consistency between the aircraft intended flight plan and the ground based flight plan.

* Broadcasting Aircraft Equipage Capability for Mixed Fleet Separation :

We have proposed in Table 3 reduced separation standards for appropriately equipped aircraft as the transition to mature Free Flight occurs. However, in a mixed fleet environment, the separation standard of the least capable aircraft should be used in an encounter. This may be accomplished in mature Free Flight by broadcasting aircraft minimum separation capability. In particular, this is needed for Alert Zone monitoring so that an appropriate separation standard is applied for potential encounters.

2.2.2 Operational Concepts for Alert Zone Monitoring

One of the fundamental limits of ground based separation is the amount of time it requires to intervene tactically to achieve separation. Some of the problem with current systems is due to sensor limitations which result in poor observability of aircraft intent. Even if this problem is overcome using ADS monitoring, the problem of time lags in resolving conflict encounters will remain. One way to overcome this limit is to transfer responsibility for separation assurance from the ground controller to the pilot, with a means provided the pilot for high integrity, high accuracy situation awareness. We assume in the following that all aircraft flying in mature Free Flight airspace will be broadcasting GPS squitters containing their current position and velocity states, to provide such situation awareness for airborne systems. Alert Zone monitoring is a concept for specially equipped aircraft to detect close encounters, and to provide autonomous guidance for safe separation during an encounter interval. The Alert Zone is the region where the guidance cues are active, and is specifically needed to provide separation assurance in same altitude, opposing encounters.

Alert Zone monitoring will require some kind of hand-off of separation responsibility from ATC to the pilot and back to ATC when an encounter is completed, in order for ATC to accept reduced separations such as those shown in Table 3. Conceptually, this may be accomplished as shown in Figure 7. At position (1) the conflict probe determines that an opposing encounter between AC1 and AC2 will occur, and alerts an appropriate sector controller. At position (2), the squitters from AC2 are detected and the pilot is notified that AC2 will be entering his aircraft Alert Zone. The pilot then activates Alert Zone monitoring which sends a message to the sector controller to the effect that aircraft AC1 is now providing self separation. At position (3), the Alert Zone monitor determines that the two aircraft have established safe separation and are on diverging paths, and deactivates Alert Zone monitoring, freeing the pilot for other tasks. A message is then sent to the controller to the effect that separation assurance for AC1

is being returned to the controller. If neither aircraft activates Alert Zone monitoring within a specified time before closest approach, then the sector controller will intervene as necessary to assure separation.

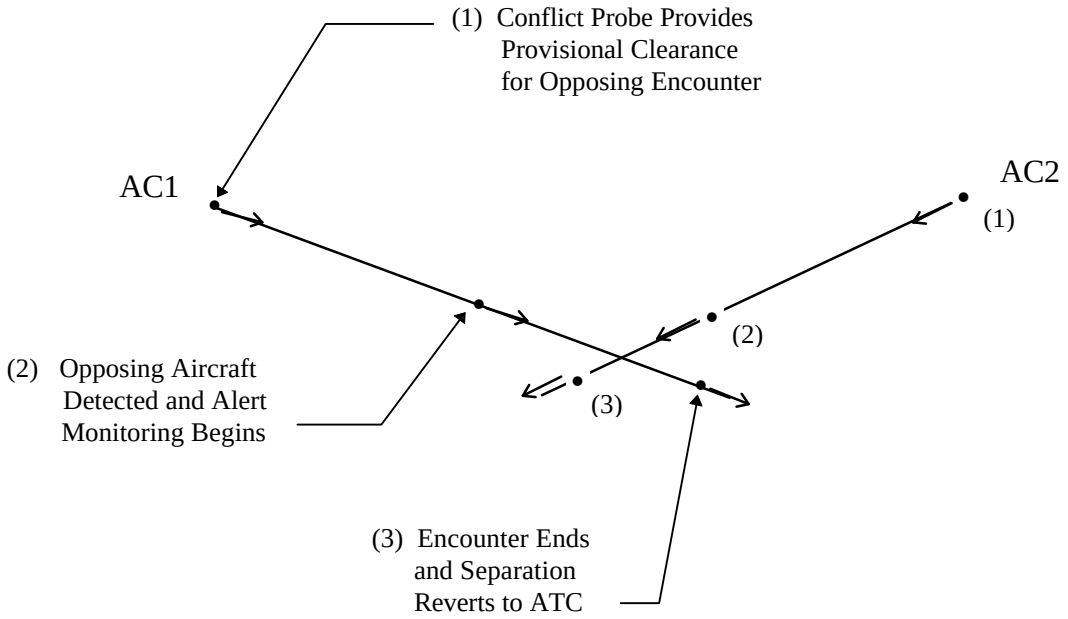

Figure 7: Cooperative Separation Concept for Alert Zone Monitoring

In our concept, an intruder enters the Alert Zone when the predicted CPA of the intruder is less than the intervention standard, the vertical separation is less than the minimum allowed, and the time to CPA is less than some threshold value, say two minutes to CPA. The aircraft remains in the alert zone until the aircraft paths diverge and the intruder range is greater than the intervention standard or vertical separation is achieved. Guidance path restrictions are continuously displayed in the Alert Zone, or earlier if the pilot has previously activated Alert Zone monitoring. The guidance restrictions prevent the pilot from heading in a direction which will intercept the intruder's protected zone. Figure 8 illustrates this concept. In the rare event that the predicted CPA becomes less than the separation standard (plus a small buffer) then the ownship path will be between the two dotted lines in the figure and the Alert Zone monitor will issue a resolution advisory (path heading / speed change) to achieve safe separation, and will send a cooperative advisory to the intruder, and an alert to the ground controller. For FMS equipped aircraft, guidance restrictions would be displayed on the navigation display and interfaced to the flight management system.

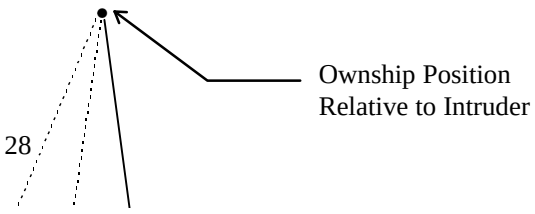

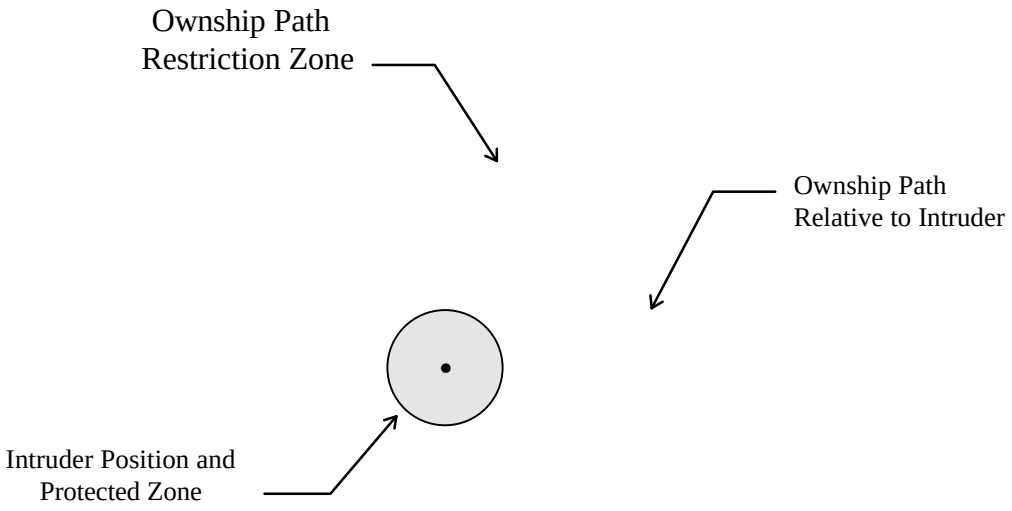

Figure 8: Alert Zone Guidance Restrictions

Now the operational concept can be summarized in terms of the following procedures:

(1) Whenever another aircraft becomes observable, the time to closest approach, time to flight level crossing, and CPA distance are monitored. If the closest approach exceeds the intervention standard, or vertical separation is assured, then the Alert Zone monitor remains in the background.

(2) If the CPA distance is predicted to be less than the intervention standard and vertical separation is not assured, then the pilot is alerted and can take responsibility for path separation, i.e. the controller is notified and the Alert Zone monitor will continuously display guidance restrictions. In the event that this CPA condition persists and the Alert Zone is entered, the monitor will notify the pilot and display guidance restrictions until Zone exit.

(3) If the intruder enters the Alert Zone, and the ownship path is in the restricted zone, i.e. the predicted CPA is less than allowed for safe separation, then the system will issue a horizontal resolution advisory to achieve the required separation and send a complementary advisory to the intruder aircraft. If this fails to be effective due to intruder maneuvering or other causes, then the TCAS system will issue a vertical resolution advisory to prevent path collision.

This concept of airborne separation is cooperative in the sense that the intruder aircraft must be able to broadcast position and velocity state information for Alert Zone monitoring, and must be able to receive some form of cooperative guidance restriction, i.e. the Free Flight aircraft may broadcast a message which is translated into an aural warning onboard the intruder aircraft, and into preventive guidance cues for CDTI

equipped aircraft. It should be observed that path resolutions are not limited by 'rules-of-the-road' which favor right hand turns by both aircraft involved in crossing or opposing encounters. Although 'rules-of-the-road' procedures are simple to understand and implement, they are not compatible with multiple aircraft encounters, or with mixed equipage encounters where one aircraft has superior situation awareness of the encounter geometry.

Other concepts have been proposed for implementing Alert Zone monitoring. The above concept was conceived as a methodology which is reasonably simple to implement for mature Free Flight (provided that all nearby aircraft broadcast GPS squitters), and which maintains the same separation parameters for ground and airborne separation assurance, providing consistency between medium term, short term, and airborne separation systems.

3.0 Operational Requirements for Separation Assurance

This section is concerned with obtaining numeric requirements for separation assurance so that tactical interventions do not grow excessively as Free Flight is progressively implemented. Most tactical interventions in the current ATC system are either for separation assurance or to manage traffic flows for high capacity operations. In order to move towards Free Flight, new concepts and implementing technologies will be needed to keep tactical interventions and controller workload at manageable levels. One of the main concepts is to implement systems which will permit reducing the size of the aircraft protection zone, eliminating the need for a substantial proportion of en route interventions. A second concept is to use automated conflict probes to determine which aircraft need to be moved due to potential path conflicts. Aircraft paths will not be changed unless there are predicted path conflicts or flow restrictions are going to be violated.

There are four routing / altitude options for transitioning to Free Flight analyzed in the studies below. The first option, denoted **Baseline** constrains the trajectories by terminal exit and entry conditions to efficiently manage terminal flows, and constrains cruise altitudes to 1000 or 2000 foot steps, segregated by east or west flying routes. This option permits the users freedom in selection of lateral routes and cruise airspeeds, and requires the least amount of ground and air infrastructure for implementation. The second option, **Baseline Plus RVSM** (Reduced Vertical Separation Minimum) reduces the vertical separation minimum and the vertical steps in cruise altitude above FL290 to 1000 feet. This option permits Baseline flight operations and more efficient use of cruise flight levels, at the cost of additional airborne avionics. The third option, **En Route UPT** (User Preferred Trajectories) removes the constraints on user preferred cruise altitudes, i.e. the user is free to select preferred altitude and speed cruise parameters as well as lateral path between terminal exit and terminal arrival points. This option permits greater freedom in route selection at the cost of greater ground and air infrastructure to achieve greatly reduced separations. The fourth option, **En Route UPT Plus RVSM** permits En route UPT flight operations with reduced vertical separation minimums. This option represents a possible end state for mature Free Flight. Other routing options are possible, but the four selected provide good insight into the trades between increased route choices and the CNS infrastructure needed to support them.

The basis of this task is a simulation of the aircraft operations in the Cleveland ARTCC (Air Route Traffic Control Center) over a one day period. Section 3.1 describes this simulation model. The simulation studies using this model are summarized in Section 3.2. These studies include benchmarking the close encounter or close proximity statistics for 1995 operations, and showing the time phased growth in encounters due to traffic growth over time, and due to implementation of successive transition steps to Free Flight. Operational requirements for Free Flight transitions are then derived in Section 3.3, based on the simulation results in Section 3.2.

3.1 Cleveland ARTCC Simulation Model

This section describes the U.S. Cleveland Air Route Traffic Control Center (ARTCC) simulation model. This model was developed using the TAAM (Total Airspace and Airport Modeler) simulation. The purpose of the model is to simulate air traffic for an en route center and count the number of close encounters between aircraft pairs. Section 3.1.1 describes the benchmark model and Section 3.1.2 describes the methodology used in the study.

3.1.1 Cleveland ARTCC Model Description

The U.S. Cleveland ARTCC was chosen to represent a high altitude en route traffic region with high density traffic peaks. The ten sectors in this region are shown in Figure 9. These sectors start at FL240 and include the airspace above FL240. The "current" air traffic for the region was obtained from the Official Airline Guide (OAG), for the day August 1, 1994. Any flight that has a direct route through the Cleveland ARTCC was selected for the study. The total number of flights simulated is 4,555. Of these 1,121 are inter-flights or flights between airports near or in the ARTCC region, 2,593 are arrivals or departures to one airport near or in the region, and 841 are overflights.

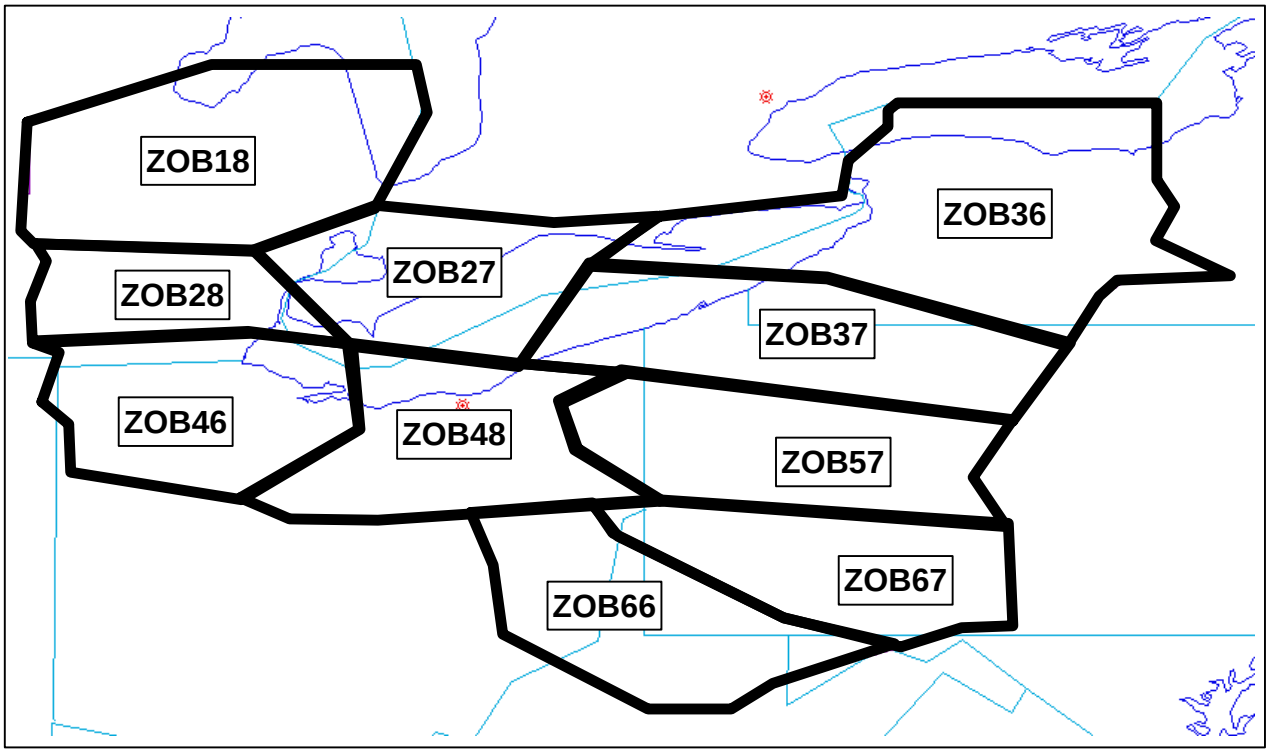

Figure 9: Sectors Used in the Cleveland ARTCC Study

The simulation models the performance of each flight based on aircraft type. The distribution of aircraft types used in the simulation is given in Table 5. In the simulation one aircraft cruise altitude is assigned for each flight. The assignment is based on the preferred aircraft cruise altitude, the flight direction, and the length of the flight. The distribution of these cruise altitudes is shown in Table 6.

Table 5. Distribution of Aircraft Types

AIRCRAFT TYPE CODE	NUMBER OF FLIGHTS	PERCENT FLIGHTS
B737	916	20.11
MD83	882	19.36
DC9	420	9.22
B757	363	7.97
B727	288	6.32
A320	224	4.92
J31	222	4.87
FK100	203	4.46
E120	200	4.39
DHC8	124	2.72
SF340	114	2.50
DC10	102	2.24
ATR42	100	2.20
B767	96	2.11
737-500	81	1.78
SWM	65	1.43
FK28	49	1.08
MD11	31	0.68
B747	22	0.48
BA146	12	0.26
A300	11	0.24
747-400	9	0.20
A310	8	0.18
J41	6	0.13
MD80	3	0.07
FK27	2	0.04
A340	2	0.04
TOTAL	4555	

For each aircraft type there is a set of simulation parameters that define the aircraft performance characteristics. Some of these parameters are preferred cruise altitude, aircraft speed, climb and descent rates. The speeds and rates vary with altitude. The parameters are contained in TAAM aircraft performance data files. These files can be modified by the user. The default parameters in these files are questionable for many of the aircraft models, but are suitable for an analysis of en route encounters. Future work should include updating the aircraft performance data files. (See Section 5)

Table 6. Distribution of Simulated Aircraft Altitudes

CRUISE ALTITUDE (FL)	NUMBER OF FLIGHTS
240	252
250	222
260	94
270	117
280	68
290	92
310	97
330	75
350	922
370	1277
390	792
410	457
430	76
450	14
TOTAL	4555

In the current simulation, airports are modeled as points and serve as a source and sink for traffic. All flights are assigned direct routes and follow great circle paths between departure and arrival airports. The airports used in the study are shown in Figure 10.

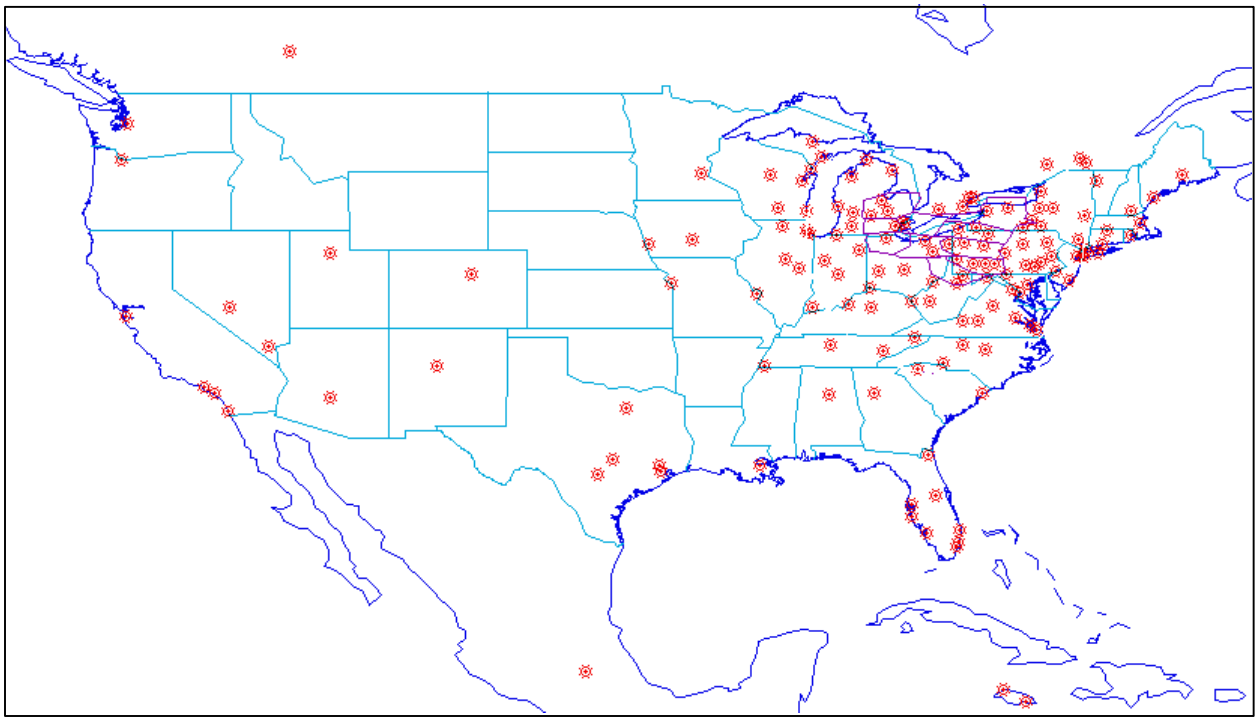

Figure 10: Location of Airports Used in the Cleveland ARTCC Simulation

Some of the city pair routes used in the study are shown in Figure 11. This figure shows the density of east/west crossing routes that makes the Cleveland ARTCC an appropriate region to study for free flight. Procedures in and out of the airport, runways, gates, etc. are not modeled. Further work could include modeling entry and exit points and procedures in and out of a terminal area or airport.

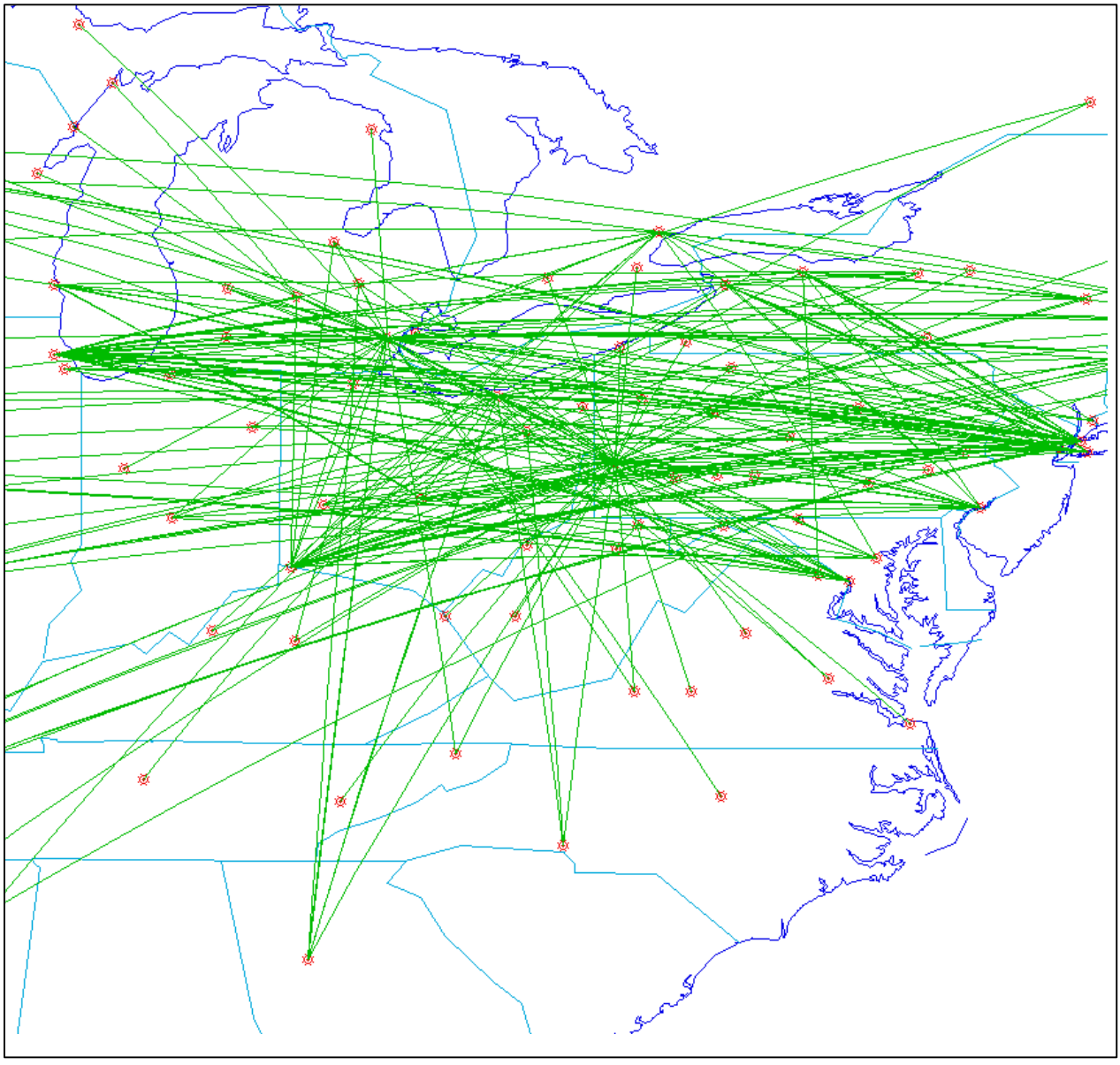

Figure 11: City Pair Routes Active During Mid-Day Traffic

In our TAAM simulation a full day of traffic is simulated. Aircraft fly undisturbed flight paths, i.e. conflicts are detected, but not resolved. As the simulation runs, the closest point of approach (CPA) between each aircraft pair is monitored. If the closest point of approach is between 0%-200% of the separation standard, an encounter is recorded.

For each encounter the distance between aircraft at the point of closest approach is recorded. The encounter data are used to compute the number of ATC interventions for a given separation requirement. These interventions are a measure of controller workload. (In this study the number of encounters which would result in a tactical intervention is used to quantify center workload. Although many other factors in reality determine controller workload, it is here assumed that encounter frequency may be used as a gross measure of workload for establishing separation requirements.)

Path conflicts are categorized by type of conflict (opposing, in-trail, or crossing) and phase of flight for the pair (descent-descent, climb-climb, cruise-cruise, climb-descent, climb-cruise, descent-cruise). Aircraft are in-trail if the difference in aircraft heading is less than 45°, opposing if greater than 135°, otherwise they are crossing. Aircraft are in climb mode prior to Top of Climb, in descent mode past Top of Descent. Otherwise they are assumed to be in cruise mode.

During a simulation, encounters are recorded. Then they are post-processed to remove encounters that are counted twice. For example, TAAM may count the same encounter twice if the pair of aircraft crosses a sector border while in conflict (counted once in each sector), or if the duration of an encounter continues to the next hour (counted once in each hour bin). Also encounters are removed if both aircraft depart from the same airport since departure procedures are not simulated.

3.1.2 Cleveland ARTCC Simulation Methodology

A total of five operational concepts are considered: the Benchmark system of today's environment, Baseline free flight, Baseline plus RVSM, En Route UPT, and En Route UPT plus RVSM. A listing of studies and their attributes is provided in Table 7.

Table 7. Operational Concepts and Their Attributes

	Attributes			
Studies	User Preferred Flight Levels	1000 Feet Flight Levels Above FL290	Unconstrained Terminal Areas	User Preferred Routes Between Terminal Areas
Benchmark	NO	NO	NO	NO
Baseline Free Flight	NO	NO	NO	YES
Baseline Plus RVSM	NO	YES	NO	YES
En Route UPT	YES	NO	NO	YES
En Route UPT Plus RVSM	YES	YES	NO	YES

User Preferred Flight Levels means a flight can use any available flight level. Cruise altitudes are still assigned by flight levels. We are not considering cruise climbs (i.e.

continuous climb during the en route phase of flight). 1000 Feet Flight Levels Above FL290 means a reduction of the current vertical separation standard above FL290 from 2000 feet to 1000 feet. Unconstrained Terminal Areas means a user is not procedurally restricted in the terminal area and can fly an optimum departure or approach profile. Optimum approach and departure profiles is desired for free flight, but our simulation model needs additional refinement for terminal area studies. Simulation of unconstrained terminal areas may be considered in future studies. User Preferred Routes Between Terminal Areas means a user can select a direct route or a minimum wind track outside of the constrained terminal areas. Users also can select their optimum speed profile.

There are four different TAAM simulations that model the four free flight options. It should be noted that the results for the benchmark studies were obtained with the baseline free flight simulation using 1995 traffic levels. For the benchmark case we have assumed that the number of encounters with direct point-to-point routes is roughly equal to the number of encounters with conventional routes. This assumption is based on results from a previous study that shows both sector loading and number of proximity events are similar for a conventional route system versus direct routing (Ref. 10). Our studies also do not model winds aloft or adverse weather conditions which may significantly alter traffic loading patterns.

In the simulation studies we evaluate encounter statistics for 1995 benchmark traffic and for traffic growth from 100% to 200% of the 1995 benchmark. If we assume a nominal 5% per year growth in traffic, then by 2002, the initial year assumed for Free Flight implementation, traffic will have grown by 140%, and by 2010 aircraft traffic will have doubled. Thus, we have chosen to evaluate the operational requirements needed for initial Free Flight using 140% traffic statistics, and the operational requirements for mature Free Flight using 200% traffic statistics. Traffic that are not included are military, cargo, and general aviation. International traffic flying outside North America also was not modeled. Their effect will be modeled in future studies. Most general aviation flights cruise at altitudes below FL240, the lowest altitude used in our study.

Statistically valid results are obtained using several Monte Carlo runs for all data sets. For each run, the departure times in the traffic schedule are varied. Sufficient runs are made to obtain consistent results.

3.2 Simulation Study Results

In this section the simulation results are presented. Results are shown for the 1995 benchmark study, and four free flight concepts: Baseline free flight, Baseline plus RVSM, baseline free flight with user preferred flight levels (En Route UPT), and En Route UPT plus RVSM. The studies show how the number of encounters change as traffic increases and as each free flight environment is introduced. For these studies an encounter is counted whenever an aircraft pair CPA is less than 10 nm. The

data from these studies are used to drive the operational requirements presented in Section 3.3, and to select preferred concepts for further study.

3.2.1 1995 Benchmark Study (Current NAS System)

This section gives the results from the 1995 benchmark simulation and establishes the relationships that hold for all studies.

The number of encounters per sector during a one day period are shown in Figure 12. The encounters are plotted hourly for each of the ten high altitude sectors in the Cleveland ARTCC (See Figure 9). An examination of the individual sector data shows considerable variation in the daily distribution of peak period encounters. Consequently, the total number of encounters over all sectors was used in this study to benchmark center workload. The number of encounters by hour for all sectors is illustrated in Figure 13. The morning peak is from 7 AM to 8 AM and the evening peak is from 5 PM to 6 PM.

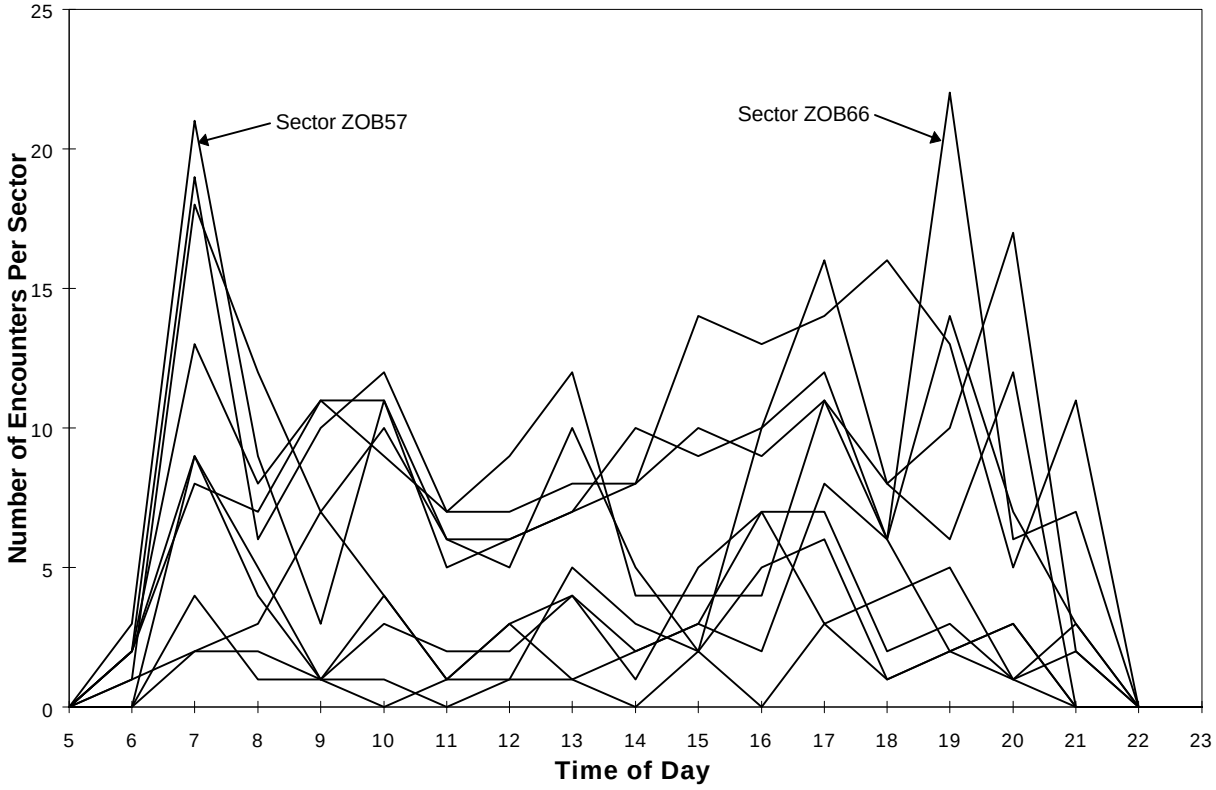

Figure 12: Benchmark Encounter Statistics Per Sector Per Hour

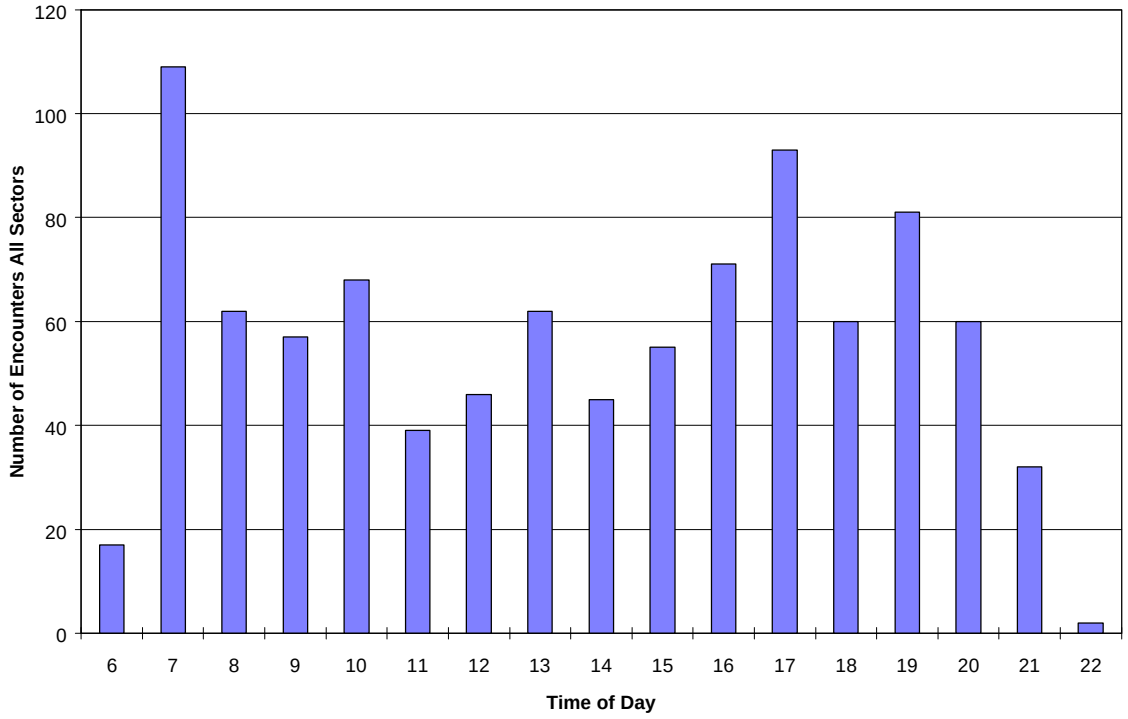

Figure 13: All Sectors Benchmark Hourly Encounters

Our measure of sector workload is based on the benchmark encounters during peak periods. Thus each free flight concept is examined over all hours and during the peak hours. For the Cleveland benchmark, the average sector peak workload is about ten encounters per hour. The busiest sectors experience about twice this rate.

3.2.2 Benchmark Encounter Statistics

The data presented in this section characterizes encounters by flight phase and type. The types of encounters are defined as in-trail, crossing, or opposing. A controller will handle each encounter differently depending on the type. An in-trail conflict develops slowly and a controller has more time to analyze the developing conflict and to resolve it. Crossing and opposing conflicts develop more rapidly and a controller has less time to analyze and resolve these types. The type of resolution action a controller takes for a crossing conflict may be different from an opposing conflict. The situation is even more complex when phase of flight is considered. The phases of flight for this study are climb, cruise, and descent.

The break down of encounters by type is shown in Table 8.

Table 8. Benchmark Encounters By Type

	Morning Peak	Evening Peak	All Hours
All Types	109	93	967
In-Trail	45	44	448
Crossing	34	20	274
Opposing	29	29	244

The benchmark encounters by flight phase and type are shown in Table 9.

Table 9. Encounters By Flight Phase and Type - All Hours

	Climb-Climb	Climb-Descent	Climb-Cruise	Cruise-Descent	Descent-Descent	Cruise-Cruise	Total
All Types	53	129	307	236	74	166	967
In-Trail	14	47	110	104	37	135	448
Crossing	19	44	85	72	22	30	274
Opposing	19	38	111	60	14	0	244

The data in these tables are averaged over several Monte Carlo runs to increase the number of samples and to remove some statistical uncertainties. Runs are varied by changing the departure times in the simulation schedule. The encounters are totaled for all sectors. Table 8 shows that the peak period and the all hours encounter data are consistent, i.e. the in-trail encounters predominate in each case, and the crossing and opposing encounters are roughly equal in magnitude.

The data in Table 9 further categorizes these encounters by flight phase. The four plots in Figures 14 to 17 illustrate the data in Table 9. The plots show the phases of flight that are most prevalent for each type of encounter. In Figure 14 the plot of all types reveals that encounters mainly involve at least one of the pair being in cruise mode. The in-trail type of encounter shown in Figure 15 usually involves at least one cruise aircraft (cruise-cruise, climb-cruise, descent-cruise), whereas crossing and opposing encounters (Figures 16,17) mainly involve climbing and descending aircraft (climb-cruise, descent-cruise, climb-descent). It may be noted that there are no cruise-cruise opposing encounters due to the east-west cruise altitude constraints.

3.2.3 Benchmark Sensitivity Studies

This section presents two benchmark sensitivity studies: the scaling law for close encounters, and the effect of procedural controls on encounters.

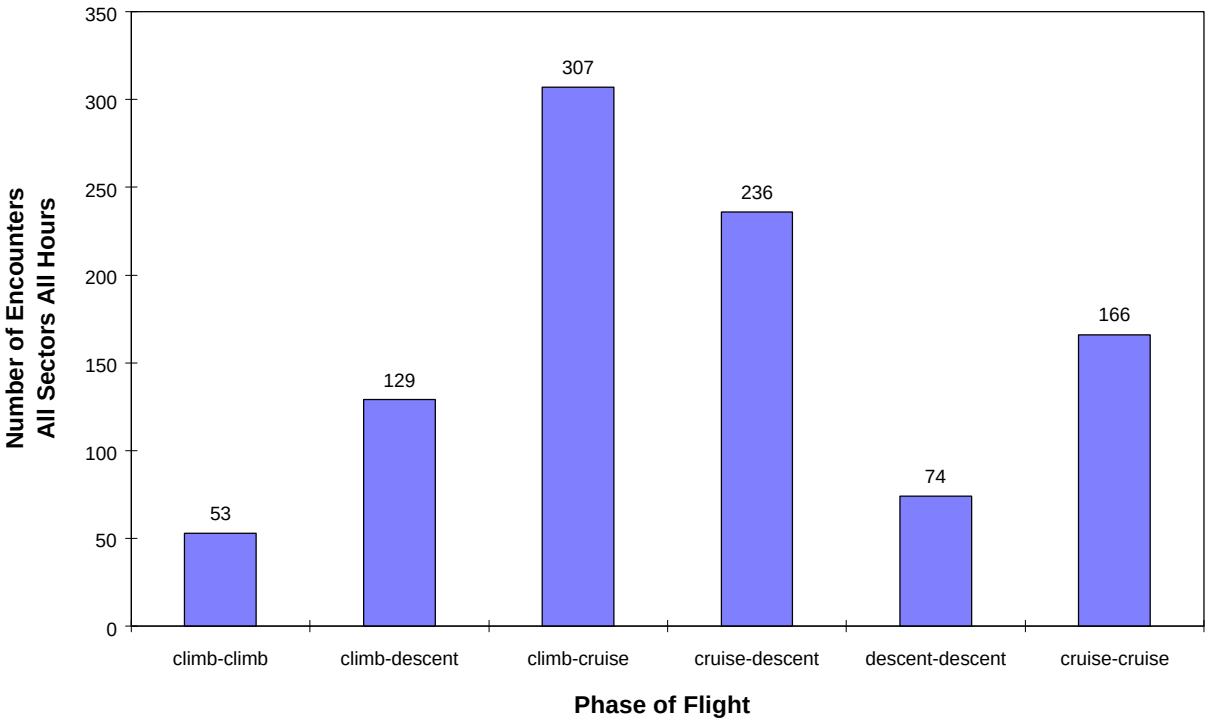

Figure 14: Benchmark Encounters By Flight Phase - All Types

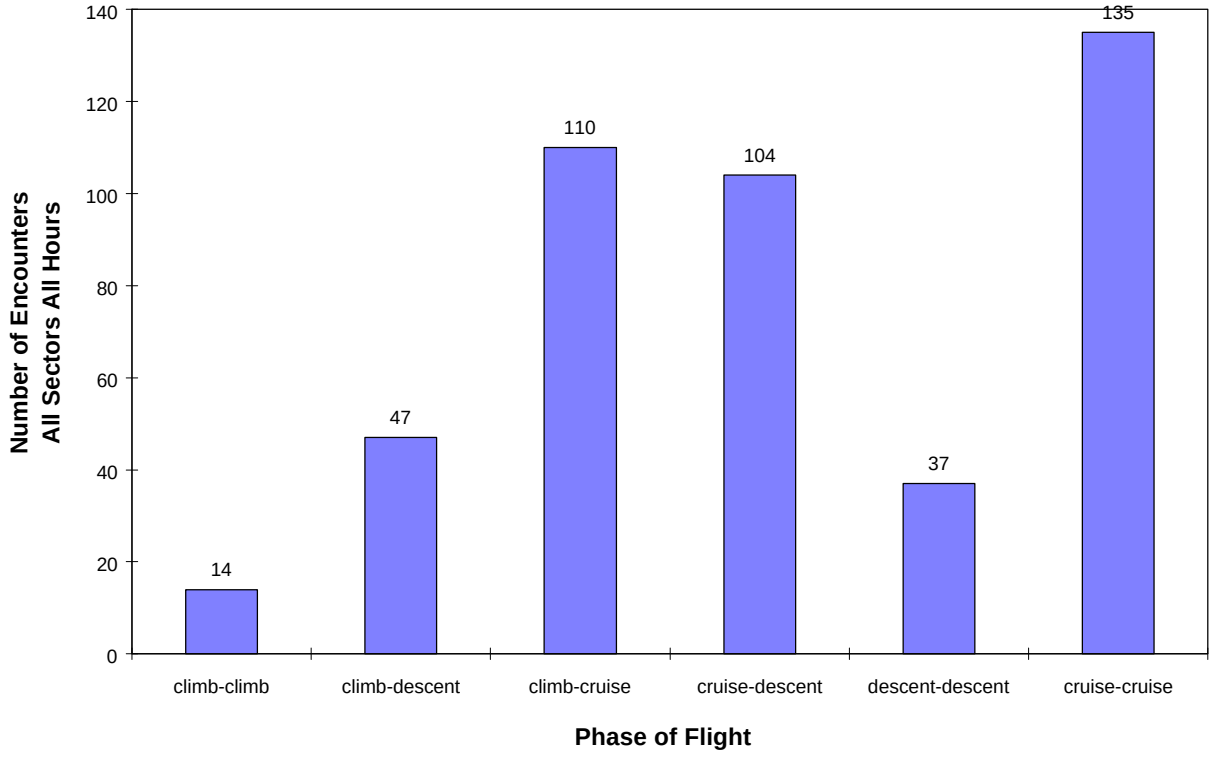

Figure 15: Benchmark Encounters By Flight Phase - In-Trail Type

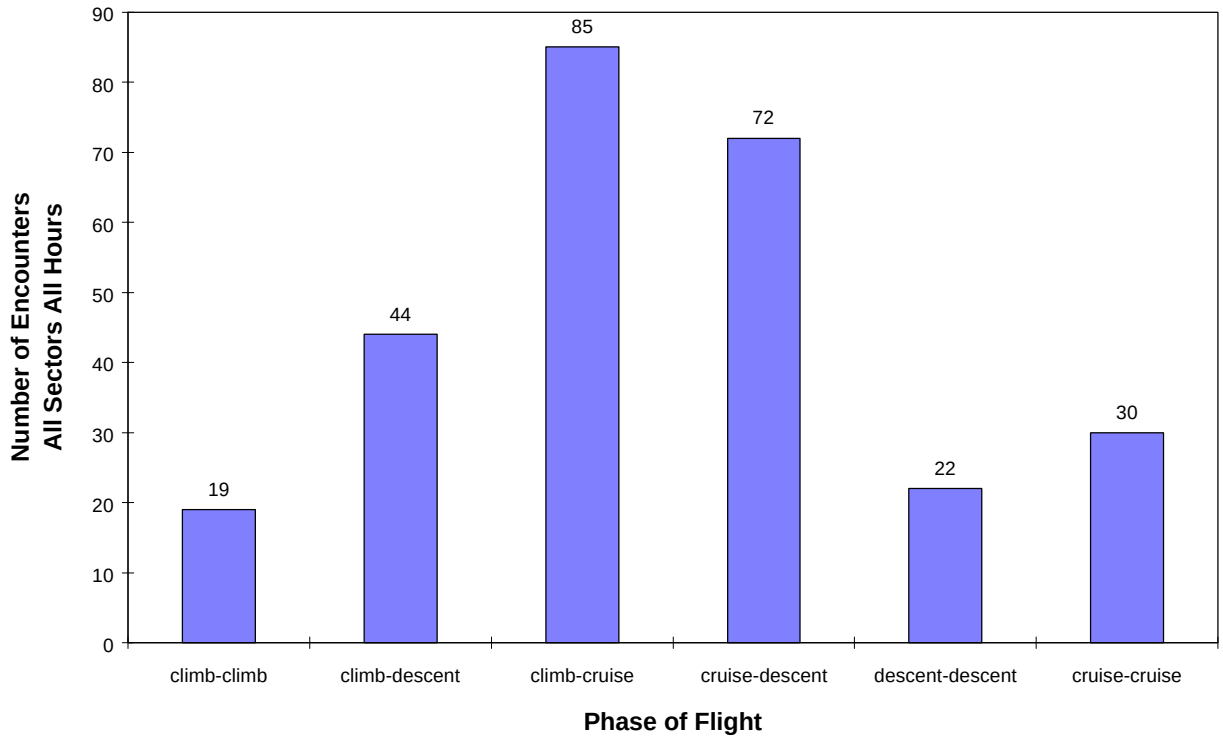

Figure 16: Benchmark Encounters By Flight Phase - Crossing Type

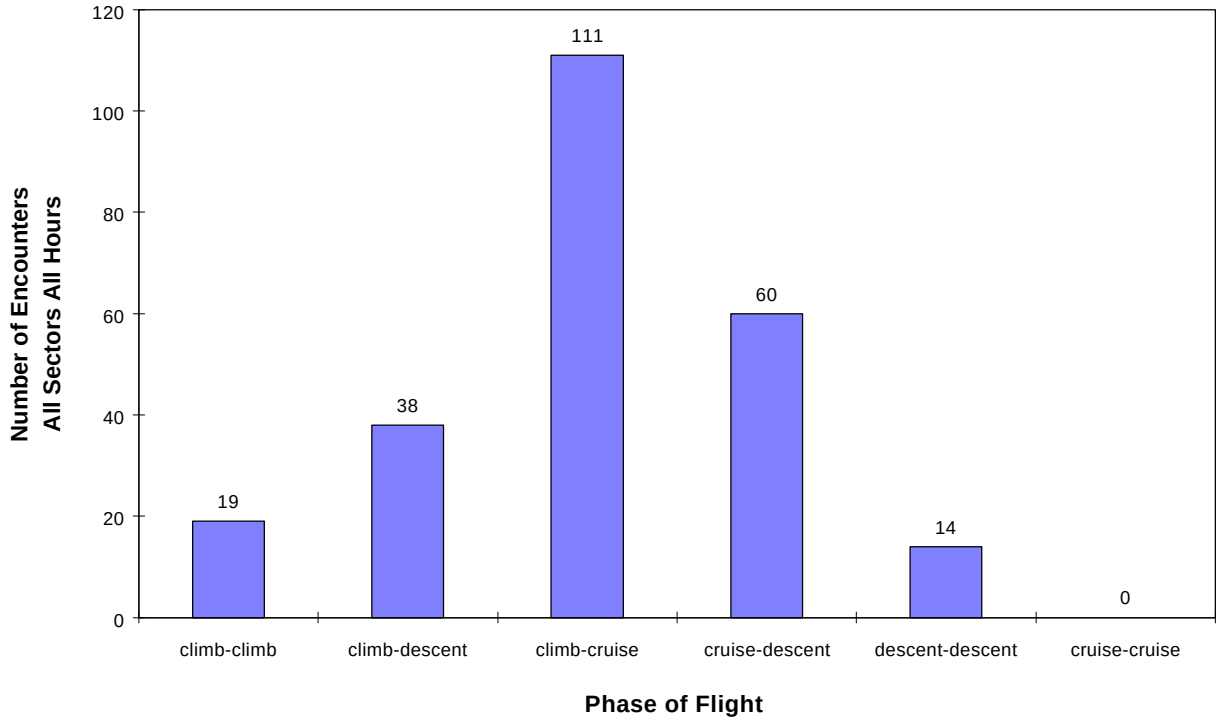

Figure 17: Benchmark Encounters By Flight Phase - Opposing Type

The scaling law for encounters defines the relationship between number of encounters and the Closest Point of Approach (CPA) between aircraft. As the CPA separation decreases the number of encounters decreases. This relationship is depicted in Figure 18 for all hours and in Figure 19 for the peak hours. For each data point the cumulative number of encounters is shown for encounters with less than the CPA distance. In both figures, the number of encounters is approximately proportional to the closest approach distance and increases somewhat more than linearly for CPA > 6 nm[1]. This implies that reducing horizontal separation has at least a proportional effect in reducing encounters and tactical interventions.

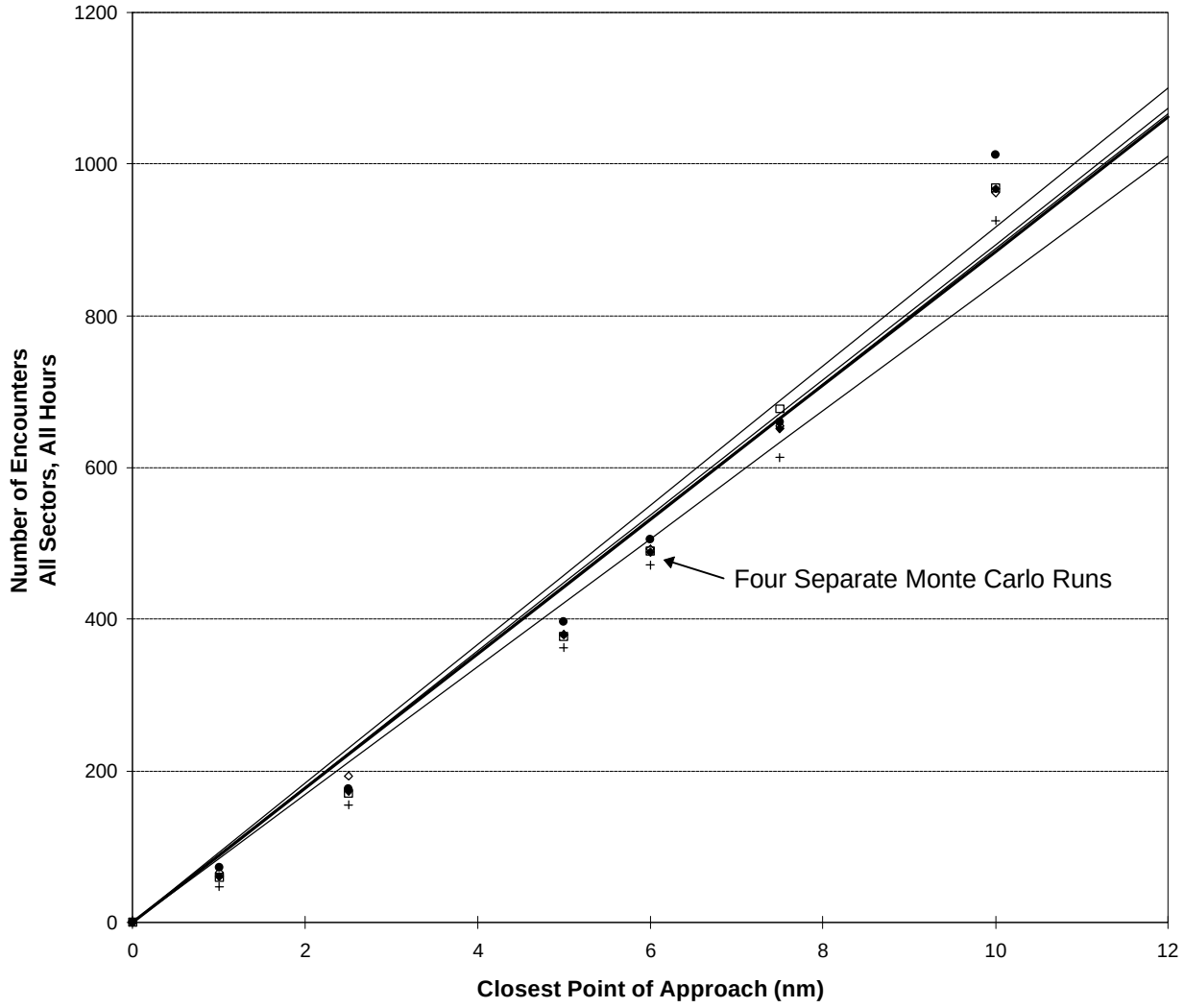

Figure 18: Scaling Law For Close Encounters - All Sectors, All Hours

[1] More recent studies show that the number of conflicts is approximately proportional to CPA raised to the 4/3 power, i.e. the number of conflicts increases 2.5 fold when CPA doubles.

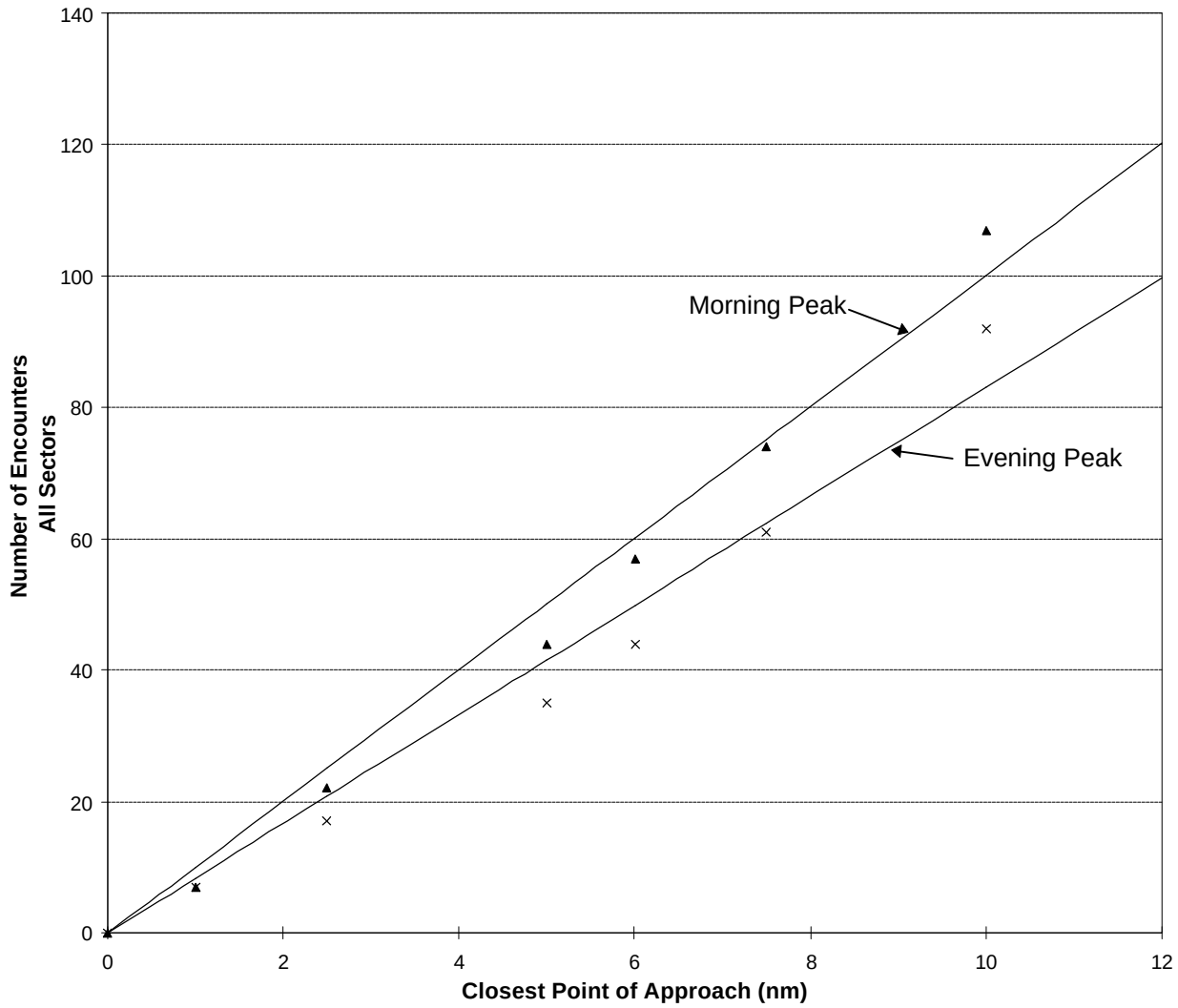

Figure 19: Scaling Law For Close Encounters - Morning and Evening Peaks

In the benchmark case there are procedural controls that limit the free flow of aircraft, and also limit the number of encounters. One procedural control is the arrival and departure constraints placed on aircraft operations in terminal areas. As aircraft approach a terminal area they transition from the en route to terminal area using procedures designed to separate arrivals from departures and to regulate flow into the airports. In the benchmark these procedures are not explicitly modeled. Instead, encounters between arrivals and departures to the same airport are removed from the encounter list. Allowing aircraft to fly unconstrained in the terminal area increases the number of encounters. The differences are shown in Figure 20. The effect is a substantial increase in the number of opposing conflicts between arriving and departing aircraft. Note that these encounters are all still at high altitudes, FL240 or above. The effect of removing terminal constraints will be much greater for low altitude sectors.

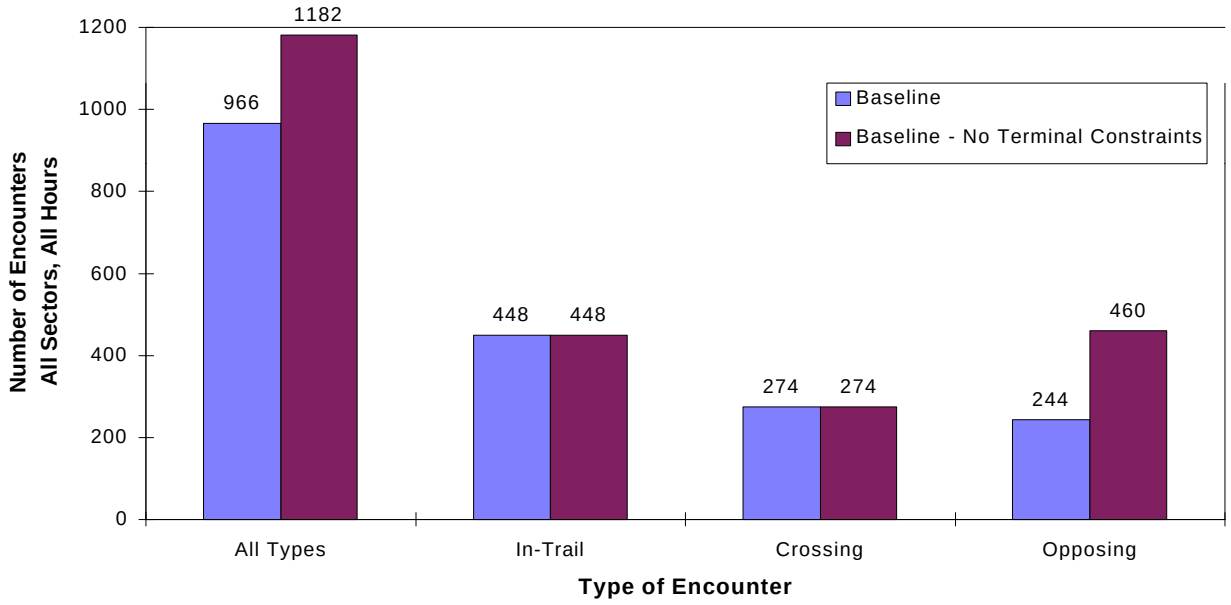

Figure 20: Effect of No Terminal Constraints

Another procedural control placed on current traffic is the segregation of cruise altitude based on direction of flight. Flights flying east are given cruise altitudes that differ from those flying west by at least 1000 feet (2000 feet above FL290). In a free flight environment aircraft would choose their cruise altitude based on optimum performance for the aircraft type, not on direction of flight. Removing the segregated altitude restriction greatly increases the number of encounters. The differences are shown in Figure 21. The biggest impact is in the increased number of opposing conflicts, i.e. more than three times as many opposing conflicts as in the benchmark case!

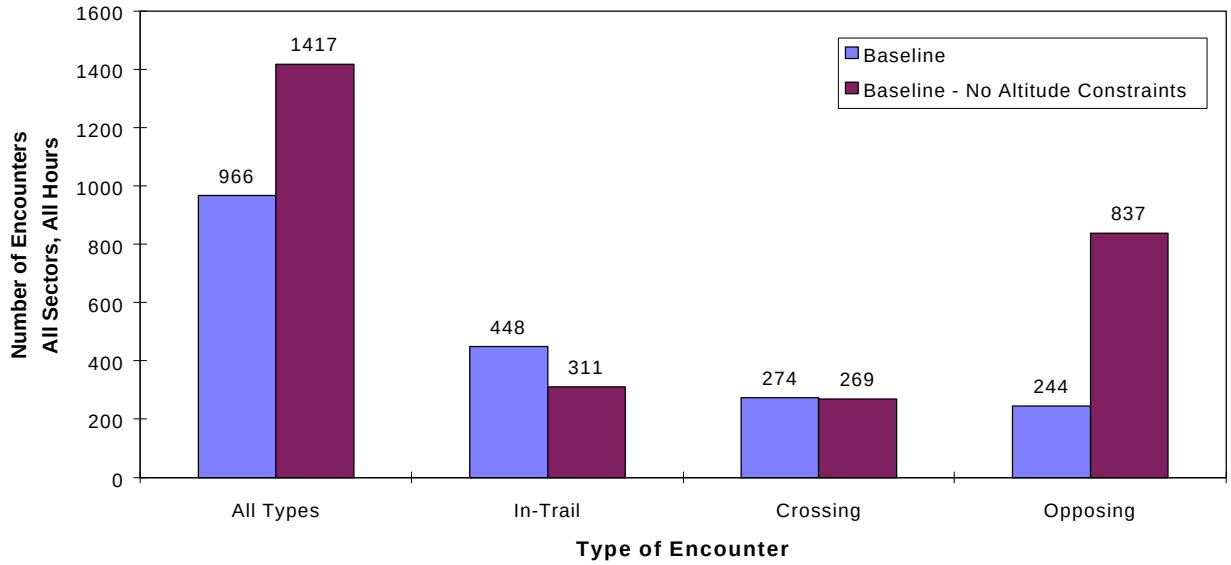

Figure 21: Effect of No Altitude Constraints

These studies illustrate the challenge in moving from procedural, constrained flight to less-constrained free flight concepts. As we remove flight restrictions, we must simultaneously reduce separation standards and potential conflicts in order to manage encounters, while maintaining or improving current safety margins.

3.2.4 Free Flight Studies - Baseline Concept

Initial free flight operations are expected to begin by the year 2002. It is assumed in this time period that the surveillance system will be radar based, but incrementally upgraded for free flight operations. The simulation studies carried out for this report assume that initial free flight will be constrained to limit the number of encounters and the controller intervention rate.

The Baseline free flight concept assumes direct routing in the en route phase, but includes terminal area constraints and en route altitude constraints to reduce aircraft conflicts. Terminal area constraints will reduce the number of conflicts between arrivals and departures to or from nearby airports. Altitude constraints will reduce the number of conflicts between opposing traffic in the en route phase of flight. Terminal area constraints control the flight profile that an aircraft follows to arrive or depart at an airport. They are needed to limit the number of arrival and departure conflicts and also to allow controllers to set up an efficient arrival stream of traffic. Flight profiles are constrained by terminal area entry and exit points that are typically located 30 nm or more from the airport. With the Baseline concept, aircraft can fly direct routes or optimum wind routes between terminal exit and terminal arrival points.

In our TAAM simulation aircraft fly direct to the airport. Terminal area procedures are not simulated, but their effect is modeled by removing encounters between arrival and departures at the same airport. Cruising altitudes are constrained by maintaining a segregated altitude structure between east bound and west bound flights.

Figure 22 shows the increase in encounters as traffic increases from 100% to 200% of the 1995 benchmark traffic. As traffic increases 40% the number of encounters increases 86%. The relationship between the number of encounters and traffic load is nearly quadratic, i.e. doubling the traffic increases the encounters almost four-fold. Such increases will necessitate major changes in the NAS system to manage the increased traffic load. The operational requirements to manage such traffic growth is addressed in Section 3.3.

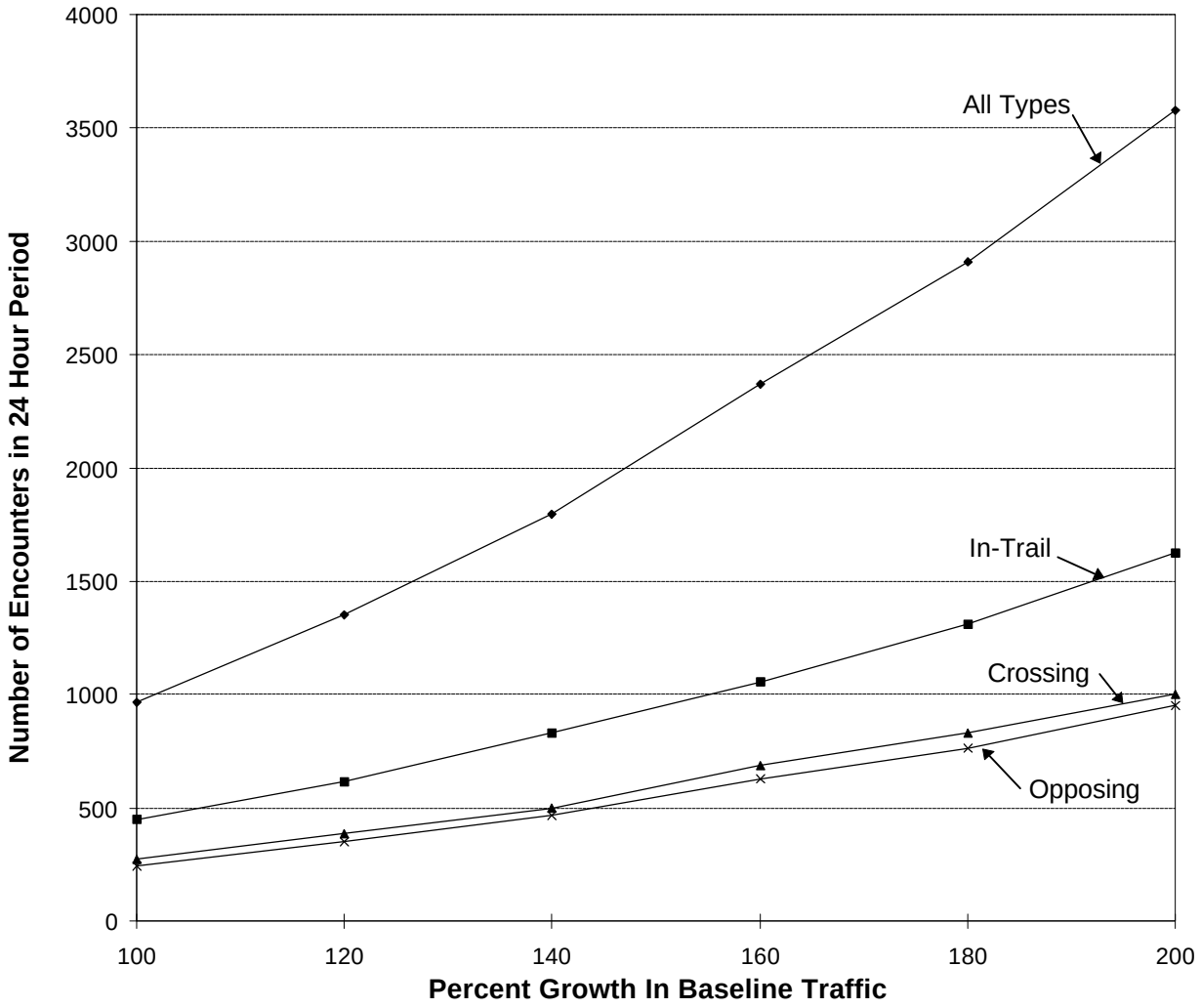

Figure 22: Growth Statistics - Baseline Free Flight

Figure 22 also shows that the predominate encounter type with the baseline concept is in-trail with crossing and opposing types composing a smaller portion of the total encounters. The number of opposing encounters is limited because opposite direction flights are separated procedurally by alternate flight levels. Since the in-trail type of encounter is presumed to be easier to resolve and because it is the predominate type of encounter, it should be relatively easy for controllers to adjust to the Baseline free flight environment. The challenge is in reducing the number of conflicts and distributing workload, e.g. use of a conflict probe to detect and resolve most potential conflicts before they become a concern to the sector controller.

Further analysis of the Baseline encounters has shown that these mainly involve one or more climbing and descending aircraft. This implies that climbing and descending path predictions need to be adequately modeled for accurate conflict predictions.

3.2.5 Free Flight Studies - Baseline Plus RVSM

The Baseline free flight plus RVSM concept allows direct routing in the en route phase and reduction of altitude separation above FL290 from 2000 feet to 1000 feet, but includes terminal area constraints and en route altitude constraints.

The modeling of the Baseline plus RVSM concept in TAAM is the same as in the Baseline free flight simulation, but includes additional cruise altitudes above flight level 290. The number of aircraft assigned the same cruise altitude above FL290 is cut in half, reducing the number of potential encounters. Cruising altitudes are still constrained by maintaining a segregated altitude structure with east bound flights using alternate altitudes from the west bound flights. However, same direction flights are within 2000 feet of the next available altitude.

Figure 23 shows the increase in encounters as traffic increases from 100% to 200% of the benchmark. As traffic increases 40%, the number of encounters increases 69%. However, compared to Baseline free flight, the number of encounters are greatly reduced by implementing RVSM. Examination of the encounter data shows that the reduction occurs mainly in encounters involving cruising aircraft. Climb / cruise encounters are reduced, for example, since the vertical separation for counting an encounter has been reduced by a factor of two.

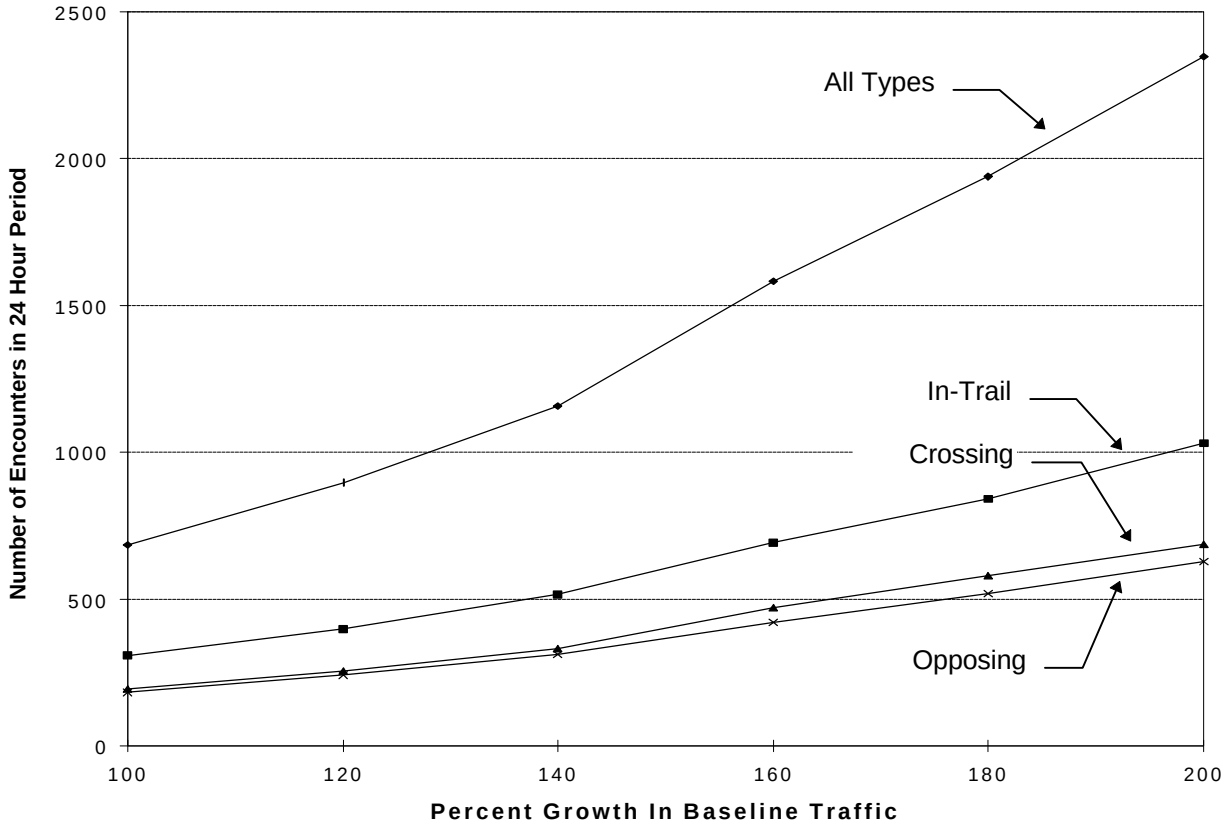

Figure 23: Growth Statistics - Baseline Free Flight Plus RVSM

One caveat to these results is that the encounter statistics assume perfect knowledge of the actual aircraft paths. In practice, interventions are based on trajectory predictions with significant path uncertainty errors. In order to reduce interventions involving climbing and descending aircraft, it may be necessary to also reduce the vertical path surveillance errors, i.e. implementing RVSM without reducing path uncertainty is unlikely to yield a significant reduction in interventions. One method to reduce vertical path uncertainty is to use ADS broadcast of altitude and altitude rate, enhancing the ability to predict level crossings of potentially conflicting aircraft.

3.2.6 Free Flight Studies - En Route User Preferred Trajectories (UPT)

In this section we examine two mature free flight options where en route altitude restrictions are removed. The first option is En Route UPT (without RVSM). The second option is En Route UPT plus RVSM.

The En Route UPT concept allows direct routing in the en route phase and removes the alternating altitude structure for east and west traffic, but still includes 2000 foot flight levels above FL290. It also includes terminal area constraints. Removing altitude constraints increases the number of conflicts between opposing traffic in the en route phase of flight, but gives the user the benefit of selecting a more fuel optimum altitude. The implementation of En Route UPT will also require additional infrastructure to manage the en route opposing conflicts.

The modeling of the En Route UPT concept in TAAM is the same as the Baseline free flight simulation, but allows east and west traffic to mix at all cruise levels. Aircraft previously assigned to one altitude are separated evenly between two altitudes with half of the aircraft remaining at the same altitude and the other half using the next lowest altitude. The number of aircraft at each en route altitude remains the same, but now there are aircraft cruising in opposite directions at the same altitude.

Figure 24 shows the increase in encounters as traffic increases from 100% to 200% of the benchmark. The opposing conflicts dominate this case, with about three times as many opposing encounters compared to crossing or in-trail encounters. Compared to the Baseline free flight and Baseline plus RVSM studies, the total number of encounters has also greatly increased. (See Figure 26).

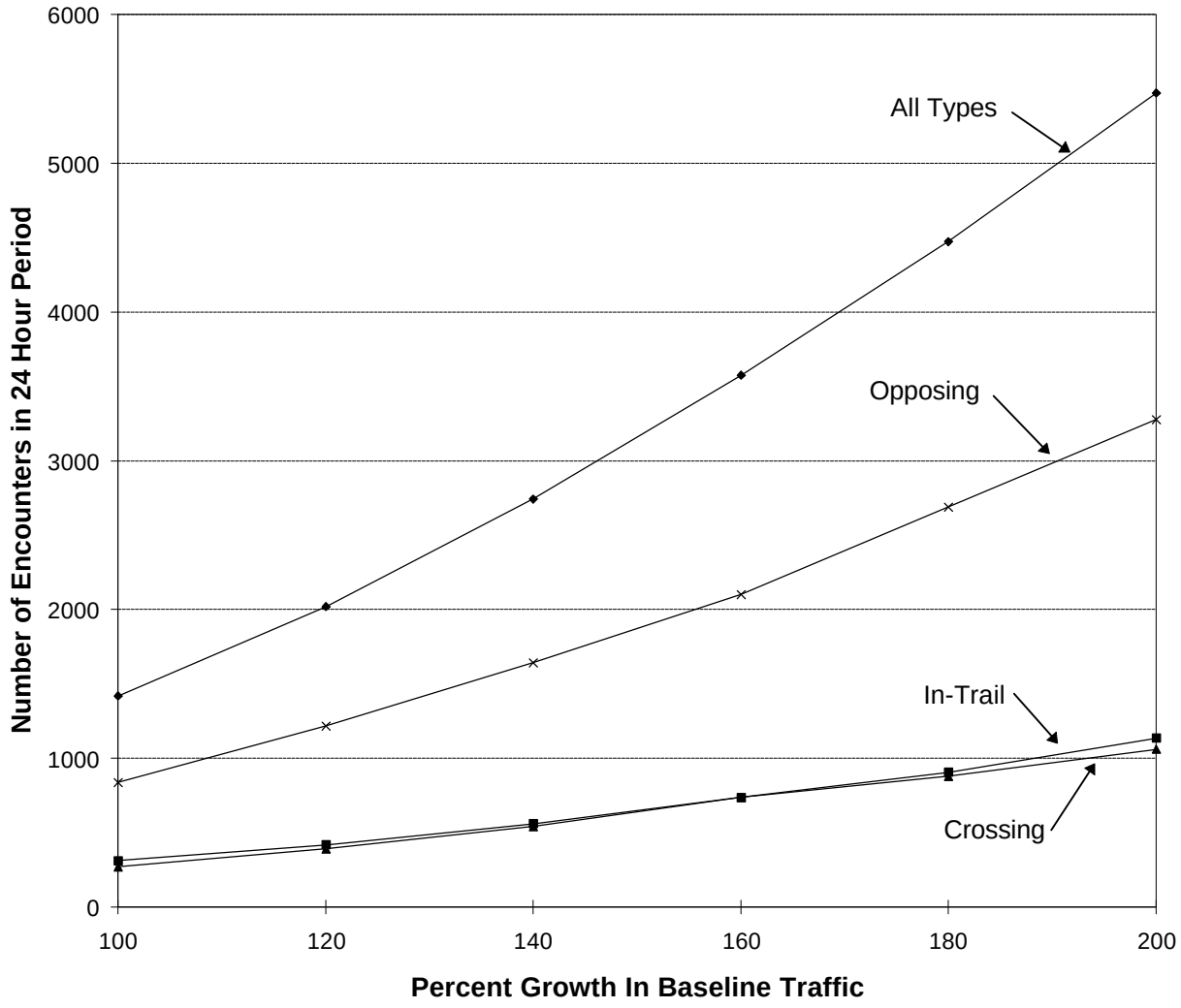

Figure 24: Growth Statistics - En Route UPT

Interviewed controllers have indicated that opposing encounters are much harder to deal with than in-trail encounters, since the time scale for conflict resolution is greatly compressed. In both the Baseline free flight and Baseline plus RVSM concepts, the predominate encounter type is the in-trail encounter. The challenge in implementing the En Route UPT concept is not only to reduce the number of conflicts, but also to resolve more difficult opposing encounters.

The second mature free flight option is En Route UPT plus RVSM. The user benefits are the same as En Route UPT. However, the number of aircraft at the same cruise altitude above FL290 is now cut in half, reducing the number of potential encounters. The results are shown in Figure 25. The number of encounters is significantly reduced from En Route UPT and is even lower than the number of encounters in the Baseline free flight option. However, en route opposing encounters predominate.

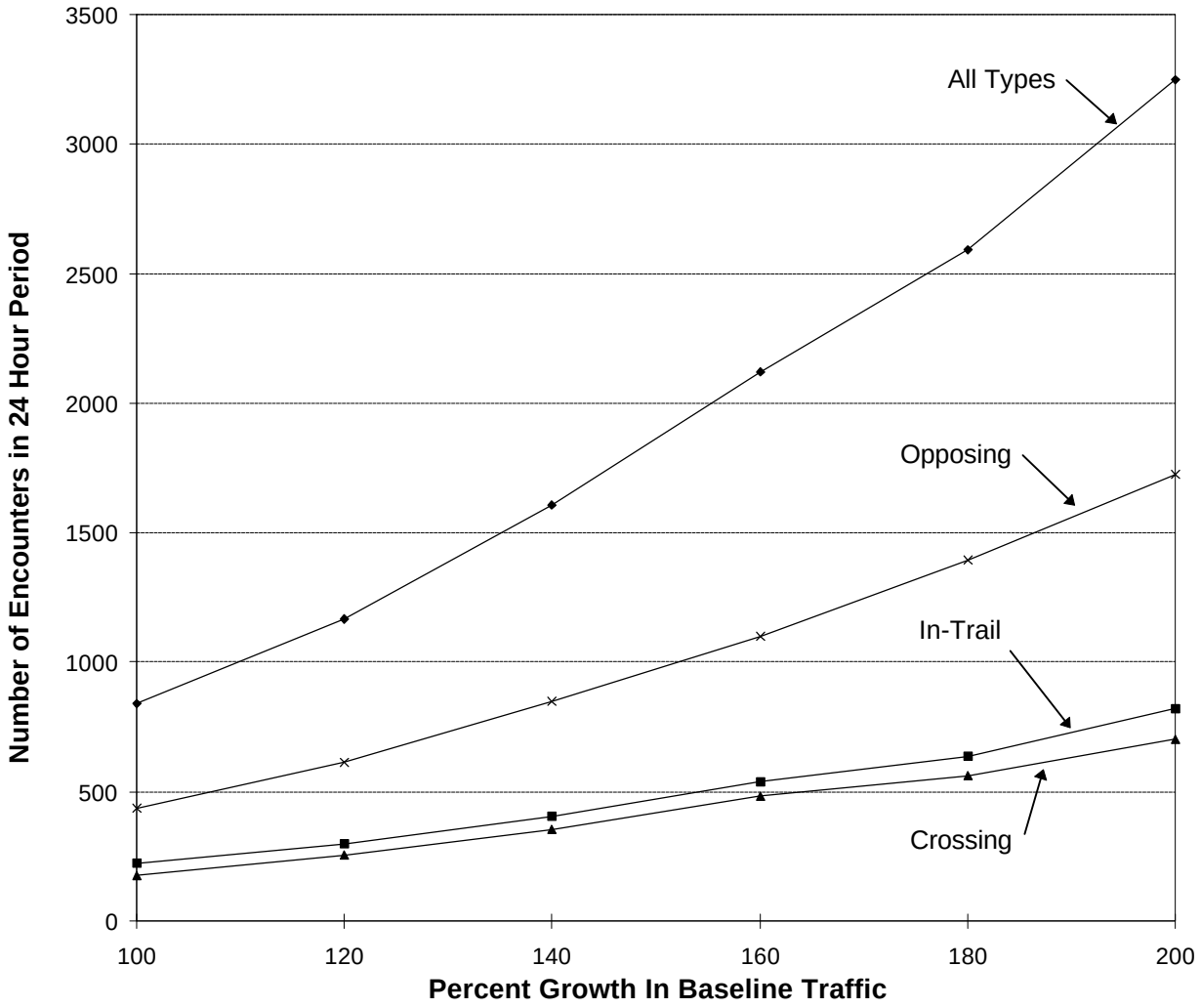

Figure 25: Growth Statistics - En Route UPT Plus RVSM

3.2.7 Summary

A total of five operational concepts have been considered: the benchmark system of today's environment, Baseline free flight, Baseline plus RVSM, En Route UPT, and En Route UPT plus RVSM.

For comparison the results of the four free flight options are shown in Figure 26. The figure shows the growth rate in encounters for the four free flight options. The options with the highest number of encounters will require the lowest separation minimums to manage intervention frequency. The relationship between growth in traffic and number of encounters is nearly quadratic for all four scenarios. The number of encounters for the benchmark study is the first point of the baseline free flight curve, about 1000 encounters. The operational requirements to implement free flight and still maintain benchmark encounter levels is explored in the next section.

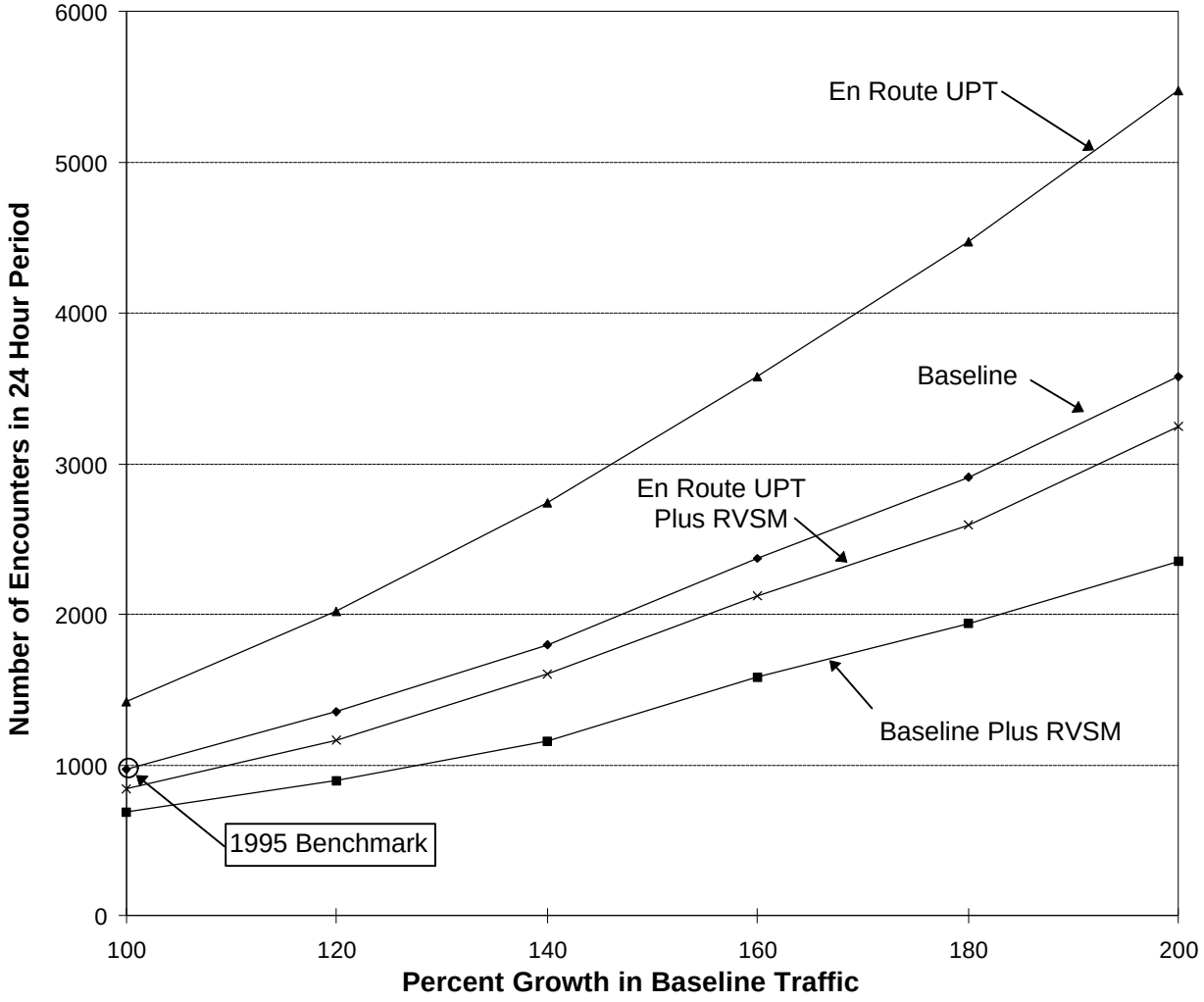

Figure 26: Growth Statistics - Four Free Flight Options

Table 10 summarizes the expected growth in encounters as traffic grows. Data is shown for all hours. Tables 11 and 12 show the expected growth in encounters for the morning peak and the evening peak respectively. We will use these tables in Section 3.3.

Table 10. Projected Growth of Encounters - All Hours

Traffic Growth	Baseline Free Flight	Baseline Plus RVSM	En Route UPT	En Route UPT Plus RVSM
100%	967	685	1418	842
140%	1795	1158	2744	1606
200%	3578	2349	5474	3248

Table 11. Projected Growth of Encounters - Morning Peak

Traffic Growth	Baseline Free Flight	Baseline Plus RVSM	En Route UPT	En Route UPT Plus RVSM
100%	109	85	157	98
140%	182	111	22	163
200%	358	226	531	295

Table 12. Projected Growth of Encounters - Evening Peak

Traffic Growth	Baseline Free Flight	Baseline Plus RVSM	En Route UPT	En Route UPT Plus RVSM
100%	93	61	158	92
140%	176	115	298	169
200%	354	230	596	361

3.3 Operational Requirements and Preferred Free Flight Transitions

The basic idea in this section is to determine system requirements such that the number of interventions for initial and mature Free Flight operations does not substantially exceed that for the 1995 benchmark. The assumption here is that the ATC workload in busy Centers is already maximized for the number of ATC controllers employed, i.e. that controllers are currently workload saturated in the operations they can handle in peak traffic. This section normalizes the total number of interventions for each Free Flight concept by applying reduced separation minimums which will limit the growth in Center operations and intervention frequency to that of the current system.

In the current NAS system, the horizontal separation standard for en route radar control is 5 nm. However, controllers will typically not intervene when the predicted CPA of an encounter is more than 10 nm, and will intervene when the predicted CPA is less than

10 nm to assure safe separation including path prediction errors such as radar errors and uncertainty in aircraft intent. The effective threshold above which a controller (or conflict alerting process) will **not** intervene is very important for Free Flight operations and is here called the **intervention standard**, in contrast with the separation standard. For the benchmark system, all the encounters examined previously would precipitate a tactical intervention to assure safe separation. One factor which we have ignored in our studies is the uncertainty in predicting aircraft altitude, i.e. the number of interventions could be much larger than the number of encounters, since the altitude buffer for interventions may be several times that of the vertical separation standard. (Future simulation studies would explicitly address this issue. See section 5.)

If the number of interventions are to be limited as traffic grows, then the intervention threshold must shrink to compensate for increased traffic encounters. If we compare the number of benchmark encounters (section 3.2.2) with the number of interventions allowed for Baseline operations with 140% traffic growth (section 3.2.7), we find that the number of interventions needs to be scaled by approximately 1000 / 1800 ~ 56%. Using the linear scaling law relating number of close encounters to CPA distance, we see that this is equivalent to reducing the intervention threshold for moving aircraft from 10 nm to about 5.5 nm. However, for current operations we made the simplifying assumption that all encounters with less than 10 nm CPA would create an ATC intervention, and all encounters greater than 10 nm would not. Thus, the reduction from 10 to 5.5 nm CPA is for a deterministic threshold based on zero sensor error, whereas an operational conflict detection system (manual or automated) has an uncertainty band defining the CPA region where most conflict detections occur.

Below we translate the number of interventions for the four Free Flight transition concepts into deterministic CPA thresholds, and then select uncertainty bands based on CNS assumptions to obtain specific separation requirements for the various options.

From the traffic intervention data in the previous section we derive the following values for the required CPA threshold corresponding to Initial and Mature Free Flight, and for Baseline, Baseline plus RVSM, En route UPT, and En route UPT plus RVSM:

Table 13. Deterministic CPA Thresholds for Proposed Free Flight Concepts

	Baseline	Baseline + RVSM	En route UPT	En route UPT + RVSM
Initial Free Flight (140% Traffic)	10* 970 / 1800 ~ 5.5 nm	10 * 970 / 1160 ~ 8.0 nm	10 * 970 / 2740 ~ 3.5 nm	10 * 970 / 1600 ~ 6.0 nm
Mature Free Flight (200% Traffic)	10* 970 / 3580 ~ 2.5 nm	10 * 970 / 2350 ~ 4.0 nm	10 * 970 / 5470 ~ 1.8 nm	10 * 970 / 3250 ~ 3.0 nm

We now translate the deterministic thresholds into separation assurance parameters. Figure 27 shows a notional sketch of the assumed detection probability for deterministic thresholding with no prediction errors, and for an operational conflict

detection process. It is required for an operational system to detect almost all of the conflicts where the CPA is less than the separation standard, and to declare conflicts on at most a few percentage of the encounters where the CPA exceeds the intervention standard, i.e. unnecessary alerts or false alarms. As a first approximation, we assume that the detection probability falls off linearly as CPA increases from the separation standard to the intervention standard, as shown in Figure 27. Then the total number of interventions for an operational system is approximately the same as that with a deterministic threshold placed at the midpoint of the CPA uncertainty region, i.e. the deterministic threshold is approximately equal to the average of the separation standard and the intervention standard.

For the Baseline flight option with an implementation date of 2002, we can allow an uncertainty band of 3.5 nm for the CPA uncertainty region, assuming fusion of Radar and Flight Plan data for path predictions. Using a deterministic threshold of 5.5 nm from Table 13 and placing this threshold near the center of the CPA uncertainty region yields a separation standard of 4 nm and an intervention threshold of 7.5 nm. In other words, if almost all of the encounters with CPA less than 4 nm are detected, and all but a few percent of the encounters with CPA greater than 7.5 nm are not , then the total number of interventions is roughly equivalent to a deterministic threshold of about 5.5 nm. In this case the separation standard reduces from 5 nm with the current system to 4 nm with Initial Free Flight, and the uncertainty band for conflict decisions shrinks from 5 nm to 3.5 nm.

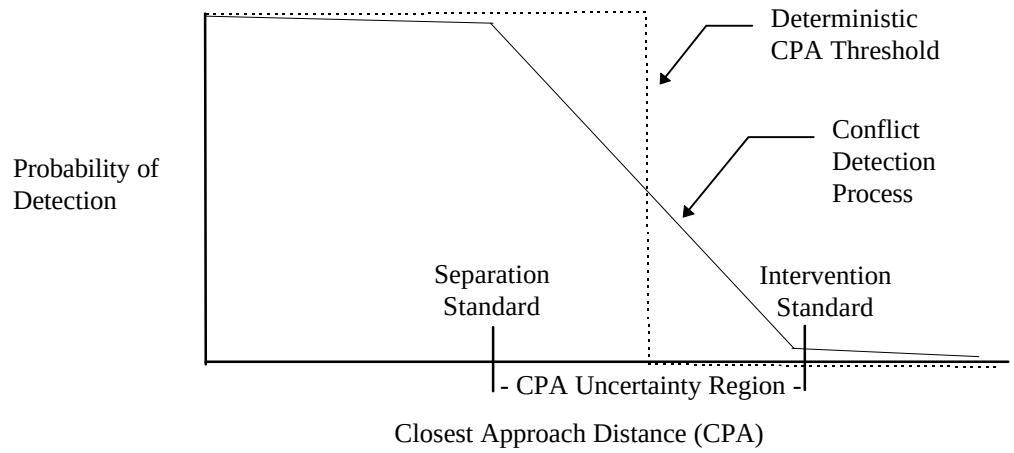

Figure 27: Sketch of Conflict Detection Thresholding Values

Now from Table 13 we obtain the following (non-unique) separation assurance requirements for Initial and Mature Free Flight, for the Free Flight Options above:

Baseline Flight

Initial Free Flight (2002) - 4 nm separation standard
7.5 nm intervention standard

Mature Free Flight (2010) - 2 nm separation standard
3.5 nm intervention standard

Baseline Plus RVSM

Initial Free Flight (2002) - 5 nm separation standard
10 nm intervention standard

Mature Free Flight (2010) - 3 nm separation standard
5 nm intervention standard

En route UPT

Initial Free Flight (2002) - 3 nm separation standard
4.5 nm intervention standard

Mature Free Flight (2010) - 1.5 nm separation standard
2.0 nm intervention standard

En route UPT plus RVSM

Initial Free Flight (2002) - 4 nm separation standard
8 nm intervention standard

Mature Free Flight (2010) - 2 nm separation standard
4 nm intervention standard

These parameters have been chosen based on examining the RNP requirements for lower separation standards and the effective CPA uncertainty band for 15 min flight predictions. For example, the separation standard should be at least 3-4 times the RNP Navigation accuracy for 95th percentile error containment. (The RGCS Panel assumes a separation of at least 7 times the RNP with adequate monitoring for lateral separation (Ref. 11). This is interpreted here as the intervention standard.) Since the rule-making bodies (RTCA, ICAO, etc.) are only now analyzing the en route separation requirements for RNP-1 precision navigation systems, it was felt that RNP-1 is the most accurate system certifiable for en route operations in the near future, and that separation standards less than 3 nm would not be feasible for Initial Free Flight.

We now consider which of these options are preferred for further analysis. For the Initial Free Flight implementation, the Baseline option is preferred compared to the other options in terms of needed infrastructure. This is because the Baseline option can be implemented using existing radar technology for surveillance, whereas we will need data-link and some form of ADS reporting for implementing the other options. (In particular, the conflict probe studies in the next section will show that with radar improvements we can reasonably expect to obtain CPA uncertainty bounds on the order of 3 - 4 nm, but to obtain uncertainty bounds on the order of 2 nm or less and satisfy reasonable lookahead constraints will require more accurate ADS based surveillance.) The Baseline option will require precision navigation (RNP-1) in order to accommodate opposing traffic conflicts, and will require substantial improvements to the radar tracking system, and implementation of several Center automation functions in order to accommodate a 4 nm separation standard and shrink the intervention standard to 7.5 nm. However, there is not a high risk in implementing these improvements since all the basic technologies are currently in place. Consequently, we have selected the Baseline flight concept with the above horizontal separation parameters for the Initial Free Flight transition.

The preferred Free Flight concept may change significantly, however as we move towards mature Free Flight, and traffic growth necessitates further reduction in separation standards. In order to implement a 2 nm separation standard and 3.5 nm intervention standard for the Baseline Free Flight concept, significant changes in both the surveillance system and in resolution of conflicts would be needed. The most significant changes are the addition of ADS surveillance to reduce the uncertainty in CPA geometry, and the implementation of an Alert Zone concept and associated Free Flight path restrictions. The problem with the Baseline concept for mature Free Flight is that even with significant changes in onboard avionics and onboard situation awareness, cruise altitudes remain limited to 4000 foot discrete steps above FL290. Consequently, it makes sense to implement RVSM when the transition to ADS occurs, as a system-wide infrastructure upgrade. Alternately, one can transition from the Baseline Free Flight system to an En route UPT system with no cruise restrictions and with a simultaneous transition to ADS surveillance and Alert Zone path restrictions.

The preferred next step to Free Flight is the Baseline Plus RVSM concept, since it has the greatest economic value for users, with the least reduction in separation parameters to accommodate future traffic growth. By contrast the Baseline and En route UPT Free Flight concepts will either require more costly infrastructure or will have less safety margin since their separation parameters are significantly smaller. However, the Baseline plus RVSM concept requires that **all airspace users flying at or above FL290**, including those not flying Free Flight paths, be equipped for RVSM. If this Free Flight option is considered too restrictive in scope, then the alternative En route UPT option may be preferred as the next step toward Free Flight.

The transition to Mature Free Flight is completed using the En route UPT plus RVSM concept, which again requires reduced separation standards compared with the Baseline plus RVSM concept. However, the horizontal separation standards are much less severe than those for the En route UPT concept without RVSM. (In fact the 1.5 nm / 2.0 nm separation parameters for Mature Free Flight are probably unrealistic requirements for automated conflict detection with a 15 minute lookahead period.) Consequently, the above transition path to Mature Free Flight was selected as the basis for the operational requirements in this study.

The operational requirements for separation assurance with the preferred Free Flight transition concepts are summarized in Table 14. The Initial Free Flight implementation is the Baseline concept with a target date of 2002. The primary infrastructure requirement onboard is an RNP-1 navigation system. Considerable ground-based infrastructure is needed in the Centers, however, to support the medium term conflict probe and the Radar controller in attaining the reduced separation parameters shown. This transitional system would be replaced sometime later in the decade with a joint radar / ADS surveillance system permitting a further reduction in both horizontal and vertical separation standards. This would require more extensive changes to the aircraft avionics and to flight procedures to safely implement the reduced separations. Even those aircraft flying current routes and procedures would need modifications for compatibility with this system, i.e. increased altitude precision and ADS capability may be required for all aircraft flying in high altitude airspace with this transition path. The final transition to En route UPT plus RVSM, where same altitude opposing conflicts may be routinely encountered, will require significant prior development and experience gained in implementing the previous steps.

The separation and intervention standards shown in Table 14 do not take into consideration the effect of wake turbulence as two aircraft approach within several nautical miles during a close encounter. Considerable research is needed to better understand the effect of wake turbulence on en route encounters and to establish the limits imposed on separation standards by the physics of such encounters. The conclusions of this section are thus preliminary, and need to be validated or modified based on research in this area.

Table 14. Selected Separation Parameters and Transition to Mature Free Flight

Separation Standard	Intervention Standard [1]	IOC Date	Ops Concept & Infrastructure
* 5 nm - Radar	* 10 nm - Manual	*Today	**NAS ATC System** * ~ 10 sec Radar Monitor
* 4 nm - Radar	* 7.5 nm - Manual + Automation Tools	* 2002	**Baseline Free Flight** * RNP-1 Navigation * Improved Tracking * Improved Wind Forecasts * 10-20 min Conflict Probe *Future Intent Display Aids
* 3 nm - Radar / ADS Monitor + 1000 ft RVSM	* 5 nm - Manual + Semi-Automated Conflict Resolution	* 2006	**Baseline Plus RVSM** * Above Plus RVSM Sensor ADS Reporting Radar/ADS/FP Fusion
* 2 nm - Radar /ADS Monitor + 1000 ft RVSM	* 4 nm - Manual + Semi-Automated Conflict Resolution	* 2010	**En route UPT Plus RVSM** * Above Plus - RNP 0.5 Navigation - High Integrity Cooperative Separation - Alert Zone Restrictions

[1]Thresholds for In-Trail & Crossing Trajectories (May be Different for Opposing)

It should be noted that the conclusions and operational requirements derived from the TAAM simulation model are tentative, i.e. substantial validation of the TAAM model is required before these results can be considered definitive. In section 5 we discuss follow-on tasks which are recommended for improving and validating the TAAM model for Free Flight studies. These tasks address the issue of validation of aircraft trajectories and airspace density using real-time ETMS data tapes, and validating the TAAM database on airplane performance. The value of the studies to date is that they give some insight into the challenges inherent in implementing Free Flight.

4.0 Conflict Probe Operational Concepts and Technical Requirements

4.1 Conflict Probe Operational Concepts

In this section we discuss the operational concepts and alternative methodologies for conflict detection between aircraft flying in the same proximate area. We first discuss the underlying methodology for predicting aircraft paths in section 4.1.1. In section 4.1.2 we discuss the process of eliminating aircraft pairs which do not conflict by using a series of sequential coarse and fine resolution tests for potential conflicts. Finally, in section 4.1.3 we outline several alternative methodologies for fine resolution horizontal conflict detection which are evaluated in section 4.2 to identify a preferred concept for medium term conflict probe.

4.1.1 Flight Path Prediction Methodology

There are three basic methodologies for predicting flight paths, which are distinguished by the time scale for the path predictions. Table 15 summarizes the prediction methodologies and the type of intent used to synthesize path predictions. The first type of prediction is that based on the strategic flight plan, which contains the waypoints to be sequenced until arrival at the destination airport, augmented with target air-speeds and altitude rates for each flight segment. This path data is then combined with wind and temperature forecasts to construct the ground speed profile, and to estimate arrival times at each future waypoint. The strategic predictions are then updated periodically by surveillance data to reinitialize the estimated arrival times (ETA's) based on current aircraft location. The strategic predictions are generally coarse estimates, since they typically do not account for flight path deviations due to weather or ATC vectoring, and do not use surveillance data to update the ground velocity profile.

Table 15: Flight Path Prediction Methodology

Intent Basis	Prediction Interval	Data Fusion Concept
* Strategic Flight Plan	* Long Term (> 30 min)	* Target Air Speed Plus Forecast Wind Used to Construct Ground Speed Profile * Periodic Surveillance Updates ETA's
* Tactical Flight Plan	* Medium Term (10 - 30 min)	* A/C Track & Altitude Profile Based on Dynamically Updated Flight Plan. * Along Track Predictions Based on Estimated Position, Velocity & Wind Shear
* Immediate Path Intent	* Short Term (< 10 min)	* Position & Velocity Extrapolation for Non-Maneuver Predictions * Uses Target Altitude / Heading & Transition Time for Maneuver Predictions

Tactical flight path predictions are based on similar intent information as for strategic flight plans, but intent will be updated either by use of ADS air-ground data-link or by a Center controller when a flight plan change is negotiated. The along track predictions are based on extrapolating estimated aircraft position and velocity states, and using along track wind shear for straight line, constant flight path segments. The methodology for predicting turn segments and vertical transitions is not explicitly discussed in this report but could be based on empirical look-up tables (Ref. 13), on assumed guidance laws during the transition phases (similar to CTAS, Ref. 14), or on ADS down-link of FMS based 4-D waypoints. Whatever method is ultimately used for such transitions, relatively high accuracy and ability to estimate prediction error growth are essential elements for medium term conflict detection. (In chapter 5 we comment further on needed research in this area, since the great majority of aircraft conflicts involve non-level flight encounters.) The use of strategic prediction methods for medium term path predictions is not recommended, since aircraft often do not follow their strategic flight plan, i.e. flight parameters such as cruise altitude, air-speed, and vertical rates may be quite different than those inferred from the flight plan or from system provided default values. (As an example, the rms error in predicting FIR-exit ETA's for overflying flights in an existing, operational system (Ref. 13) is on the order of five times larger than results obtained for the Baseline conflict probe, which assumes more accurate path prediction methodologies.) Moreover, accurate predictions may require sophisticated flight tracking and conformance monitoring to validate the parameters and guidance laws assumed for the current flight segment.

Short term path predictions typically do not use wind forecasts or flight plan data, and are based on simple extrapolation of the current velocity vector over the forecast period. However, experience with both the Conflict Alert algorithm used in the ATC Centers and TCAS shows the importance of including short term intent (especially target altitude) for modifying path forecasts based on intent. This type of information may be broadcast in an ADS-B event report in future systems, i.e. prior to and at the start of a flight transition. Otherwise, such intent data must be input to the prediction system by a controller or by lookup from the current flight plan. Short term predictions are usually fairly simple and have limited accuracy due to limitations in the surveillance system, i.e. large lags and noise errors in estimating velocity vector and altitude rate. Consequently, lookahead time for Conflict Alert is typically limited to a few minutes, and does not exceed 3.5 minutes with current technology radar surveillance (Ref. 15).

The accuracy of medium term path predictions using the above methodology changes dynamically and has different error mechanisms for lateral, vertical, and longitudinal axes. In the lateral axis, the primary error sources are navigation and Flight Technical Error (FTE), since the lateral prediction is based on the tactical flight plan. For an RNP-1 navigation system, the total rms lateral errors should not exceed 0.5 nm, independent of prediction time, although larger lateral errors may be assumed during turn maneuvers. Although we do not explicitly model vertical predictions in this report, the covariance methodology discussed below may be appropriate for climb and descent transitions, and a single rms parameter may be applicable for cruise and level flight segments. In the longitudinal direction, the rms prediction errors grow rapidly with

prediction time, reflecting uncertainty in estimating path velocity due to surveillance and wind forecast errors. In addition, the path length during turning maneuvers is uncertain, which adds to uncertainty in the longitudinal axis following such maneuvers. Figure 28 illustrates the covariance methodology for modeling horizontal prediction errors as a time varying ellipse with major axis typically along the longitudinal axis, and minor axis along the lateral axis. For two proximate aircraft, the size and shape of such error ellipses at the time of closest approach are vital elements in predicting assured separation or detecting potential conflicts in a probe lookahead period.

As an example, suppose we are predicting the one sigma error ellipse for an RNP-1 aircraft with surveillance rms errors = 5 knots, i.e. using the CNS requirements specified in section 1.5. Then the lateral axis rms is 0.5 nm, and the longitudinal rms error grows at the rate of 0.5 nm per 6 minute prediction period. Thus the rms longitudinal error roughly equals the lateral error at T = 6 minutes lookahead, is about twice the lateral error at T= 12 minutes, and is about three times the lateral error at T= 18 minutes. This rapid growth in error uncertainty has important consequences for conflict alerting and use of the conflict probe in an operational setting. Using similar logic, we find that the short term prediction method for Conflict Alert has smaller lateral error uncertainty than the medium term Conflict Probe for lookahead periods less than 6 minutes, in this example. Thus the medium term prediction method should only be used for lookahead times greater than that for short term Conflict Alert, i.e. we recommend complementary use of both short term and medium term conflict alerting.

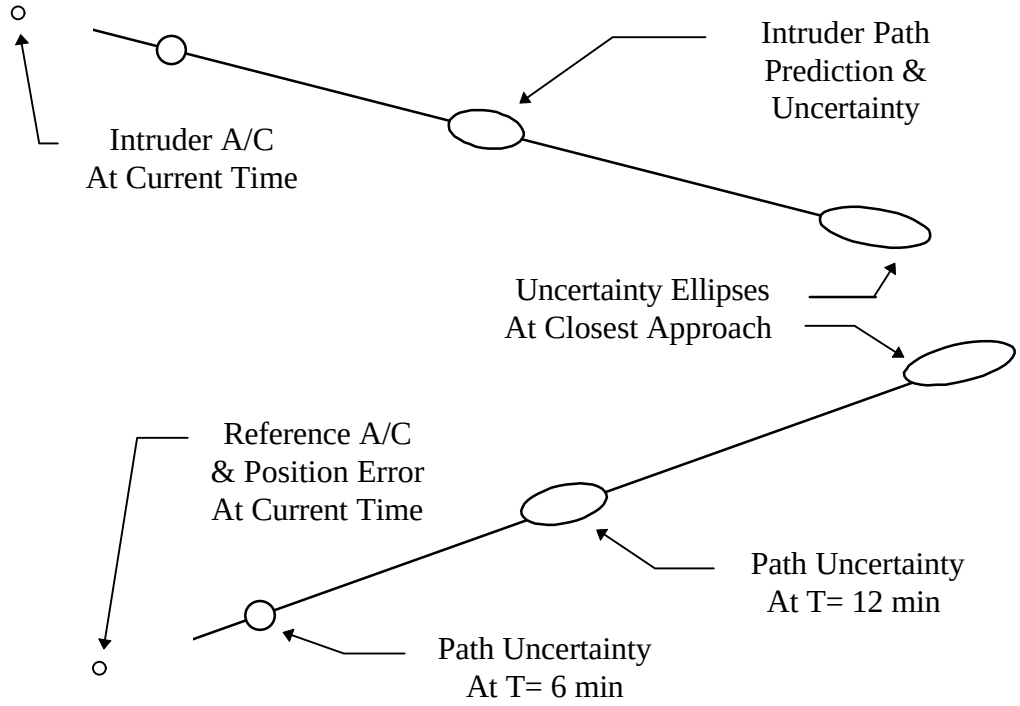

Figure 28 : Aircraft Crossing Path Horizontal Geometry (Covariance Modeling)

4.1.2 Conflict Detection Automation Process

Figure 29 illustrates the process used to detect conflicts for the probe operational concept described in section 2.1.2. At each conflict probe update time, or as needed for trial flight planning, the predicted flight plan of a reference aircraft is subjected to conflict processing to validate flight plan separation with other aircraft, or to identify and alert the controller to potential conflicts. The first step is to use a coarse conflict filter to identify potential intruder aircraft and time segments where the intruder path is near the reference aircraft during a lookahead period. These potential intruders are then subjected to finer resolution tests to declare potential conflicts and to eliminate safely separated aircraft from further probe testing on later probe updates. For newly identified aircraft pairs, the probe tests at regular intervals, e.g. one minute updates, until either a no-conflict or a conflict alert is declared for the aircraft pair. The probe then inhibits further testing on this pair until either a time-out (nominally = 5 min) is exceeded, or one of the aircraft is declared out of conformance with its intended flight plan. Thus, a conflict / no-conflict declaration typically remains in effect for some time period, and then the aircraft pair is again subject to conflict processing.

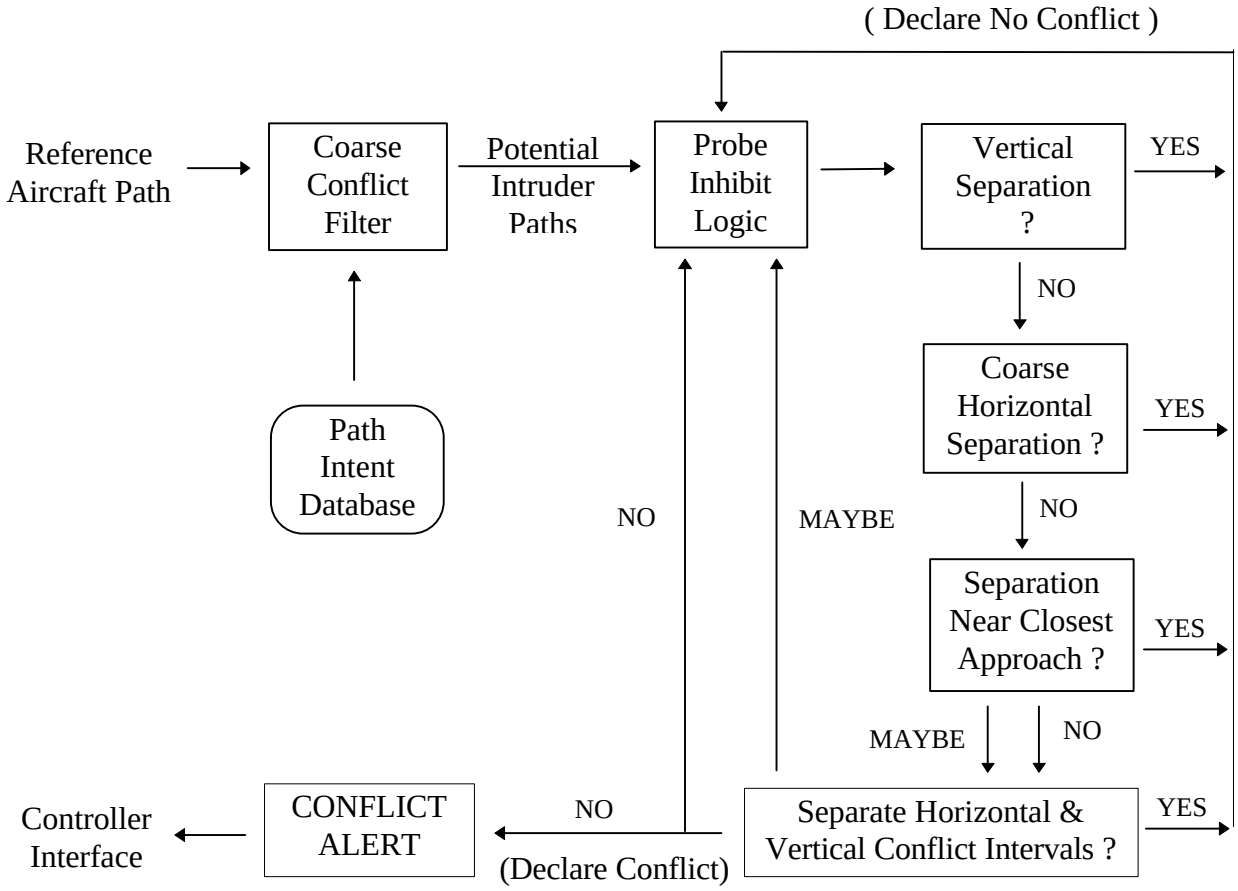

Figure 29 : Aircraft Pair Filtering and Conflict Detection Process

The fine resolution conflict probe consists of several sequential steps, each of which acts as a filter to eliminate potential conflict pairs. The first test shown is that of

determining if vertical separation is achieved, and if not, the time interval when vertical separation is not adequate. The second test is a coarse test for horizontal separation. In our simulation this consists of calculating the time and CPA distance for the closest approach point, and applying threshold tests to CPA time and CPA distance. (For details see Appendix A.6.) Then a fine resolution test is applied to those pairs which remain. Two separate thresholds are used for conflict / no-conflict decisions, and the decision logic must be confirmed on at least one successive probe update to declare a horizontal conflict or to declare no conflict. (The three valued logic in Figure 29 is required since noisy CPA estimates will otherwise lead to unreliable conflict decisions.) If both vertical and horizontal tests identify a potential conflict, then the intervals of vertical and horizontal loss-of-separation are compared and a potential conflict is declared if there is a time overlap. Otherwise the times of separation loss do not coincide, and a no-conflict declaration is issued for the aircraft pair. If no declaration is issued, the conflict probe continues to process the potential conflict pair at successive update times until a declaration occurs. The inner loop logic is similar to that of existing systems, such as the Conflict Alert used in NAS Centers (Ref. 15).

Now our simulation studies in section 3 showed that the vast majority of proximate encounters in en route airspace involves at least one aircraft climbing or descending through the altitude of the other. We see from the structure of the conflict declaration logic the value of accurately estimating both time to vertical crossing, and time to CPA in such cases, since large time uncertainties in either axis will greatly increase the chances for overlap of potential vertical and horizontal separation-loss intervals. With current methodology, the uncertainty in estimating such times is relatively poor, i.e. ~50 sec one sigma errors in predicting outbound and transit ETA's and ~90 sec one sigma errors in predicting inbound ETA's to a terminal fix have been measured in an existing system (Ref. 13). Although we primarily study the horizontal conflict probe and requirements in this report, it is clear that similar requirements on prediction accuracy need to be developed for the vertical axis. Our objective for Free Flight operations is to reduce the one sigma errors in estimating vertical and horizontal crossing times to ~15 sec. or less (~30 seconds time uncertainty with 95% probability). (This is the level of accuracy achievable with CTAS fix metering, and is consistent with the system requirements for Free Flight specified in section 1.5) Improvements in surveillance and intent infrastructure such as improved trackers and use of ADS reporting may enable future systems to achieve such objectives.

We note that the coarse conflict filter in Figure 29 also can play a role in the conflict resolution process when a potential conflict is detected. Although most conflict encounters between aircraft occur as discrete pairs, occasionally other aircraft are in the proximate vicinity of the conflicting aircraft, and may be adversely affected by the tactical resolution method selected. Since the coarse conflict filter identifies potential intruders with the reference aircraft, these aircraft (and others for the conflicting aircraft) can become inputs into the resolution process to help select an intervention tactic which does not propagate into a downstream problem. Any trial resolution would be processed and cleared through the conflict probe prior to activation, in any case.

4.1.3 Alternative Conflict Detection Concepts

Three concepts for horizontal plane conflict detection were selected for detailed analysis and study. The Fixed Threshold concept uses fixed thresholds on CPA time and CPA distance to declare conflicts and non-conflicts, and is a relatively primitive conflict detection method. The Covariance Method explicitly models path uncertainty as a function of surveillance, wind forecast and FTE errors, and uses the covariance errors to dynamically determine conflict declaration thresholds. The Conformance Bound Method models lateral, vertical, and longitudinal conformance bounds on path uncertainty, based on parametric values typical for medium term predictions. The Conformance Bound Method then determines conflict thresholds to assure that the conformance regions of aircraft pairs are adequately separated. These concepts are further described below:

* Fixed Threshold Conflict Detection - In this concept, the CPA time and distance of closest approach are first obtained for each potential path conflict pair. Two thresholds are used to declare conflicts and non-conflicts, respectively. If the CPA time is outside a fixed lookahead interval, or if the CPA distance is larger than an outer_threshold (nominally 10 nm for an advanced radar tracker) then the aircraft pair is declared non-conflicting, and is removed from the list of potential conflict pairs. If the CPA time is inside the probe lookahead interval and if the CPA distance is less than an inner_threshold (nominally 5 nm) then the aircraft pair is declared conflicting. In order to make the detection process more robust to tracker noise errors, conflicts must be detected two times in a row on successive probe updates for a horizontal conflict declaration to be issued. (Once a given aircraft has been checked for path conflicts and found non-conflicting with all other pairs, it may be cleared by the automation system for unconstrained flight until the next sector is reached, or the aircraft is detected out of conformance with the predicted flight path.)

* Covariance Method Conflict Detection - In this concept, error ellipse path uncertainty regions are computed at the closest approach time together with CPA distance for each potential path conflict pair. These error ellipses are based on covariance matrix calculations obtained by modeling tracker surveillance errors, wind forecasting errors, and aircraft path following errors (Appendix B.1). Figure 30 illustrates the horizontal conflict detection concept as viewed relative to the reference aircraft. The intruder path relative to the reference path is just a straight line with closest approach distance Rmin at time Tmin. The horizontal separation standard is a protected circular region around the origin with fixed radius Rsep. An intruder path is non-conflicting if the predicted uncertainty ellipse at each time point does not intersect the Rsep circle. The uncertainty ellipse shown is an aggregate error obtained by combining individual errors in predicting the reference and intruder paths. (For details, see Appendix B.2) To simplify calculations, the uncertainty ellipse is only evaluated at the minimum approach time Tmin. The closest approach is then found by sliding the ‘frozen’ ellipse along the intruder path, generating the dotted line in Figure 30. The uncertainty error Runc can be determined analytically as the maximum distance of the ellipse from the intruder path. If $R_{min} < R_{sep} + R_{unc}$, then a potential conflict exists. In this case, the initial

time (final time) of the conflict is found by sliding the ellipse backward (forward) in time until the circle and ellipse just touch. The methodology for covariance based conflict detection is summarized in Appendix B.

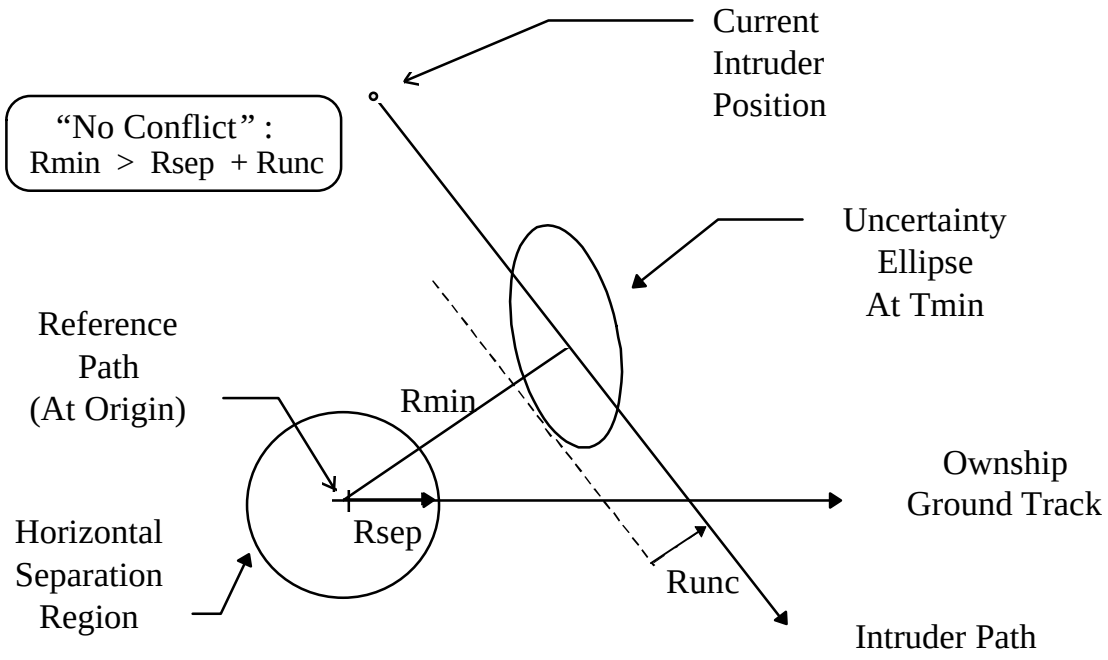

Figure 30: Covariance Method Conflict Detection Concept

In practice, two error ellipses are used for conflict decisions. The main difference between declaring conflicts and non-conflicts is in the size of the uncertainty ellipses used. The error ellipse used to declare non-conflicts is relatively large, on the order of two to three times the one sigma prediction errors, in order to reduce the missed detect probability to an acceptable level. The outer threshold for eliminating non-conflicting pairs is the sum of Rsep and Runc for the large error ellipse. Similarly, the error ellipse used to declare conflicts is relatively small, typically less than one sigma, in order to avoid excessive false alerts resulting in unnecessary tactical interventions. The inner threshold for identifying potential conflicts is the sum of Rsep and Runc for the small error ellipse. The thresholds with this method are dynamic and depend on the geometry of the conflict and the time to closest approach. The detection logic for declaring conflicts and non-conflicts is similar to that with Fixed Thresholds, once the inner and outer thresholds are computed.

* Conformance Bound Conflict Detection - This concept is a generic version of the conflict detection method proposed for the AERA-2 program (Ref. 2, 3). As originally proposed, each Center maintains a strategic, 4-D flight plan for all aircraft entering into Center controlled airspace. This flight plan reflects the current aircraft intent and is kept updated by path conformance monitoring and surveillance based flight plan reconformance if the actual position drifts too far from the predicted flight plan. Conflict detection with this concept is performed periodically on each aircraft between entry and

exit from Center airspace, and whenever aircraft paths are out of conformance with the intended plan. Fixed size error ellipses are used to model horizontal conformance bounds for level flight path following (nominally, 1 nm lateral semi-axis by 2 nm longitudinal semi-axis for conflict declarations). These conformance regions are expanded during vertical transitions and turn maneuvers. Figure 31 illustrates horizontal conflict detection with this method. As in figure 30, the intruder path and location at minimum approach are shown relative to the reference aircraft (ownship). The conformance bounds for both ownship and intruder paths are represented here as ellipses centered on the predicted aircraft paths. The conformance ellipses are obtained by rotating from standard NED coordinates to ownship coordinates with x-axis along the ownship track. The intruder is considered conflicting if the minimum approach distance between the conformance bounds becomes less than the separation standard Rs, as the intruder transits the minimum approach point. This is easily determined by analytic calculations to calculate the maximum lateral extent of each conformance ellipse (R1 and R2) in the direction of the minimum approach point. If Rmin < R1 + R2 + Rs then the aircraft pair are potentially conflicting, i.e. an inner threshold is obtained by summing R1, R2, and Rs. The detection logic for declaring non-conflicts is similar to that above, with the outer thresholds for declaring non-conflicts based on larger size conformance ellipses, nominally 1.6 times the size of the inner bounds.

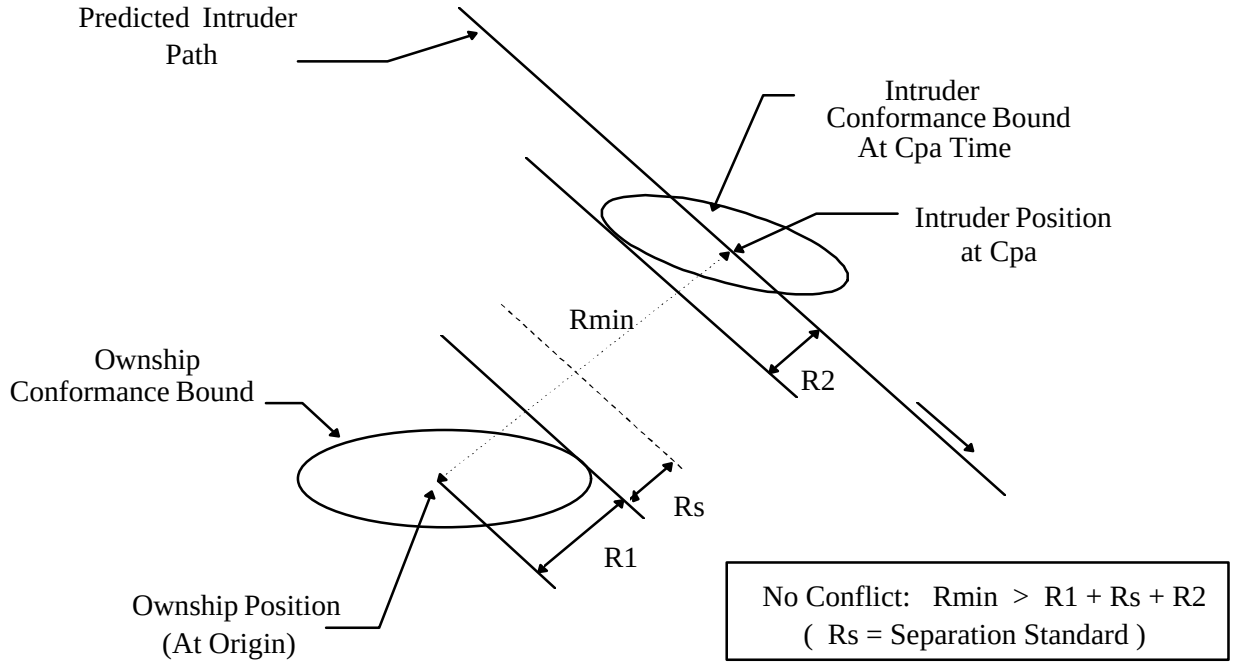

Figure 31: Conformance Bound Conflict Detection Concept

The conformance method is inherently more conservative in declaring conflicts than the covariance method. This is partly due to the covariance method using dynamically updated bounds on relative prediction error whereas the conformance method uses

a-priori uncertainty bounds, and partly due to maintaining separation between two conformance bounds rather than using an aggregate bound on prediction errors.

4.2 Baseline Comparisons of Alternative Probe Concepts

In this section we compare the conflict detection performance of the alternative probe concepts identified in section 4.1. Rather than using surveillance and prediction assumptions relevant for today's ATC system, we here assume conditions relevant to the Baseline Free Flight concept, i.e. with enhanced radar tracking and enhanced weather forecasting assumed available in the ATC Centers by 2002. (In section 4.3 we show the effect of using coarse tracking and weather forecasting assumptions on probe performance.) The navigation systems for simulated aircraft encounters also assume low navigation errors and FTE path following errors, consistent with RNP-1 quality airborne avionics. These assumptions are based on the operational requirements for initial Free Flight developed in section 3.3. Encounters between aircraft with lower quality avionics can also be simulated, but the separation and intervention standards would be larger with such encounters.

The modeling assumptions and methodology for evaluating the alternative probe concepts are first described in section 4.2.1. Section 4.2.2 then presents comparisons of important performance measures such as missed detections, false alarms, and conflict warning time, and shows the expected number of probe-based conflict interventions relative to benchmark results for the Cleveland Center simulation. Section 4.2.3 recommends a preferred concept for further study and sensitivity analysis, and summarizes the performance characteristics of the preferred concept.

4.2.1 Baseline Assumptions and Conflict Probe Performance Analysis

The conflict probe studies are based on Monte-Carlo simulation of horizontal encounters between aircraft pairs. Figure 32 shows the geometry of a single encounter between two aircraft denoted the "ownship" and "intruder". For each trial, the nominal encounter geometry is fixed and the initial entry conditions are chosen such that a direct collision results if both aircraft fly their flight plan with no FTE errors, and with no random wind errors. A wind field is generated for each trial, based on a fixed mean wind with exponentially correlated random wind errors (Ref. 16). In effect, the random wind errors perturb the along-track velocity vectors of the aircraft at the initial entry times, and create along-track wind shear which changes the ground speed of the aircraft as they move toward the crossing fix. In addition, aircraft navigation and FTE errors are modeled as a constant lateral offset chosen randomly from trial to trial. The result of the random wind field and the lateral offset errors is a close encounter rather than a direct collision, as the aircraft transit the crossing fix. (Our covariance model can also include longitudinal FTE error modeling, but these errors are ignored in our studies, since wind and surveillance velocity errors will typically dominate such errors even with assumed technology enhancements for 2002 operations.)

For each Monte-Carlo study, the mean time for the aircraft to reach the crossing fix is 25 min. (This assures that the simulation time exceeds the max lookahead time for the conflict probe.) Three different crossing angles are evaluated in our studies: 30 deg crossing (intrail conflict), 90 deg crossing (crossing conflict), and 150 deg crossing (opposing conflict). The rms error in lateral offset for each aircraft is 0.5 nm, i.e. on each trial the ownship and intruder are offset laterally from the nominal flight path by a random distance with mean zero and standard deviation = 0.5 nm. Random winds were simulated in our studies with mean value = 40 knots, random along-track rms error = 25 knots, and correlation distance = 670 nm for cross-correlation between winds at different locations. (The along-track wind shear is about 10 knots rms per 100 nm with this model. See Appendix A.2 for modeling details.) This level of wind and FTE errors produces close encounters with most CPA distances less than 10 nm and most CPA times within 2 minutes of the mean crossing time (25 min).

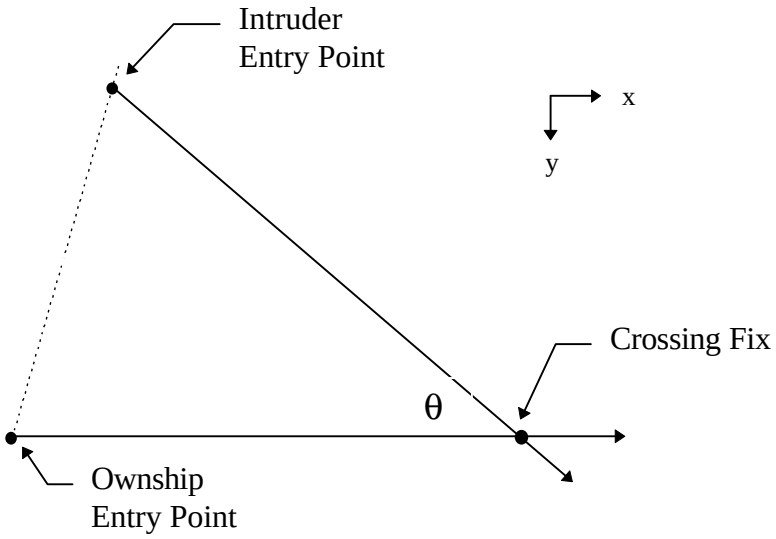

Figure 32 : Conflict Probe Simulation Encounter Geometry

At each probe update time (nominally every two minutes from simulation start) the ownship and intruder paths are predicted forward using pseudo-tracker estimates of along track position and speed, and estimated along-track wind shear. A two step recursion is used to estimate CPA distance and CPA time, and then the conflict detection algorithms are applied to evaluate conflict probe performance. The pseudo-tracker model evaluates the 'truth' values of along-track position and speed at each update time, and then adds on random tracker induced errors. A simple alpha-beta tracker model is assumed for our studies, with the pseudo-tracker simplifying calculations by generating random errors at each probe update time, rather than at each sensor update (nominally 10 second updates for radar sensors). The estimated wind shear is generated from the 'truth' values of wind shear assuming both scale factor and additive random errors in wind forecasts. Nominal surveillance and wind forecast rms errors for CPA predictions assumed in our studies are:

* Radar sensor along-track position error = 0.15 nm
* Along-track wind forecasting error = 6 knots
* Along-track wind shear uncertainty = 4 knots per 100 nm
* Radar tracker steady state velocity error = 3.8 knots
(alpha = 0.20 & beta = 0.022 for ~ 2 minute track settling time)

As discussed earlier in section 1.5, these assumptions are consistent with current state-of-the art wind forecasting and target tracking given modern monopulse radar sensors.
Our assumption is that these enhanced systems will be integrated into the ATC Centers in the time period that medium term conflict probe becomes available.

The system requirements for En Route conflict probe were previously discussed in section 1.5. They are repeated here for completeness. The main requirements for our study are :

* Missed detects < 2% of close encounters, i.e. the probability of not generating a conflict alert on aircraft pairs with true CPA < Separation_Std is less than 2%, where the separation standard for RNP-1 equipped aircraft = 4nm.

* False alerts < 6% of close encounters (with CPA < 10 nm), i.e. the probability of generating a conflict alert on aircraft pairs where true CPA > Int_Std is less than 6%, where intervention standard for equipped aircraft is Int_Sep = 7.5 nm.

* Max_lookahead for conflict probe evaluations = 17 min for Intrail (30 deg crossing) scenarios and 20 min for Crossing and Opposing scenarios.

In practice, the max_lookahead times for path predictions are fixed constants. However, the covariance method will wait until path prediction uncertainty is sufficiently small before attempting conflict detections. This will occur at about 17 min for the Intrail scenarios, and at max_lookahead = 20 minutes for the other cases. We used these values for all methods to obtain equivalent probe performance for comparisons.

4.2.2 Conflict Probe Methods Performance Comparison

Each of the three conflict probe concepts were evaluated with three crossing scenarios and common error sources, and subjected to over 2000 Monte-Carlo trials to evaluate conflict probe performance under common baseline assumptions. The threshold parameters were tuned as needed to attain a missed detection probability (where no alert is issued for a true conflict) of less than 2 %. Probe performance statistics including missed detects, false alarms, and averaging warning time from first detection were evaluated. The results of these studies are summarized in Table 16. The statistics show that conflict detection warning times are similar for all three methods,

with the longest warning times obtained for the Crossing and Opposing scenarios. However, the Conformance method has significantly more false alarms than the Covariance and Fixed Threshold methods. If this method were adopted, then max_lookahead would need to be reduced substantially, i.e. to 10 minutes or less to meet the specified requirement on false alarm rate. The reason for this disparity in performance is seen in examining missed detects for the Conformance method, which are significantly lower than those for the other methods. The Conformance method chooses thresholds which are biased toward detecting potential conflicts, but would result in an excessive number of false alerts requiring attention by Center controllers. The missed detect and false alarm rates for the other methods are very similar, and either method would be acceptable for medium term conflict probe. This shows that most conflict detections occur in a fairly narrow time interval, and that the detection thresholds for the Fixed Threshold and Covariance methods are similar at the average warning time for first detect.

Table 16: Conflict Probe Methods Performance Summary

Conflict Probe Method	Missed Detects %	False Alarms %	Warning Time (min)
Covariance:			
In-Trail (30 deg)	1.8	5.0	14.1
Crossing (90 deg)	1.0	6.4	18.2
Opposing (150 deg)	0.0	0.0	18.7
Fixed Thresholds:			
In-Trail (30 deg)	1.7	5.1	13.9
Crossing (90 deg)	0.8	5.6	17.9
Opposing (150 deg)	0.5	0.0	18.6
Conformance:			
In-Trail (30 deg)	0.0	25.0	14.2
Crossing (90 deg)	0.2	21.5	18.4
Opposing (150 deg)	0.0	4.6	18.6

Another method to measure conflict probe performance is in terms of total conflict interventions per unit time period. Even though our studies only measure horizontal conflicts, we can estimate the relative performance of the three methods by multiplying the number of close encounters per encounter category and CPA region (obtained in our Cleveland simulation) by the percentage of conflict detections to estimate total probe conflict interventions for the Cleveland baseline simulation with 2002 traffic. The results of this study are summarized in Figure 33.
This figure shows expected number of conflict alerts over a one day period. The results show that the Covariance method has the best performance, and results in only 9% more interventions than the benchmark, even though the simulated traffic load has

grown by 40 % from the 1995 benchmark. The Fixed threshold method also performs well, compared to Covariance based conflict detection. Of these two, the Covariance method is preferred since it is more easily adapted to changes in CNS system performance, and parameter tuning is easier than with the Fixed threshold method. The Conformance method is not competitive with the other concepts. It is simply too conservative in choosing detection thresholds, which results in very few missed detections, but excessive false alerts. (A false alert is generated whenever a conflict is declared even though the true CPA distance is greater than the intervention standard.)

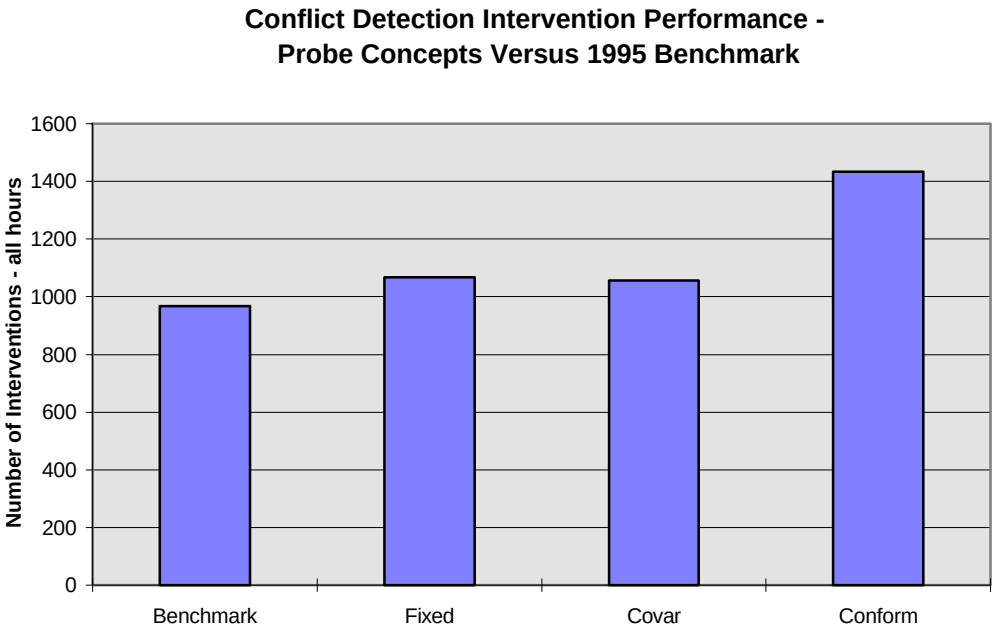

Figure 33: Conflict Probe Concepts - Intervention Performance

4.2.3 Preferred Conflict Probe Concept - Covariance / Data Fusion Methodology

We have identified in sections 2.1 and 4.1 the desirability of sophisticated trajectory synthesis for predicting aircraft paths from all available information sources: wind forecasts, surveillance data on current aircraft states, and flight path intent, in order to obtain accurate medium term path predictions for separation assurance. The covariance methodology is a means of incorporating the prediction uncertainty associated with such forecasts using simple error models to represent the dominant prediction error sources. Covariance methodology allows many of the problems with separation assurance to be formulated and solved simply, i.e. calculation of detection thresholds, problem entry and exit times, and graphical display of path uncertainty can be obtained with straightforward analytical calculations. As we show in Appendix B, the additional code for this method is relatively small, i.e. covariance methodology does not greatly increase either the size or the complexity of code for medium term conflict

probe. We have shown in the previous section that this methodology is competitive or superior to other probe concepts in terms of missed detect, false alarm, and detection warning time. Thus, this methodology is recommended for future conflict probe studies, and was adopted as the preferred concept for our Free Flight requirements analysis.

Of equal importance, is the supporting infrastructure for the conflict probe. The earlier studies in Ref. 1 showed the importance of accurate ground velocity vector and accurate wind forecasts for medium term path predictions. Both our current studies and the experience of the CTAS project (Ref. 12) reinforce this viewpoint, i.e. the development of advanced automation systems for regional ATM will require enhancements to our current surveillance and weather forecasting infrastructure. We have assumed such enhancements in our baseline studies.

The anticipated performance of the Covariance method for En Route conflict probe is illustrated in Figure 34. This figure shows conflict detection probability per aircraft encounter as a function of true CPA distance for an in-trail scenario, based on 2100 Monte-Carlo trials. The results show better than 99% detection probability for encounters with CPA < Separation Standard= 4nm, a rapid fall-off in detection probability between CPA= 4.5 nm and CPA = 8 nm, and less than 6% false alerts for CPA > Intervention Standard=7.5 nm. These results show the potential for implementing medium term separation with reduced horizontal separation standards, and support mid-term (~ 2002-2005) implementation of direct routing operations.

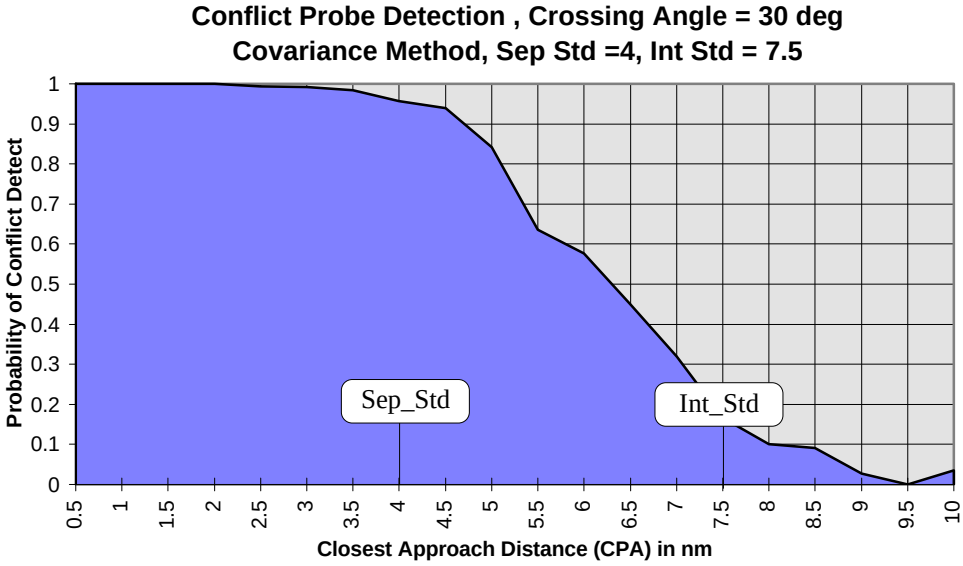

Figure 34: Conflict Detection Performance - Baseline Assumptions

4.3 Conflict Probe Sensitivity Studies

Several sensitivity studies were performed to evaluate the effect of important parameters and error sources on conflict probe performance. Two of these studies, the sensitivity to probe update rate - section 4.3.1, and the sensitivity to surveillance

system errors - section 4.3.3, use the Monte Carlo simulation method described in the previous section. The other studies are based on covariance analysis using the conflict detection thresholds generated by the Covariance method. These studies include sensitivity to conflict geometry (airplane crossing angle) - section 4.3.2, sensitivity to wind forecasting errors - section 4.3.4, sensitivity to lateral FTE /NAV errors - section 4.3.5, and sensitivity to vertical crossing conflicts - section 4.3.6.

4.3.1 Sensitivity to Probe Update Rate

One of the most important parameters for the conflict probe is the update time between successive probes. As update time is shortened, one would expect that average warning time would increase. However, as probe update time is shortened, the number of calculations increases and a point of diminishing returns is reached, where small increases in performance require large increases in probe calculations. Figure 35 shows the cumulative probability of conflict detection as a function of conflict warning time for update times between 0.5 and 4 minutes, based on 1500 Monte Carlo trials. The baseline assumptions of the previous section were used in this study, and the results are for a 30 degree crossing angle scenario. The figure shows significant improvements in warning time as probe update time (tau) is decreased from four to one minute. However, the decrease in warning time in shortening tau to 0.5 minutes is not significant, except at the 95% probability level and higher. This indicates that the probe conflict logic needs improvement (2 detects out of 3 probes is recommended to replace the current logic for 2 detects on 2 sucessive probes). With improvements to probe logic for marginal cases, one minute conflict probe updates are recommended.

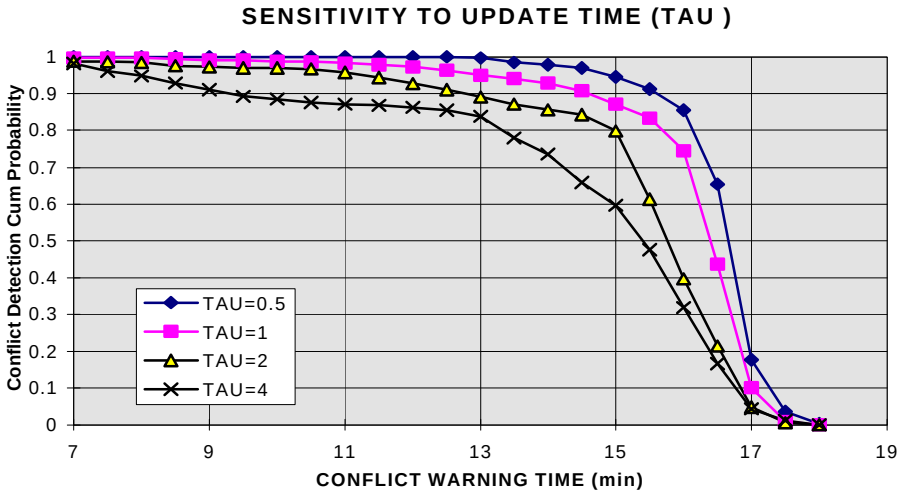

Figure 35 : Sensitivity to Probe Update Time - Baseline Assumptions

4.3.2 Sensitivity to Conflict Geometry (Airplane Crossing Angle)

Our baseline Monte-Carlo studies indicated that conflict detection is most difficult for In-trail scenarios where the crossing angle is less than 30 degrees. This sensitivity to crossing angle was confirmed by evaluating the inner and outer conflict detection thresholds for conflict / no-conflict decisions at a fixed 15 min lookahead time, for

crossing angles varying from 0 to 180 degrees. The detection thresholds reflect the uncertainty in predicting CPA distance as a function of conflict geometry and the modeled uncertainty in path predictions. Figure 36 shows the result of this sensitivity study. It is seen that the detection thresholds (and CPA error uncertainty) increases to a maximum as crossing angle increases from 0 to 20 degrees, remains relatively flat between 20 and 30 degrees, and decreases slowly as crossing angle increases from 30 to 180 degrees. This study confirms the difficulty of detecting in-trail conflicts with 15-30 degree crossing angles. Although such conflicts are a worst case from the point of view of conflict detection, they are typically easier to resolve for controllers since more time is available for course corrections. Opposing conflicts, on the other hand, are easily detected and uncertainty errors in CPA time and CPA distance are minimized.

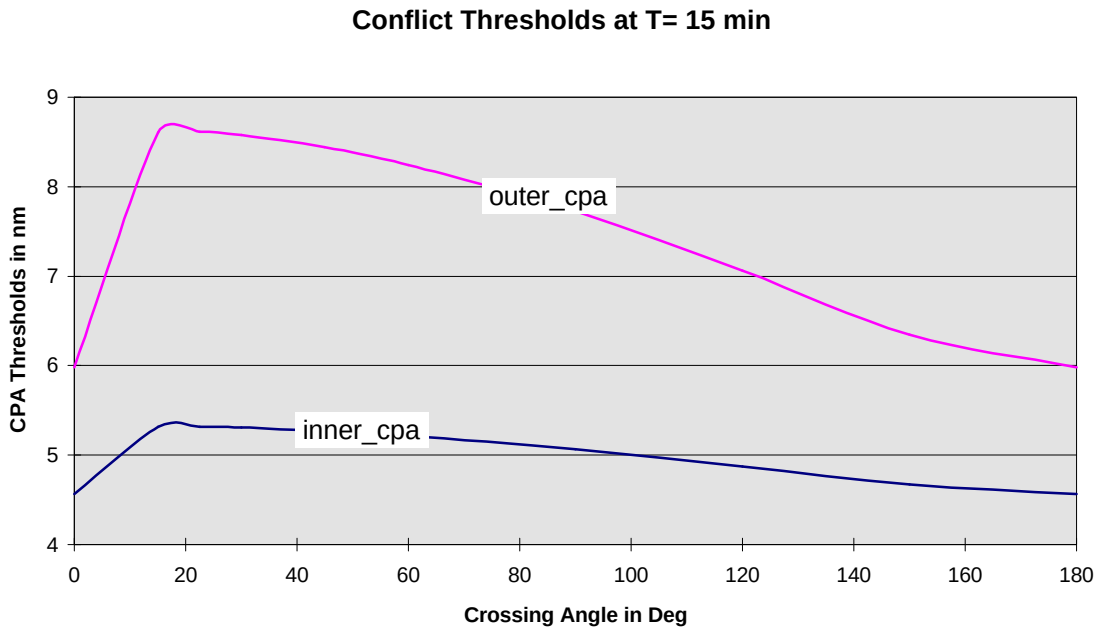

Figure 36: Conflict Probe Baseline Sensitivity to Crossing Angle

4.3.3 Sensitivity to Surveillance Errors

A previous sensitivity study using the covariance method (Ref. 1) showed that conflict probe performance is very sensitive to assumptions on surveillance and tracking errors. In this study we examined the relative effect on conflict probe performance of three technology options for surveillance: (1) retaining the current surveillance and tracking system, (2) enhancing the radar-based tracking software as described earlier in section 4.2, and (3) implementing ADS or ADS-B surveillance assuming non-augmented GPS avionics aboard participating aircraft.

The Monte-Carlo study results of probe performance assuming the current surveillance system characteristics were not promising. The study assumed slightly worse radar errors - 0.25 nm one sigma errors versus 0.15 nm errors for the baseline, and much less smoothing in the tracking filter - alpha = 0.32 for 10 second update smoothing versus alpha= 0.20 for the baseline. The net result is that the steady state velocity error = 15 knots rms for the current technology study versus 4 knots rms error for the assumed baseline. This level of velocity error is consistent with observations from current en route radar systems as verified recently in CTAS studies (Ref. 12). This study also assumed the current horizontal separation standard = 5 nm. The results of our studies for the 30 deg in-trail crossing scenario showed that the effective lookahead time for the conflict probe shrank to about 8 minutes, and the mean conflict warning time was only 5.3 minutes. Although these results could be improved by further algorithm tuning, they show that with current NAS surveillance and trackers, prediction errors are unacceptable for lookahead times exceeding about 8 minutes. In fact, two existing systems that perform medium term predictions, i.e. CTAS and the Dutch conflict probe (Ref. 13), use their own modified trackers to obtain sufficient data smoothing for medium term path predictions. We concluded from these studies that current NAS radar trackers, which compromise between accurate steady state tracking and timely maneuver response, will not support medium term conflict probes.

By contrast, the probe results with ADS-based surveillance show much improved performance compared with the assumed baseline system. With ADS based surveillance and some data smoothing to reduce SA noise, the steady state velocity error drops below 0.5 knots rms, assuming unaugmented GPS position and velocity measurements. Figure 37 shows the results for ADS equipped aircraft using 2100 Monte Carlo trials. This study assumed the same level of lateral errors and wind forecast errors as the baseline system, so that the study measures the effect of reduced surveillance and tracking errors only. The probe thresholds were tuned for a 3 nm horizontal separation standard and 5 nm intervention standard. It is seen that the conflict probe will support the reduced separation standards if both aircraft are ADS equipped, i.e. missed detect, false alarm, and warning time requirements are all satisfied. We also evaluated the effect of reducing the wind forecast errors by about a factor of two. In this case the CPA uncertainty region decreased about 0.5 nm compared with Figure 37, showing that further reductions in separation standards may be possible with ADS surveillance, reduced RNP levels, and enhanced weather forecasting.

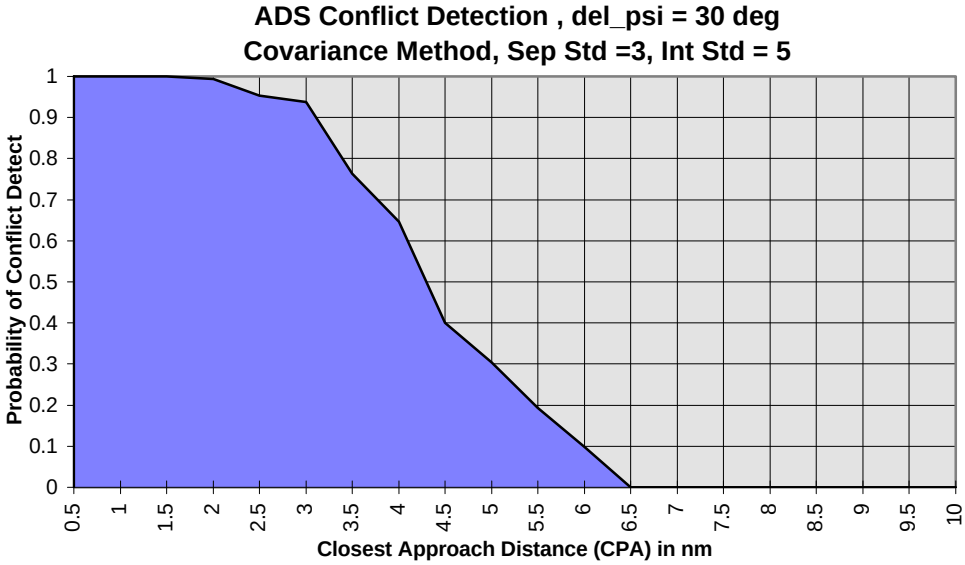

Figure 37: ADS Conflict Detection Performance - 30 Deg Crossing Scenario

4.3.4 Sensitivity to Wind Forecasting Error

This study examined the effect of varying the along-track forecasting error on the conflict detection thresholds at a15 min lookahead time. (The effect of wind forecasting error grows with lookahead time and 15 min represents the desired lookahead for medium term conflict detection and resolution.) Baseline assumptions and errors are used except for the sensitivity to forecasting error. The results of a covariance analysis are shown in Figure 38. This figure shows that with enhanced surveillance and the other baseline assumptions, the 'knee' of the curve for medium term forecasting is in the 6 to 9 knot rms range, with smaller forecasting errors not changing the CPA uncertainty or detection thresholds very much. Consequently, the desired goal for medium term predictions is forecast error < = 6 knots rms. (The forecasting error tolerance for climbs and descents was not examined in this study, but is assumed to be tighter than that for cruise predictions.)

There is one strong caveat to this study which should be noted. The covariance error model assumes that the correlation distance for cross-correlation between two along-track wind forecast points is on the order of 500 nm. However, there is some evidence (Ref. 17), that for rapidly updated (< 3 hr), dense grid (< 60 km) forecasts, the correlation distance may be much smaller, e.g. on the order of 75 -125 nm. What is needed here is an analysis of the RUC forecast errors to validate the forecast correlation distance for use in our covariance modeling. If a shorter correlation constant is validated, i.e. there is little predictability in the wind error for medium term predictions, then the covariance error sensitivity to forecast errors shown in Figure 38 is overly optimistic, and even tighter tolerances on wind forecast error are desirable.

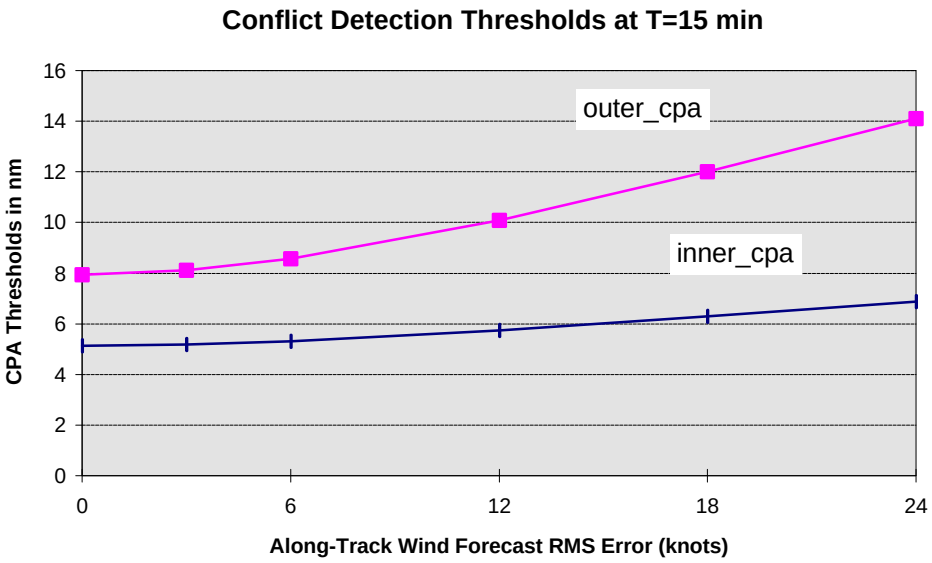

Figure 38: Sensitivity to Wind Forecasting Error - 30 Deg Crossing Scenario

4.3.5 Sensitivity to Lateral FTE and Navigation Errors

As noted before, medium term conflict detection is not very sensitive to lateral FTE and navigation errors. This is shown in Figure 39 which compares the CPA uncertainty at two threshold levels for lateral error rms values up to 2 nm, and for a 15 min lookahead interval. Conflict detection is much more sensitive to lateral errors at short lookahead times, i.e. for T< 5 min, since the lateral errors dominate covariance uncertainty at short lookahead times. This does not mean that the lateral FTE errors are unimportant for medium term separation assurance, however. The RNP tolerance on lateral errors is extremely important in determining minimum horizontal separation (Ref. 11).

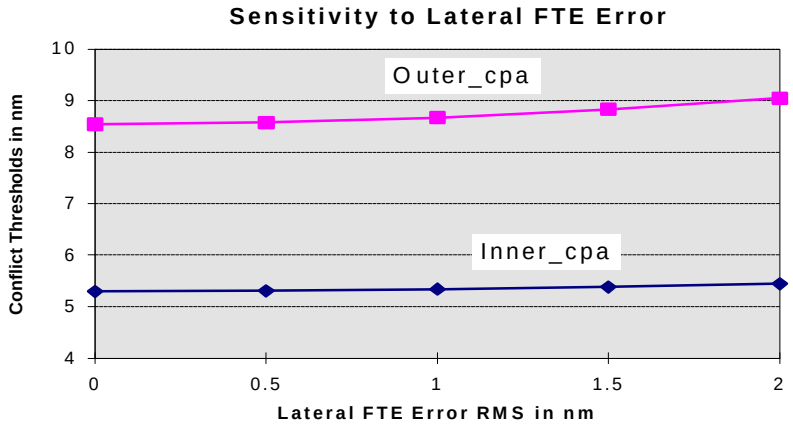

Figure 39: Sensitivity to Lateral FTE Error at 15 min Lookahead

4.3.6 Sensitivity to Vertical Crossing Conflicts

The Cleveland Center simulations in section 3 showed that most of the potential conflicts between aircraft involve one of the aircraft passing through or crossing the flight level of the other. It is of great interest to identify the ability of an enhanced radar system to perform medium term conflict detection for aircraft performing vertical transitions. However, the path dynamics in both the vertical and horizontal planes are more complicated than those for cruise, since both ground speed and vertical rate are non-constant in climb and descent flight phases. An in-depth study of 3-D conflicts was beyond the scope of the current study. However, a simplified covariance analysis was used to bound the potential lookahead capability for conflicts involving level crossings. To keep the analysis simple, an alpha-beta-gamma tracker was assumed to process radar (or ADS-B) along-track position measurements, and to predict the future horizontal path based on a constant acceleration model during vertical transitions.

For this study, we assumed somewhat smaller radar sensor errors, since the climb and descent phases are usually closer to a terminal radar, i.e. radar sensor rms noise error = 0.1 nm was assumed, compared to an rms value = 0.15 nm for the baseline studies. An alpha-beta-gamma filter was tuned for ~ 2 minute convergence in both position and velocity axes. Figure 40 shows the normalized autocorrelation for the position and velocity estimates of the tuned tracking filter. This figure shows that the filter correlation between current data and older measurements decays to small levels (autocorrelations < 0.1) in about 2 minutes, i.e. filter performance is equivalent to that for the baseline alpha-beta filter. With these assumptions, steady state rms velocity error ~ 2.2 knots, about 60% of the error level assumed for the baseline studies.

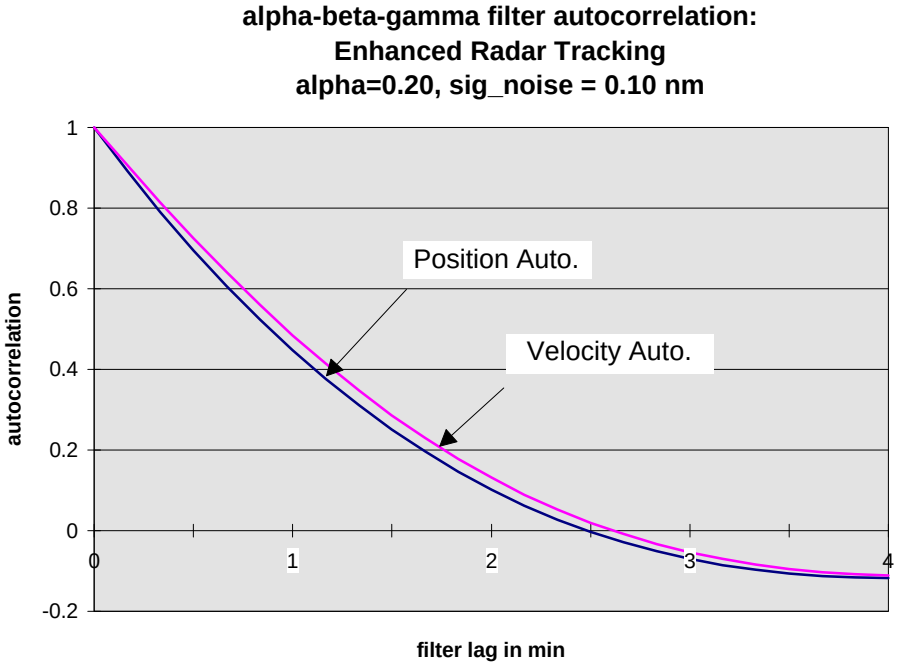

Figure 40: Alpha-Beta-Gamma Filter Design for Vertical Path Tracking

Conflict probe sensitivity to lookahead time for the alpha-beta-gamma tracker model is shown in Figure 41. In our studies, the effective lookahead for the covariance method is based on the time when the outer threshold for no-conflict declarations is less than 10 nm. This study shows that the effective lookahead time shrinks to about 11 min for the more complex path dynamics associated with vertical transitions. Although this meets the requirement of at least a 10 minute lookahead period, it is clear that more research is needed to validate our modeling assumptions, and to establish precise velocity tracking requirements for path predictions during vertical transitions. (See Section 5.2 for further details on recommended vertical transition studies.)

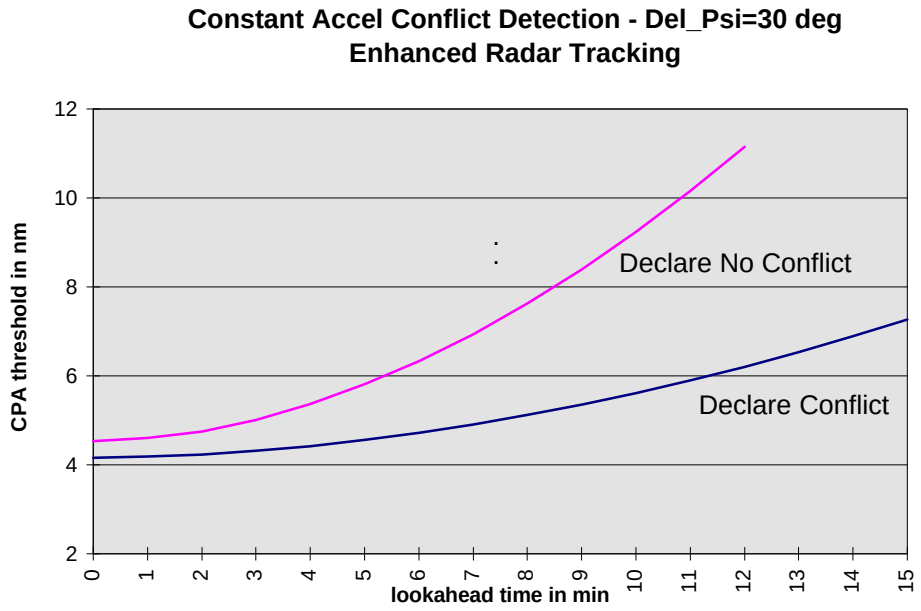

Figure 41: Conflict Lookahead Capability with Enhanced Radar Tracking

It should be noted that much better path prediction performance is achievable if the aircraft is equipped with ADS-B or ADS capability, enabling air-ground data link of aircraft ground vector (ground track, ground speed, vertical rate). Whereas the radar tracker must utilize long filter smoothing times to obtain accuracies on the order of 2-4 knots, an ADS system could deliver near real time estimates of aircraft velocity with rms accuracies on the order of 1 knot or better. Significantly improved ADS surveillance will allow the lookahead times for vertical transitions to be expanded, and may enable reductions in separation standards. However, path prediction capability will still be limited by wind forecast errors, and the ability to determine the aircraft guidance law and energy-rate dynamics during vertical transitions. All of these factors must be examined to determine the potential benefit of ADS equipage for improved climb and descent path predictions.

4.4 Technical Requirements for Initial Free Flight

The technical requirements for initial Free Flight operations are summarized in Section 1.5. This section is meant to expand on the basis for these requirements, and is complementary to the summary in Section 1.5. The requirements for Conflict Probe Automation are first addressed, followed by Navigation, Surveillance, and Communication requirements, and ending with Weather Forecasting requirements.

Conflict Probe Automation Requirements

We have assumed a 2% missed detection rate and a 6% false alert (nuisance) rate for conflict probe technical performance. This assumption assumes redundancy in performing separation assurance, i.e. sector controllers providing primary separation services as in the current system. It is possible to provide much tighter detection criteria such as 10^{-5} detection rates, using larger detection thresholds and multiple opportunities for conflict detections. However, this will have the negative effect of greatly increasing nuisance alerts and controller workload. The assumed detection and false alert rates must be validated with controller-in-the-loop simulations. These initial values are designed to balance the need to detect and resolve potential conflicts early, while minimizing the number of unnecessary interventions.

Similarly, the selection of a 20 minute lookahead period is based on the desire to provide early resolution of potential conflicts, reducing the severity of path disturbance for resolving conflicts. Recent studies at NASA Ames have shown that ~14 minute intervention times are optimal for resolving potential conflicts, considering the uncertainty in trajectory predictions due to surveillance and wind forecasting errors (Ref. 18). This study validates the requirement for 20 minute probe lookahead, since several minutes are typically needed to generate a conflict alert, and several minutes more may be needed for controller resolution decisions. Our studies in Section 4 support the use of a 20 minute lookahead for aircraft in cruise, but show that little more than 10 minutes lookahead may be feasible for conflict decisions with climbing and descending aircraft, using current surveillance technology. (However, these results assume open loop trajectory prediction. The use of closed loop arrival time control procedures such as RTA to a meter fix or to top-of-climb may improve trajectory prediction uncertainty for climbing and descending aircraft.)

Finally, the selection of a one minute rate for probe updates is based on a sensitivity study in Section 4.3, using baseline probe assumptions. However, the update rate should be increased if probe lookahead is reduced, i.e. ~ 30 second probe updates may be needed if the lookahead interval shrinks to 10 minutes or less, in order to maximize warning times for conflict resolutions.

Navigation Requirements

We have stated a requirement for precision RNAV equivalent to RNP-1 navigation capability for initial Free Flight operations. This requirement is derived from the operational requirement derived in Section 3.3 to support a 4 nm horizontal separation standard. Recent RGCSP studies (Ref. 11) have proposed the use of RNP standards as a basis for reduced lateral route separation, and for reduced longitudinal (in-trail) separation. Route based separation minimums as low as 3.5 nm have been proposed for RNP-1 aircraft with radar conformance monitoring. Thus, RNP-1 aircraft should be capable of supporting the proposed 4 nm separation standard for initial Free Flight.

Surveillance Requirements

Probably the most important surveillance requirement for initial Free Flight is that of obtaining an along-track steady-state velocity error of 5 knots rms or better. This value is considerably better than current NAS trackers, e.g. the somewhat enhanced tracker used for recent CTAS studies was observed to have a 15 knot rms error for cruise trajectories. The ~5 knot surveillance criterion is the basis for the 4 nm separation / 7.5 nm intervention standard assumed for initial Free Flight, i.e. enhanced surveillance is key to reducing minimum separations and intervention thresholds for Free Flight operations. On the other hand, various simulation studies such as Ref. 4, 6 have consistently shown that the use of modern Kalman filter based multi-sensor trackers are capable of achieving this level of tracking performance (or better) using modern ATC radars. Another method of achieving this requirement is to use longer interval data filtering to reduce velocity noise. However, this solution is not recommended for general tracking needs, since fast response is also desirable for tracking maneuvering aircraft. The preferred solution methods are to improve the radar sensor and to improve the ATC tracking software.

For aircraft in vertical transition, the required velocity accuracy may be considerably tighter than for cruise to sustain 10 min or better lookahead times. The sensitivity study in Section 4.3 indicates that the required velocity accuracy may be on the order of 2.5 knots rms, for the simple dynamics model evaluated. This may be at the practical limit of single source trackers using monopulse radars. Consequently, multiple source trackers may be required to achieve this level of tracking accuracy. At least three alternative methods may be considered to achieve this level of tracking accuracy:

* multi-sensor radar tracking blending the inputs from several nearby sensors,

* use of primary radar position and Doppler range-rate inputs, and

* data fusion of radar position and ADS broadcast velocity data.

The latter is preferred for eventual upgrade of the current surveillance system, but may not be available for Initial Free Flight operations. The other alternatives do not require enhancements to the existing surveillance sources, but require significant changes to the existing terminal and en-route tracking software.

Communication Requirements

Although some form of medium term separation can be implemented prior to the introduction of Controller-Pilot Data Link (CPDLC), it's usage is vital for later stages of Free Flight. From the point of view of Center operations, CPDLC is essential for distributing workload from the sector controller to other positions. Simulation studies (Ref. 19) have shown that CPDLC allows more efficient usage of controller teams, based on distributed situation awareness of user intent and current flight plan clearances. This is exactly what is needed to implement medium term separation assurance, since the planning controller using a conflict probe needs some capability to resolve conflicts outside the current sector. Moreover, the implementation of complex procedures such as the use of RTA restrictions and Top-of-Descent restrictions will require CPDLC for reliability of communications.

The other requirement for later stages of Free Flight involves the direct communication of user intent whenever that intent changes and at the time of handover from the current ATC Center to a downstream Center. The communication of user intent can be implemented using CPDLC or ADS interrogation. ADS communications are preferable from the point of view of reducing pilot and controller workload, since these communications can be automated.

Weather Forecasting Requirements

Most of the Monte-Carlo studies and covariance analysis studies assumed forecast wind component errors on the order of 6 knots rms, based on studies reported in Ref. 7. Since that time, the author has found several other studies (Ref. 12, 20) which show that weather forecast errors for 3-6 hr forecasts are more likely to have component errors on the order of 10 knots rms. The sensitivity study to wind forecast errors in Section 4.3 showed that acceptable results are obtained for 15 min probe lookahead if the wind forecast rms errors are in the 6 - 9 knot region. However, this study may be somewhat optimistic since the distance parameter for wind error correlation was set at 500 nm, whereas recent studies (Ref. 20) show that the correlation in wind forecast errors is about one-third this value. Redoing this sensitivity with the distance parameter set at 133 nm showed that somewhat better forecasts with errors in the 4 - 6 knot rms range are desirable for medium term conflict probe. Consequently, we have concluded that 3 - 6 hr forecasts are not sufficient for 20 min conflict probes, since accuracies on the order of 5 knots rms are required for best results. This will probably require more sophisticated update techniques such as Waftage (Ref. 20) or the Integrated Terminal Weather System (ITWS) (Ref. 7), which updates the background numerical weather forecasts on an hourly or better basis.

5.0 Conclusions and Recommended Studies

In this study we have examined a number of issues related to separation assurance and the use of advanced automation systems such as conflict probe for transitioning to Free Flight. Many of the analyses in this report are preliminary explorations of these issues, and the study results are tentative in the sense that much further work remains in order to validate both the study methodology and the working assumptions used to represent current and future CNS / ATM technology. We here summarize some of the fundamental concepts which underlie this study, and point to further work which is needed to validate and extend these concepts:

* The basic thesis behind this study is that separation assurance can be subdivided into distinct time scales, i.e. medium term, short term, and immediate separation assurance. For the proposed initial step to Free Flight, extended studies are needed to evaluate the feasibility of medium term separation using advanced decision support tools such as conflict probe and trial resolution planning. These studies should include Controller-in-the-Loop real time simulation of the conflict probe / conflict management process and its effect on workload and controller productivity. In addition, the effect of system failures must be analyzed, and fall-back procedures developed which will allow the operators to safely transition to manual operations when decision support tools are not available or not reliable due to failures.

* A Cleveland Center simulation model was used to develop scaling laws and relationships between encounter rates and separation standards, and the effect of these parameters as a function of traffic growth. Further studies are needed to validate encounter rate as a gross measure of Center workload, and to evaluate the influence of other factors which were ignored in this analysis. For example, other factors which could be important as traffic increases include

  * the effect of sector handoffs and transfers of control,
  * the effect of local aircraft density, and
  * the effect of multiple aircraft encounter scenarios.

Controller-in-the-loop simulations will be required to resolve this issue, and to develop more refined measures for specifying future system operational requirements.

* A horizontal plane conflict probe simulation was used to evaluate the relationship between horizontal separation standards and encounter CPA distance. However, the Cleveland Center simulation showed that over 80% of the encounters involved at least one of the aircraft in climb or descent mode. Thus, the conflict probe methodology needs to be extended to evaluate 3-D encounter scenarios, and to evaluate the effect of horizontal and vertical conflict resolution strategies. The difficulty of this problem arises from the complex dynamics involved in vertical transitions compared with those for cruise. However, improved data fusion and trajectory synthesis methodologies are essential for development of reliable and accurate 3-D

conflict probes. The development of a 3-D conflict probe should include estimates of critical parameters for encounters, and covariance uncertainty in these estimates. For example, the following parameters may be required for 3-D conflict detection:

* CPA time and CPA distance
* Entry and Exit Times of horizontal encounter (separation less than acceptable)
* Entry and Exit Times of vertical encounter (separation less than acceptable).

Some method of accommodating prediction uncertainty is necessary, since the definition of when a vertical or horizontal encounter will occur needs to include a buffer for prediction uncertainty in addition to the applicable separation standard.

* The allocation of CNS requirements to meet specified separation standards is implicitly based on an underlying collision risk methodology, e.g. the specification of RNP levels consistent with a given separation standard. A formal collision risk methodology needs to be developed which includes attributes of accuracy, integrity, and availability for development of future CNS systems explicitly designed to provide specified levels of Required System Performance (RSP). This methodology should include as a minimum :

- the effect of Navigation and FTE errors, in normal operating mode, and considering gross navigation errors reflecting system failures,

- the effect of surveillance and conformance monitoring, including failure to detect aircraft conflicts and gross path deviations, and

- the effect of ATC and controller-pilot communications in resolving and intervening tactically when necessary to prevent loss-of-separation.

Although simulations such as those in this study may be used to provide data for the collision risk analysis, it is essentially seen as an allocation of probabilities of rare events which are constrained to meet some specified target level of safety.

In the text which follows we briefly describe three specific study areas which are recommended for follow-on work. These areas were selected as especially promising for future research based on insight gained in this study, and based on common Boeing / NASA interest in Free Flight and advanced CNS / ATM systems.

5.1 Operational Concepts and Requirements for Free Flight

The proposed study task focuses on further development and refinement of our Cleveland Center traffic simulation model for examining operational concepts for Mature Free Flight, and for developing operational requirements consistent with workload constraints at the En Route Centers. This task would include:

* Cleveland Center benchmark traffic model validation,

* model refinement of encounter statistics based on Conflict Probe alerting,

* modeling and simulation of mature Free Flight concepts such as cruise climbs and dynamic density routing constraints.

The first sub-task includes validation and refinement of the 1995 benchmark simulation using ETMS data to validate Cleveland Center traffic loads and encounter rates, and developing a refined database of aircraft performance parameters for TAAM simulations. The objective of this sub-task is to validate that the benchmark simulation adequately models traffic and aircraft encounters within the Cleveland Center. The ETMS data will also be analyzed to evaluate other traffic measures such as local traffic density and relative frequency of multiple aircraft encounters.

The second sub-task is based on the premise that considerably more interventions may be required due to surveillance and prediction uncertainty than are actually necessary due to proximate encounters. In our studies we approximated the number of encounters requiring intervention as a function of CPA distance, but we did not account for the uncertainty in predicting times of horizontal and vertical loss-of-separation. This sub-task would provide model refinements to remedy this deficiency in modeling encounter statistics.

The third sub-task would examine the effect of Free Flight operational concepts beyond those evaluated to date. This would include explicit modeling of terminal area routing constraints and the effect of such constraints on traffic encounters and traffic density, and the effect of permitting en route cruise climbs for properly equipped aircraft.

5.2 Conflict Probe and Surveillance Requirements for Vertical Transitions

This proposed study task would examine tracking and data fusion concepts for accurate synthesis of climb and descent trajectories, and application of this technology to 3-D conflict detection. The objectives of this study task would be to evaluate and recommend preferred concepts for medium term prediction of vertical transition paths, and to develop technical requirements for wind forecasting, surveillance, and path intent data needed to implement an advanced 3-D conflict probe. The proposed study would include at least three sub-tasks:

* evaluation of advanced tracking / fusion concepts for vertical transitions including limited simulations of one or more concepts, i.e.

    - use of conventional, constant acceleration model Kalman filter trackers,

- use of Interacting Multiple Model (IMM) technology to track complex aircraft guidance laws such as constant IAS flight segments,

- use of nominal energy state tables and energy state error parameters for integrated vertical path tracking and path predictions.

* synthesis and evaluation of three-dimensional conflict probe, extending the covariance methodology and methods of the current study, and

* evaluation of technical requirements for data fusion sources including surveillance and weather forecasting requirements.

Although several conflict probes have been developed in past studies, this study would focus on areas which have not been examined in depth, in order to obtain substantially more accurate trajectory forecasts and accurate estimates of conflict parameter uncertainty. The focus of these studies would be to improve the tracking algorithms for integrated tracking and path prediction during vertical transitions, and to utilize covariance methodology to estimate CPA uncertainty and to estimate the times of vertical and horizontal loss-of-separation.

5.3 Cooperative Separation Concept Evolution & Requirements Analysis

In this report we have briefly described a concept for airborne based separation for mature Free Flight operations. However, airborne separation based on ADS broadcast and Cockpit Display of Traffic Information (CDTI) technologies will probably evolve gradually, beginning with In-Trail stationkeeping and climb applications, and eventually including complex, Free Flight conflict management of crossing and opposing encounters. This proposed task would examine the evolution of CDTI concepts and technical requirements for cooperative separation applications, i.e.

* En Route Stationkeeping & Offset Passing,

* En Route / Oceanic Path Merging, and

* Mutual Separation Assurance for Free Flight (alert zone guidance concept).

The focus of these studies would be to develop the operational concepts in sufficient depth for first principles analysis of CNS and other avionics technical requirements to perform the required separation function. For the stationkeeping application, this would include analysis of data rates, sensor errors, and data latency for transition & maintenance of longitudinal, In-Trail separation. These applications would include analysis of CNS requirements for conflict detection, and limited simulation of the conflict resolution concepts to evaluate feasibility of the operational concepts.

6.0 References

(1) A. Warren, " ATCA Conference Paper on En Route Conflict Detection", BE43B-C94-089, Aug. 1994.

(2) B. Fordham, *AERA 2 Operational Description*, MTR-85W00066, Rev. 2, The Mitre Corporation, McLean, VA, 1990.

(3) B.C. Wetherby, J.C. Celio, S.M. Kidman, M.A. Stanley, *Full AERA Services Operational Description,* MTR-93W0000061, The Mitre Corporation, McLean, VA, Sept. 1993.

(4) K. Kastella and M. Biscuso, " Tracking Algorithms for Air Traffic Control Applications", Air Traffic Control Quarterly, Vol. 3, No. 1, 1995.

(5) J.L. Gertz, " Multi Sensor Surveillance for Improved Aircraft Tracking", The Lincoln Laboratory Journal, Vol. 2, No. 3, 1989.

(6) H.A.P. Blom and Y. Bar-Shalom, " The Interacting Multiple Model Algorithm for Systems with Markovian Switching Coefficients", *IEEE Trans. Auto. Contr.,* Vol AC-33, Aug. 1988.

(7) R.E. Cole and F.W. Wilson, "The Integrated Terminal Weather System Terminal Winds Product", The Lincoln Laboratory Journal, Vol. 7, No. 2, 1994.

(8) V.A. Orlando and G.H. Knittel, " GPS-Squitter: System Concept and Performance", Air Traffic Control Quarterly, Vol. 1, No. 4, 1994.

(9) *ICAO Draft Manual on Mode-S Specific Services*, SICAS Panel Working Group 1, WP /1, Mar. 1995.

(10) M. Ball, J.S. DeArmon and J.O. Pyburn, " Is Free Flight Feasible? Results from Initial Simulations", Journal of Air Traffic Control, Jan-Mar. 1995.

(11) RGCSP Working Group A, Working Paper 26, Appendix E, Sept. 1994.

(12) C. G. Hunter. et. al., "CTAS Trajectory Sensitivity Analysis and Potential Benefits Study", TM96150-1, Seagull Technology, Inc. , May 1996.

(13) J.N.P. Beers, et. al., " The Application of Trajectory Prediction Algorithms for Planning Purposes in the Netherlands ATC - System", *Aircraft Trajectories, Computation - Prediction - Control*, AGARD - AG- 301, Vol. 2, May 1990.

(14) H. Erzberger and L. Tobias, "A Time-Based Concept for Terminal-Area Traffic Management", Proceedings of the 1986 AGARD Conference No. 410, Efficient

Conduct of Individual Flights and Air Traffic, Brussels, Belgium, June 1986.

(15) R.A. Tornese, et. al., “Observations on the En Route Conflict Alert Function”, 37th Air Traffic Control Association Conference, Atlantic City, Nov. 1992.

(16) Handbook of Geophysics and Space Environments, S.L. Valley, ed., McGraw-Hill, 1968.

(17) J.E. Sanders and D.A. Forrester, “The Improvement of Meteorological Data For Air Traffic Management Purposes”, Stage 3 Report for Eurocontrol, PHARE Programme Task TM 02, Nov. 1995.

(18) H. Erzberger, “Conflict Detection and Resolution in the Presence of Trajectory Prediction Error“, 1996 AIAA Air Transportation Technical Committee Workshop, Washington DC, March 1996.

(19) C. A. Shingledecker and E.R. Darby Jr., “ Effects of Data Link ATC Communications on Controller Teamwork and Sector Productivity“, Air Traffic Control Quarterly, Vol. 3, No. 2, 1995.

(20) D. A. Forrester and G. C. Dean, “ Improvement of Meteorological Data for Air Traffic Management Purposes “, Air Traffic Control Quarterly, Vol. 2, No. 2, 1994.

(21) M. Haest and B. Govaerts, “ A Statistical Hypothesis Testing Approach to the Determination of Supportable Aircraft Separation Standards “, IEEE AES Systems Magazine, June 1995.

Appendix A: Conflict Probe Performance Evaluation Model

A.1 Purpose and Methodology

Purpose: The purpose of the Performance Evaluation Model (PEM) is to evaluate various conflict probe concepts on a common statistical basis, and to refine promising operational concepts. The model will incorporate predominant aircraft trajectory prediction error sources, so that the effect of CNS infra-structure can be evaluated and requirements levied for future Free Flight operations.

Methodology: A simple, 2-D conflict scenario between two en-route aircraft (the ownship and an intruder aircraft) is simulated. (A future version may extend this model to include 3-D encounters between climbing, constant altitude, and descending aircraft.) Many Monte-Carlo trials are used to simulate crossing conflicts and near encounters, and the effect of various prediction error sources in detecting and resolving conflicts. Sufficient Monte-Carlo trial runs are used to generate a continuous spectrum of encounters with Closest Point of Approach (CPA) varying from Mid-Air Collision distances out to 20 nm or more. The model uses random noise generation techniques to simulate error uncertainties in predicting aircraft trajectories over lookahead intervals of one to 30 minutes. The error uncertainties which are modeled include

* Flight Technical Error (FTE) in tracking the intended flight path,
* Wind field spatial variations and forecast error uncertainty,
* Surveillance errors including Radar tracker noise in estimating aircraft position and velocity states.

Simplified models of various conflict probe concepts are embedded in the model and evaluated statistically using multiple Monte-Carlo trials. Statistical measures of performance are then obtained including:

* Missed Conflict Detections
* False Alarms, i.e. unnecessary trajectory interventions
* Detection Times relative to time of closest approach.

Figure A-1 shows the top-level flow diagram for the Performance Evaluation Model.

A.2 Wind Prediction Error Modeling

The uncertainty in predicting along-track wind is one of the major error sources and limiting factors in any conflict probe method. Although the vector winds aloft are difficult to model with precision, fairly simple statistical models of wind variation as a function of altitude and along-track distance have been used by meteorologists to characterize the nominal behavior of the mean wind. We here use an exponential

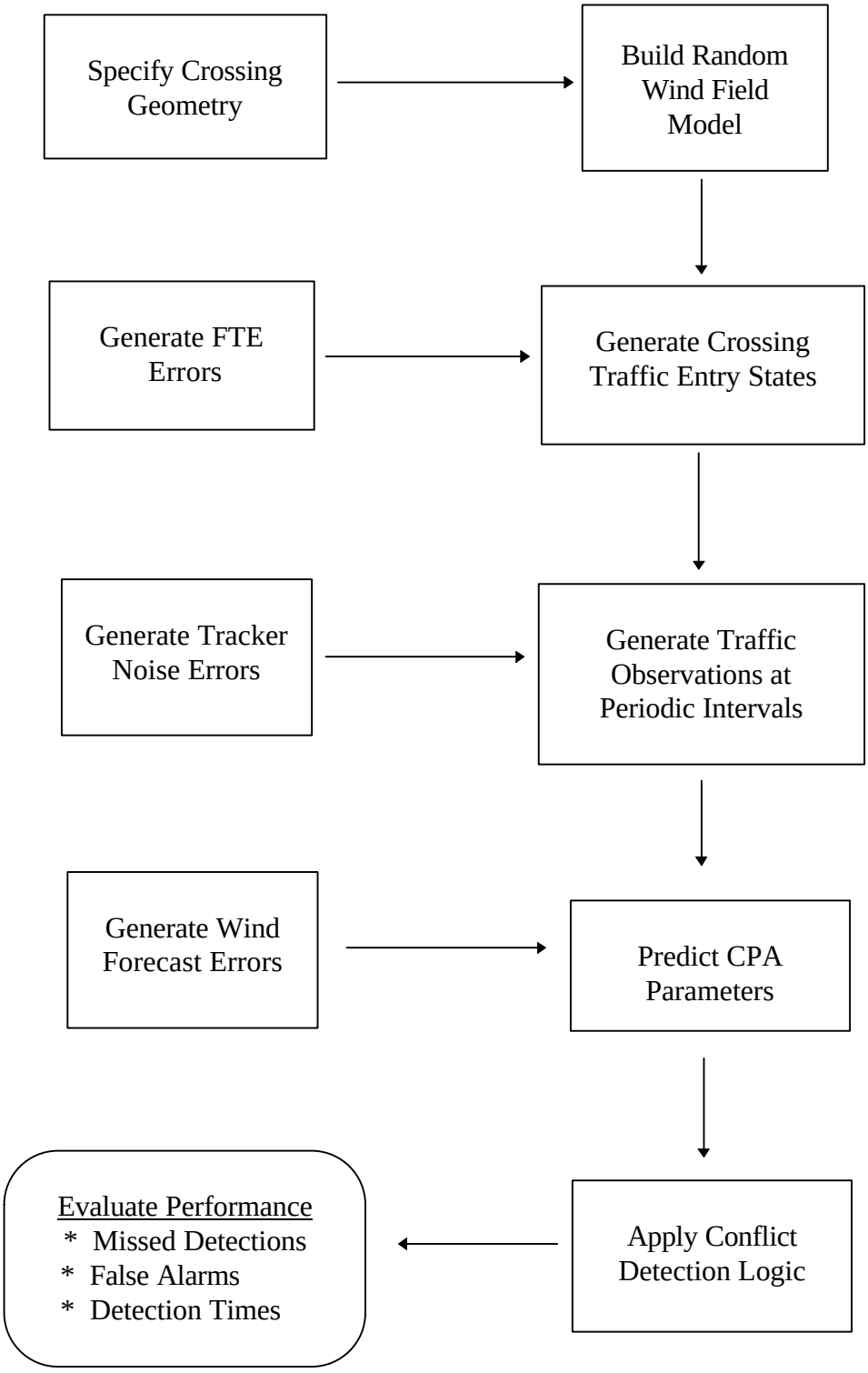

Figure A-1: Performance Evaluation Model Flow Diagram

autocorrelation function (Ref. 16) for constant altitude wind variations as a function of spatial distance to generate random along-track wind and wind shear variations for the ownship and an intruder aircraft during a crossing encounter. The wind variations are generated using independent random variables at each Monte-Carlo trial, but are assumed constant over the time interval of a crossing encounter, i.e. the wind field is frozen in time but varies spatially for a single trial run.

The geometry of a crossing encounter is shown in figure A-2. For convenience, the x-axis is defined along the ground track of the ownship aircraft, and the entry times of the aircraft into the simulation are such that without random wind variations, the intruder and ownship will arrive at the crossing fix simultaneously. Suppose V1 denotes the predicted ground speed of the ownship including nominal cruise airspeed and mean along-track wind, and V2 denotes the corresponding ground speed of the intruder aircraft. Then the distances D1 and D2 to the crossing fix in figure A-2 are selected such that

$$D1 = V1 * T$$
$$D2 = V2 * T,$$

where T denotes the nominal time from aircraft entry to arrival at the crossing fix.

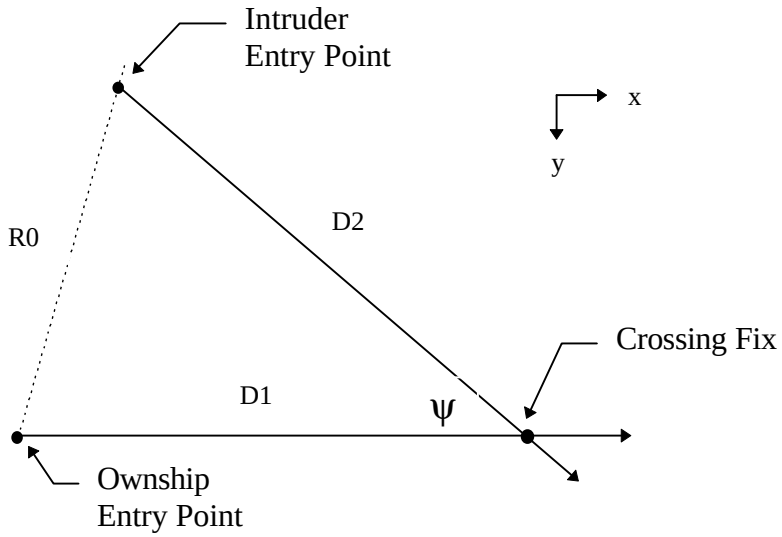

Figure A-2: Crossing Traffic Encounter Geometry

The vector wind uncertainty at the three points in Figure A-2 is first generated and then used to compute along-track wind and wind shear components. We define the following wind error components:

(Wxo, Wyo)' = vector wind uncertainty at the ownship entry point,

(Wxi, Wyi)' = vector wind uncertainty at the intruder entry point,

(Wxc, Wyc)' = vector wind uncertainty at the crossing fix point.

The winds are assumed to be circular normal errors at each point, i.e. the x and y components are assumed independent and identically distributed random variables with mean zero and standard deviation = σ_w. The correlation between the wind components is assumed exponential, i.e. the cross-correlations are only functions of the distances between two points. For the x components this means that

$$E\ Wxo^*\ Wxo = E\ Wxi^*Wxi = E\ Wxc^*Wxc = (\sigma_w)^2$$

$$E\ Wxo^*Wxi = (\sigma_w)^2 \exp(-R0 / L), \quad E\ Wxo^*Wxc = (\sigma_w)^2 \exp(-D1/ L)$$

$$E\ Wxi^*Wxc = (\sigma_w)^2 \exp(-D2 / L),$$

where L is a correlation constant, nominally = 670 nm. (The y axis components are given by similar equations.)

Let $\mathbf{s_x}$ denote the random vector consisting of the x axis components above, i.e.

$$\mathbf{s_x} = (\ Wxo,\ Wxi,\ Wxc\ )' \qquad (A.2\text{-}1)$$

Then the covariance matrix for the vector $\mathbf{s_x}$ is given by

$$\mathbf{Sx} = E\ \mathbf{s_x}\ \mathbf{s_x}' = (\sigma_w)^2 \begin{vmatrix} 1 & \exp(-R0 / L) & \exp(-D1 / L) \\ - & 1 & \exp(-D2 / L) \\ - & - & 1 \end{vmatrix}$$

where the lower diagonal terms are not explicitly represented since the covariance matrix is symmetric.

Now the question is how to generate a normal random vector with the specified covariance matrix **Sx**. Essentially, the answer is to generate a square-root factorization of the covariance matrix **Sx**. Suppose the random vector $\mathbf{s_x}$ is generated using three independent normal random variables z1,z2,z3 with mean zero and unit variance and a matrix transform of the form:

$$\mathbf{s_x} = \begin{vmatrix} G11 & 0 & 0 \\ G21 & G22 & 0 \\ G31 & G32 & G33 \end{vmatrix} * \begin{vmatrix} z1 \\ z2 \\ z3 \end{vmatrix} \qquad \text{(A.2 -2)}$$

Then the transform matrix **G** must satisfy the matrix equation

$$\mathbf{Sx} = \mathbf{G * I * G'} = \mathbf{G * G'} \qquad \text{(A.2 -3)}$$

Solving the above matrix equation for individual scalar terms yields:

$G11 = \sigma_w$

$G21 = \sigma_w * \exp(-R0 / L)$

$G31 = \sigma_w * \exp(-D1 / L)$

$G22 = \sigma_w * (1 - \exp(-2*R0 / L))^{1/2}$

$G32 = ((\sigma_w)^2 \exp(-D2 / L) - G21*G31) / G22$

$G33 = ((\sigma_w)^2 - G31*G31 - G32*G32)^{1/2}$

Consequently, the wind vectors are generated by computing the G terms above and then using (A.2 -2), i.e.

$Wxo = G11 * z1$

$Wxi = G21*z1 + G22*z2$

$Wxc = G31*z1 + G32*z2 + G33*z3,$

where z1, z2, z3 are normal random samples which are recomputed for each Monte-Carlo trial. The y component terms are generated similarly using three independent random samples to obtain independent x and y wind components.

In practice, only the along-track wind terms are needed since the aircraft navigation and autopilot systems automatically adjust for cross-wind errors. Consequently, the wind model reduces to computing the along-track wind and spatial shear terms for the ownship and intruder:

Wxo = along-track wind for ownship

dWxo = spatial derivative of along-track wind = (Wxc - Wxo) / D1

Wli = along-track wind for intruder

$$= \quad \cos\psi * Wxi + \sin\psi * Wyi$$

$$dWli = \text{spatial derivative of along-track wind}$$

$$= \quad \cos\psi * (Wxc - Wxi) / D2 + \sin\psi * (Wyc - Wyi) / D2$$

The aircraft along-track dynamics for the ownship and intruder are then approximated by simple differential equations which can be solved analytically:

Ownship Along-Track Dynamics:

The ground speed including wind shear is approximately given by

$$dx/dt = xo\_dot + (x - xo) * dWxo \qquad \text{(A.2-4)}$$

with $xo\_dot = V1 + Wxo$. Solving the differential equation (A.2-4) yields

$$x(t) - xo = xo\_dot * (\exp(t * dWxo) - 1) / dWxo \qquad \text{(A.2-5)}$$

$$x\_dot(t) = xo\_dot * \exp(t * dWxo) \qquad \text{(A.2-6)}$$

Approximating the exponential above by a first order Taylor series yields

$$x\_dot(t) \sim (V1 + Wxo)(1 + t * dWxo) \quad \text{Ownship speed}$$

$$x(t) - xo \sim (V1 + Wxo)(t + (t^2/2) * dWxo) \quad \text{Ownship distance}$$

Intruder Along-Track Dynamics:

The intruder dynamics and closed form predictions are similar to those above:

$$Li\_dot(t) = V2 + Wli + (Li - Lo) * dWli$$

$$\sim (V2 + Wli)(1 + t * dWli) \quad \text{Intruder speed}$$

$$Li(t) - Lo \sim (V2 + Wli)(t + (t^2/2) * dWli) \quad \text{Intruder distance}$$

where in the above expressions, xo and Lo denote the along-track axes at the entry fix, x(t) and Li (t) denote along-track distances as functions of time since arrival at the entry fixes, and x_dot (t) and Li_dot (t) denote the corresponding ground speed.

A.3 Closest Approach Truth Modeling

A “truth model” of two aircraft crossing in a close encounter is constructed based on: 1) the crossing angle between the two aircraft on ground tracks; (this angle is typically set at constant values of 30, 90, and 150 degrees per simulation), 2) random variables which model aircraft groundspeed and along-track wind shear, and initial lateral offset from the nominal path. For each Monte Carlo simulation these variables change and generate a stochastic traffic flow pattern culminating at the crossing fix. For each individual run, these variables are used to determine the crossing positions and times for both the ownship and the intruder. As such, the “truth model” calculates the closest position of approach (cpa) and closest time of approach (cpa_tim). Without wind shear, cpa and cpa_tim can be computed analytically. However, wind shear complicates the dynamics of path prediction and we must know cpa_tim accurately in order to analytically compute the ownship and intruder locations at the point of closest approach. This problem is solved in the following way: First, we compute the ownship and intruder positions at the nominal crossing time **Tc** of the two ground tracks. We know that cpa_tim is close to **Tc** by the method used to generate these paths. We then use the analytic solution for finding cpa_tim and cpa, given the aircraft positions at time **Tc**, ignoring wind shear. The following is a general outline of the steps required to generate the above:[1]

First, the **lateral offset** for ownship (**yoff1**) is computed based on a normally distributed random variable with a zero mean value and a standard deviation (**siglat**), which is nominally 0.5 n.m. based on precision RNAV performance. Then the lateral state components of the ownship are given by:

y1dist=yoff1,

y1dot=0.

Second, the initial **ground speed xo_dot** is calculated as the sum of a nominal ground speed and the along-track wind component Wxo which is modeled in Section A.2. That is, for the ownship:

xo_dot = V1+Wxo where

V1=target airspeed+along-track mean wind

Third, the nominal along track position x1dist and velocity x1dot at time **Tc** is a function of the distance between the aircraft at the entry point and crossing fix (D1), the mean crossing time (**Tc**), and the wind shear (**dwxo**). That is:

[1] Due to symmetry between the ownship and intruder aircraft calculations, the analytical description below is generic and applicable to both.

$x1dist = -D1 + xo\_dot*(1 + a/2 + a^2/6)*Tc$ and

$x1dot = xo\_dot*(1 + a + a^2/2)$ where

$a = dwxo*Tc$

$D1 = V1*Tc$

Note: Nominal values for the above parameters are: mean cross_time=25 min; target airspeed =480 knots; mean wind magnitude=40 knots; mean wind angle=-45 deg.

The calculations for the intruder states at time **Tc** are similar, except that we also rotate from along-track to x-y coordinates.

Fourth, **cpa_tim** and **cpa** are calculated by using the relative intruder geometry shown in Figure A-3:

cpa_tim = $-Rc*Rcdot/delvsq + Tc$

cpa = $Rc*(1-Rcdot^2/delvsq)^{1/2}sign(cross)$ where

$cross = delx*delydot - dely*delxdot$

$Rc = (delx^2 + dely^2)^{1/2}$

$Rcdot = (delx*delxdot + dely*delydot)/Rc$

$delx = x2dist - x1dist$

$dely = y2dist - y1dist$

$delxdot = x2dot - x1dot$

$delydot = y2dot - y1dot$

$delvsq = (delxdot)^2 + (delydot)^2$

Intruder position delx and dely at Tc

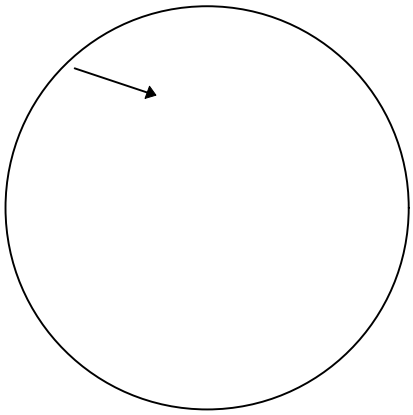

$\Delta V=(delxdot^2+delydot^2)^{1/2}$

$Rcdot=(delx.delxdot+ dely.delydot)/Rc$

$Dc=Rc.\cos\omega$

$\cos\omega=-Rcdot/\Delta V$

$cpa\_tim = Tc+Dc/\Delta V$

$=Tc-Rc.Rcdot/\Delta V^2$

$cpa=Rc.(1-(\cos\omega)^2)^{1/2}$

Figure A-3: Geometry for Computing cpa_tim

A.4 Surveillance System/Tracker Noise Modeling

The traffic model consists of modeling the trajectory for both an Ownship and an Intruder aircraft. Their position and velocity is estimated by a tracker which introduces both position and velocity errors relative to each observation point. This model utilizes the aircraft trajectory information embedded in the flight plan and fuses it with the tracker observations. Only the along-track surveillance information is retained for path predictions. In the context of a Monte Carlo simulation of the above traffic model, tracker noise associated with these observations needs to be modeled as an additional error source that contributes to the total prediction uncertainty for both the Ownship and Intruder aircraft.

To generate the tracker noise for along-track performance requires the following concepts and relationships:

Let the true along-track position and velocity of an aircraft be denoted by:

$$\mathbf{s_t} = (x_t , v_t)^T$$

and let the estimated position and velocity due to radar/tracker surveillance be denoted by:

$$\mathbf{s'_t} = (x'_t , v'_t)^T$$

the error then is defined as the difference between the true and estimate:

$$\mathbf{e_t} = s_t - s'_t = (x_t - x'_t, v_t - v'_t)$$

We assume here that the tracker can be modeled using a steady state α–β filter as defined by Kalata[2], i.e. α and β are the filter coefficients associated with the steady state position and velocity gains K_x and K_v.

The mean and covariance of the error $\mathbf{e_t}$ at each observation time t are given by:

$$E\mathbf{e_t} = 0.$$

and

$$E\mathbf{e_t}\mathbf{e_t}^T = \mathbf{S} = \sigma^2\mathbf{D} \text{ where}$$

[2] For more details see for example, Paul RKalata "The Tracking Index: A Generalized Parameter for α–β and α–β–γ Target Trackers", in IEEE Transactions On Aerospace and Electronic Systems Vol. AES-20. No. 2 March 1984.

$$\mathbf{D} = \begin{bmatrix} \alpha & \beta/T \\ \beta/T & [(2\alpha-\beta)\beta/2(1-\alpha)T^2] \end{bmatrix}$$

where T = update time of the tracker (min)

σ = RMS noise in the raw radar data reports (measurement noise) (nm)

α = gain constant design parameter

$\beta = 2(2-\alpha)-4(1-\alpha)^{1/2}$

Generation of Initial Tracker Error

To generate an initial Normally distributed tracker error $\mathbf{e_0}$ at the arrival time (initial start time for Ownship and Intruder Monte Carlo traffic simulation) and a covariance matrix defined by:

$$\mathbf{S} = \begin{bmatrix} S_{xx} & S_{xv} \\ S_{xv} & S_{vv} \end{bmatrix}$$

Let, ζ_1 , ζ_2 ~ be normally distributed random variables with zero mean and unity variance, and

$\rho^2 = (S_{xv})^2 / S_{xx}S_{vv}$, $\sigma_x = (S_{xx})^{1/2}$, $\sigma_v = (S_{vv})^{1/2}$

$h_{xx} = \sigma_x$, $h_{xvp} = \rho\sigma_v/\sigma_x$, $h_{vv} = \sigma_v(1-\rho^2)^{1/2}$

Then the initial error $\mathbf{e_0}$ is generated by:

$e_x = h_{xx}\zeta_1$ and $e_v = h_{xvp}e_x + h_{vv}\zeta_2$

$\mathbf{e_0} = (e_x, e_v)^T$ where e_x is position and e_v is velocity error

Therefore the estimated tracker position and velocity states at the arrival time are:

$x'_0 = x_0 - e_x$ and $v'_0 = v_0 - e_v$

Recursive Generation of Tracker Errors at Probe Update Times

Now, suppose that the conflict probe performs conflict detection at intervals of $\tau = mT$ (for example, m=6 if T=1/6 min, τ=1 min). Then the tracker noise is correlated from one update to the next update interval. It can be shown that (Bryson[3], section 11.2) correlation between $\mathbf{e}_t$ at the current time and $\mathbf{e}_{t-mT}$ at the last update satisfies the recursion:

$$\mathbf{C}_m = E\mathbf{e}_t \cdot \mathbf{e}^T_{t-mT} = \mathbf{A} \cdot \mathbf{C}_{m-1} \quad = \mathbf{A}^m \cdot \mathbf{C}_0 \qquad \text{(A.4-1)}$$

where $\mathbf{C}_0 = \mathbf{S}$ and

$$\mathbf{A} = \begin{bmatrix} (1-\alpha) & (1-\alpha)T \\ -\beta/T & (1-\beta) \end{bmatrix}$$

We will use this equation to derive a recursive formula for tracker noise $\mathbf{e}_t$ given the last error state $\mathbf{e}_{t-mT}$ as:

$$\mathbf{e}_t = \mathbf{F}_m \cdot \mathbf{e}_{t-mT} + \mathbf{G} \begin{bmatrix} n_1 \\ n_2 \end{bmatrix} \qquad \text{(A.4-2)}$$

where F_m and G are constant 2X2 matrices, and n_1 and n_2 are independent Normal (Gaussian) random variables with zero mean and unity variance.

Now, from equation (A.4-2) we find that the covariance of the current and the last error state is given by:

$$\mathbf{C}_m = E\mathbf{e}_t \cdot \mathbf{e}_{t-mT} = \mathbf{F}_m \cdot (E\mathbf{e}_{t-mT} \cdot \mathbf{e}^T_{t-mT}) + 0$$

$$\text{„} \qquad = \mathbf{F}_m \cdot \mathbf{S}$$

or $$\mathbf{F}_m = \mathbf{C}_m \cdot \mathbf{S}^{-1} = (\mathbf{A}^m \cdot \mathbf{S}) \cdot \mathbf{S}^{-1} = \mathbf{A}^m \qquad \text{(A.4-3)}$$

Similarly, the covariance of $\mathbf{e}_t$ is given by:

[3] See section 11.2 inBryson, A. E., Ho, Yu-Chi Applied Optimal Control,Blaisdell 1969.

$$\mathbf{S} = E\mathbf{e}_t \cdot \mathbf{e}^T_t = E\mathbf{e}_t(\mathbf{e}^T_{t-mT} \cdot \mathbf{F}^T_m + (n_1, n_2)\mathbf{G}^T)$$

$$\mathbf{S} = \mathbf{C}_m\mathbf{F}^T_m + E(\mathbf{F}_m\mathbf{e}_{t-mT} + \mathbf{G}\begin{bmatrix} n_1 \\ n_2 \end{bmatrix})(n_1, n_2)\mathbf{G}^T$$

$$\mathbf{S} = \mathbf{F}_m \cdot \mathbf{S}\mathbf{F}^T_m + \mathbf{G}\mathbf{G}^T \qquad \text{(A.4-4)}$$

without loss of generality we can assume that **G** has the special form:

$$\mathbf{G} = \begin{bmatrix} G_x & 0 \\ G_{xv} & G_v \end{bmatrix}$$

then, from (A.4-4) we find that

$$\mathbf{G}\cdot\mathbf{G}^T = \begin{bmatrix} G^2_x & G_xG_{xv} \\ G_xG_{xv} & G^2_v + G^2_{xv} \end{bmatrix} = \mathbf{S} - \mathbf{F}_m \cdot \mathbf{S} \cdot \mathbf{F}^T_m = \mathbf{Q} \qquad \text{(A.4-5)}$$

solving for the components of **G** yields:

$$G_x = (Q_{xx})^{1/2}, \quad G_{xv} = Q_{xv}/G_x, \quad G_v = (Q_{vv} - G^2_{xv})^{1/2} \qquad \text{(A.4-6)}$$

Now, the solution method for obtaining $\mathbf{F}_m$ and **G** given by equations (A.4-3) thru (A.4-6) reduces to the following:

Step 1: Recursively generate $\mathbf{F}_m$:

The matrix equation $\mathbf{F}_m = \mathbf{A} \cdot \mathbf{F}_{m-1}$ reduces to the following four scalar equations:

$$F_{11}(m) = (1-\alpha)(F_{11}(m-1) + TF_{21}(m-1))$$

$$F_{21}(m) = (1-\beta)F_{21}(m-1) - (\beta/T)F_{11}(m-1)$$

$$F_{12}(m) = (1-\alpha)(F_{12}(m-1) + TF_{22}(m-1))$$

$$F_{22}(m) = (1-\beta)F_{22}(m-1) - (\beta/T)F_{12}(m-1)$$

where $$\begin{bmatrix} F_{11}(1) & F_{12}(1) \\ F_{21}(1) & F_{22}(1) \end{bmatrix} = \mathbf{A} = \begin{bmatrix} (1-\alpha) & (1-\alpha)T \\ -\beta/T & (1-\beta) \end{bmatrix}$$

Step 2: Compute the matrix $\mathbf{Q} = \mathbf{S} - \mathbf{F_m} \cdot \mathbf{S} \cdot \mathbf{F^T_m}$ using $\mathbf{R} = \mathbf{F_m} \cdot \mathbf{S}$

$$R_{11} = F_{11}S_{xx} + F_{12}S_{xv}$$

$$R_{12} = F_{11}S_{xv} + F_{12}S_{vv}$$

$$R_{21} = F_{21}S_{xx} + F_{22}S_{xv}$$

$$R_{22} = F_{21}S_{xv} + F_{22}S_{vv}$$

$$Q_{xx} = S_{xx} - (R_{11}F_{11} + R_{12}F_{12})$$

$$Q_{xv} = S_{xv} - (R_{11}F_{21} + R_{12}F_{22})$$

$$Q_{vv} = S_{vv} - (R_{21}F_{21} + R_{22}F_{22})$$

Step 3: Solve for G_x, G_{xv}, G_v using equation (A.4-6)

Now, for each Monte Carlo trial run we can recursively generate the position and velocity surveillance errors at update time t, using equation (A.4-2):

$$e_x(t) = F_{11}(m)e_x(t-\tau) + F_{12}(m)e_v(t-\tau) + G_x n_1$$

$$e_v(t) = F_{21}(m)e_x(t-\tau) + F_{22}(m)e_v(t-\tau) + G_{xv} n_1 + G_v n_2$$

The along-track position and velocity estimates at time t including tracker noise are then given by:

$$x'_t = x_t - e_x(t) \quad \text{and} \quad v'_t = v_t - e_v(t)$$

A.5 Estimated Closest Approach Modeling

Section A.3 described the "truth model" which generates the appropriate parameters that define the modeled trajectories, times, and positions in space for both the ownship and intruder. This section describes the estimated/predicted or observed/measured flight path parameters for both the ownship and intruder. The simulation models the ownship and intruder conflict detection performance in the midst of uncertainties introduced by surveillance errors, wind and wind shear estimates, and other error sources (e.g. Flight Technical Errors). In the context of these uncertainties an estimated (observed) closest approach position **cpa_o** and time **cpa_tim_o** are calculated as the basis for the conflict detection algorithms.

It is assumed that the aircraft will follow the current flight plan with small lateral tolerances. Consequently, we can discard the lateral position and velocity states from the tracker in favor of the known flight plan based ground track, and use only the along-track position and velocity states for medium term predictions. Suppose ψ_o and ψ_I denote the ground track angles relative to North in a NED[4] system for the ownship and the intruder aircraft. The ownship and intruder velocity components at prediction time Δt are approximated by:

$$v_{xo}(\Delta t) = v_o(1+\Delta t S_f)\cos\psi_o \qquad \text{(A.5-1)}$$

$$v_{yo}(\Delta t) = v_o(1+\Delta t S_f)\sin\psi_o$$

$$v_{xI}(\Delta t) = v_I(1+\Delta t S'_f)\cos\psi_I$$

$$v_{yI}(\Delta t) = v_I(1+\Delta t S'_f)\sin\psi_I$$

where v_o and v_I denote the current ground speed estimates for the ownship and intruder (including tracker noise), and S_f, S_f' denote the wind shear forecasts over the prediction period along the ownship and intruder flightpath (See A.2-4 to A.2-6). There are two sources of wind shear forecast error: 1) time correlated errors due to forecast data time lag, and 2) position or grid related errors due to observation errors at discrete points.

The time correlated errors will tend to be highly correlated in time and distance and are represented by an exponential correlation. The grid related errors are more like independent noise sources which will result in shorter correlation lengths when interpolating winds across a grid system. A simple method to represent these sources was used in the Monte Carlo simulation, i.e. if S_T denotes the true along-track wind shear, then the forecasted wind shear S_f is modeled as:

$$S_f = bS_T+\sigma_s\zeta \qquad \text{where,}$$

[4] NED is North, East, Down convention (right hand rule).

b is a gain constant with nominal value b=0.75, ζ is a normal (0, 1) random variable and σ_s is a wind shear error constant with numerical value σ_s = 0.0005 which corresponds to 3 knots wind error per 100 nm:

0.0005per min = (3 kts)/(100 nm)(60 min)

The b constant is chosen to obtain the desired level of exponentially correlated noise corresponding to forecast lag, and the σ_s constant is chosen to represent the measurement error in the grid interpolation process.

Integrating the above velocity equations (A.5-1) yields the position components which are:

$$x_o(\Delta t) = x_o+v_o(\Delta t+\Delta t^2 S_f /2)\cos\psi_o \qquad \text{(A.5-2)}$$

$$y_o(\Delta t) = y_o+v_o(\Delta t+\Delta t^2 S_f /2)\sin\psi_o$$

$$x_I(\Delta t) = x_I+v_I(\Delta t+\Delta t^2 S_f' /2)\cos\psi_I$$

$$y_I(\Delta t) = y_I+v_I(\Delta t+\Delta t^2 S_f' /2)\sin\psi_I$$

where (x_o, y_o) and (x_I, y_I) denote the current horizontal position of the two aircraft as projected onto their intended ground track. Now from the velocity estimates (A.5-1) and position (A.5-2) component equations we obtain the predicted position of the intruder relative to the ownship:

$$\Delta x(\Delta t) = (x_I-x_o)+(v_I\cos\psi_I -v_o\cos\psi_o)\Delta t+(v_I S_f'\cos\psi_I -v_o S_f\cos\psi_o)\Delta t^2/2 \qquad \text{(A.5-3)}$$

$$\Delta y(\Delta t) = (y_I-y_o)+(v_I\sin\psi_I -v_o\sin\psi_o)\Delta t+(v_I S_f'\sin\psi_I -v_o S_f\sin\psi_o)\Delta t^2/2$$

$$\Delta v_x(\Delta t) = (v_I\cos\psi_I -v_o\cos\psi_o)+\Delta t(v_I S_f'\cos\psi_I -v_o S_f\cos\psi_o)$$

$$\Delta v_y(\Delta t) = (v_I\sin\psi_I -v_o\sin\psi_o)+\Delta t(v_I S_f'\sin\psi_I -v_o S_f\sin\psi_o)$$

We now obtain an implicit equation and a two step iteration for the time of minimum approach t_{min}, for two converging aircraft (R_dot<0). From (A.5-3), the predicted distance-squared for the two aircraft as a function of Δt is given by:

$$R^2(\Delta t) = \Delta x^2(\Delta t)+\Delta y^2(\Delta t) \qquad \text{(A.5-4)}$$

$$=(\Delta x_o+\Delta t\Delta v_x(\Delta t/2))^2+(\Delta y_o+\Delta t\Delta v_y(\Delta t/2))^2$$

where $\Delta x_o = x_I - x_o$, $\Delta y_o = y_I - y_o$. Differentiating (A.5-4) to find the minimum distance yields an orthogonality condition at $\Delta t = t_{min}$:

$$0 = (\Delta x_o + t_{min}\Delta v_x(t_{min}/2))\Delta v_x(t_{min}) + (\Delta y_o + t_{min}\Delta v_y(t_{min}/2)\Delta v_y(t_{min}) \qquad \text{(A.5-5)}$$

Solving (A.5-5) for t_{min} yields the implicit equation:

$$t_{min} = -(\Delta x_o \Delta v_x(t_{min}) + \Delta y_o \Delta v_y(t_{min}))/ \qquad \text{(A.5-6)}$$

$$(\Delta v_x(t_{min}/2)\Delta v_x(t_{min}) + \Delta v_y(t_{min}/2)\Delta v_y(t_{min}))$$

In practice, this equation can be solved in a few iterations or alternatively by analytically solving the cubic equation for t_{min} in (A.5-5). Ignoring the wind shear terms yields an initial estimate:

$$t_1 = -(\Delta x_o \Delta v_x(0) + \Delta y_o \Delta v_y(0))/(\Delta v_x^2(0) + \Delta v_y^2(0)), \quad \text{and then}$$

$$t_{min} = -(\Delta x_o \Delta v_x(t_1) + \Delta y_o \Delta v_y(t_1))/$$

$$(\Delta v_x(t_1/2)\Delta v_x(t_1) + \Delta v_y(t_1/2)\Delta v_y(t_1)).$$

The min distance or cpa_o is then obtained from (A.5-4):

$$R_{min} = cpa\_o = (R^2(t_{min}))^{1/2} \qquad \text{(A.5-7)}$$

The following is a list of the equations used to calculate **cpa_tim_o** and **cpa_o**. The definition of these variables are provided in the Nomenclature. First, the observed velocity and forecasted wind shear are computed using:

vgndop=vgndo-Ev

vgndip=vgndi-E2v

dwxop=Fore_const*dwxo+sig_shear*N(0, 1)

dwxip=Fore_const*dwxi+sig_shear*N(0, 1)

where N(0, 1) denotes a Gaussian random variable with mean zero and unit variance. Then the observed relative position and velocity states are calculated:

s1dist_o = -D1+vgndop*(dt+dwxop*dt^2/2)+Ex

s2dist_o = -D2+vgndip*(dt+dwxip*dt^2/2)+E2x

s1dot_o = vgndop*(1+dwxop*dt)

s2dot_o = vgndip*(1+dwxip*dt)

delx_o = s2dist_o*costhe-s1dist_o

dely_o = s2dist_o*sinthe

delxdot_o = s2dot_o*costhe-s1dot_o

delydot_o = s2dot_o*sinthe

The first iteration for cpa_tim_o is then given by:

dotp = delx_o*delxdot_o+dely*delydot_0

delvsq_o = $delxdot\_o^2$+$delydot\_o^2$

timo = -dotp/delvsq_o

The first iteration for cpa_tim_o is then calculated:

temp1 = s2dot_o*dwxip*costhe-s1dot_o*dwxop

tempx = timo*temp1

delvx2 = delxdot_o+tempx/2

delvx=delxdot_o+tempx

temp2=s2dot_o*dwxip*sinthe

tempy=timo*temp2

delvy2 = delydot_o+tempy/2

delvy=delydot_o+tempy

denom = delvx2*delvx+delvy2*delvy

cpa_tim_o = -(delx_o*delvx+dely_o*delvy)/denom

Finally, the estimated cpa is given by:

delx2 = delx_o+cpa_tim_o*delvx2

dely2 = dely_o+cpa_tim_o*delvy2

cross_o = delx2*delvy-dely2*delvx

$delv = (delvx^2 + delvy^2)^{1/2}$

cpa_o = $(delx2^2+dely2^2)^{1/2}$ *sign(cross_o)

A.6 Conflict Detection and Performance Modeling

The conflict detection methods in this report are based on two dominant characteristics of the estimated CPA parameters (cpa_o and cpa_tim_o):

(1) The quality of the CPA estimates improve as the time to closest approach decreases, since path prediction errors decrease with reduced cpa_tim_o,

(2) The cpa_o estimate may be quite noisy from one probe update time to the next, even if the aircraft tracks are heavily smoothed.

As a result the detection algorithm modeled here examines the cpa_o and cpa_tim_o estimates at each probe update time and then sets a detect_flag into one of three possible states:

* detect_flag = 0	'No Conflict Declaration' state	
	= 1	'Decision not possible' state
	= 2	'Conflict Alert Declaration' state.

If detect_flag =0, then the aircraft pair are deleted from the list of potential conflicts, until some delta_time interval has passed or one of the aircraft is found no longer in conformance with the last path predictions. Similarly, if detect_flag =2 then the controller is notified of the potential separation violation and time-to-violation. However, if detect-flag =1, then the algorithm in effect waits until the quality of the estimates improve and a better conflict decision is possible. In addition, tracker noise will sometimes result in large CPA deviations which can result in wrong conflict decisions based on single probe data. Thus, the algorithm also checks the consistency of the cpa_o estimates using two successive probe updates and sets detect_flag =1 if the results are not consistent, i.e. no declaration is made unless the cpa_o values cross a decision threshold on two successive update times. Although more sophisticated detection logic is feasible, this approach was easily prototyped and proved fairly robust for the conflict probe studies in this report.

The conflict probe uses four parameters at each probe update:

max_looktime = the maximum lookahead for path predictions

min_looktime = the minimum time for effective conflict alerting

inner_cpa = CPA decision threshold for conflict alert declarations

outer_cpa = CPA decision threshold for no-conflict pair declarations.

Once the estimated cpa_o and cpa_tim_o are computed for a potential conflict pair, the following steps are applied:

(1) cpa_tim_o checking:

If cpa_tim_o > max_looktime, then the quality of the CPA parameters is questionable and consequently we set detect_flag =1. Similarly, if cpa_tim_o < min_looktime (where min_looktime is less then or equal to the lookahead time for the Short Term Conflict Alert algorithm), then the conflict pair is being managed by the sector controller and we set detect_flag = 1 to take no further action. Otherwise, if cpa_tim_o is within these time limits we proceed to step (2).

(2) conflict status detection logic:

If cpa_o< inner_cpa on two successive probes, then we declare a conflict alert, i.e. detect_flag = 2. The inner_cpa threshold is chosen at some value exceeding the separation standard, i.e. for the fixed threshold algorithm when sep_std = 4, we typically set inner_cpa = 5 nm, in order to keep the probability of missed detections less than 2%. (See Figure A-3.) The covariance method and conformance method algorithms select the inner_cpa dynamically, depending on CPA uncertainty and conflict geometry, whereas the fixed threshold method selects inner_cpa based on worst case conditions at maximum lookahead and at crossing angles of 20 - 30 deg. (For further details on relative performance of these algorithms see Section 4.)

If cpa_o > outer_cpa on two successive probes, then we declare this pair conflict free, i.e. detect_flag = 0. The outer_cpa threshold should be selected large enough to prevent an excessive number of false alerts, and significantly larger than the inner_threshold in order to avoid missed detections. However, the outer_cpa threshold should change dynamically with CPA uncertainty, in order to minimize the number of false alerts when CPA can be estimated accurately. For the fixed threshold algorithm, we set outer-cpa larger than the intervention standard (See Figure A-3), so that the algorithm performs well in worst case conditions. The covariance method selects the outer_cpa threshold dynamically, and typically does not begin making any decisions until outer_cpa is slightly larger than the intervention standard. Both the outer and inner thresholds then vary dynamically with approach time. (See Figure 5).

If neither of the above conditions holds, then detect_flag=1, and the current estimates of cpa_o and cpa_tim_o are stored for use on the next probe update.

The performance of the conflict detection algorithms is assessed by counting the number and percentage of missed detects and false alerts, and by evaluating warning time statistics, where warning time is the estimated time remaining until a separation violation occurs, measured from time of first alert. For each Monte Carlo run, we first determine the detect_flag status when the conflict probe ended, and the truth cpa status as defined by the following ‘truth_flag’ :

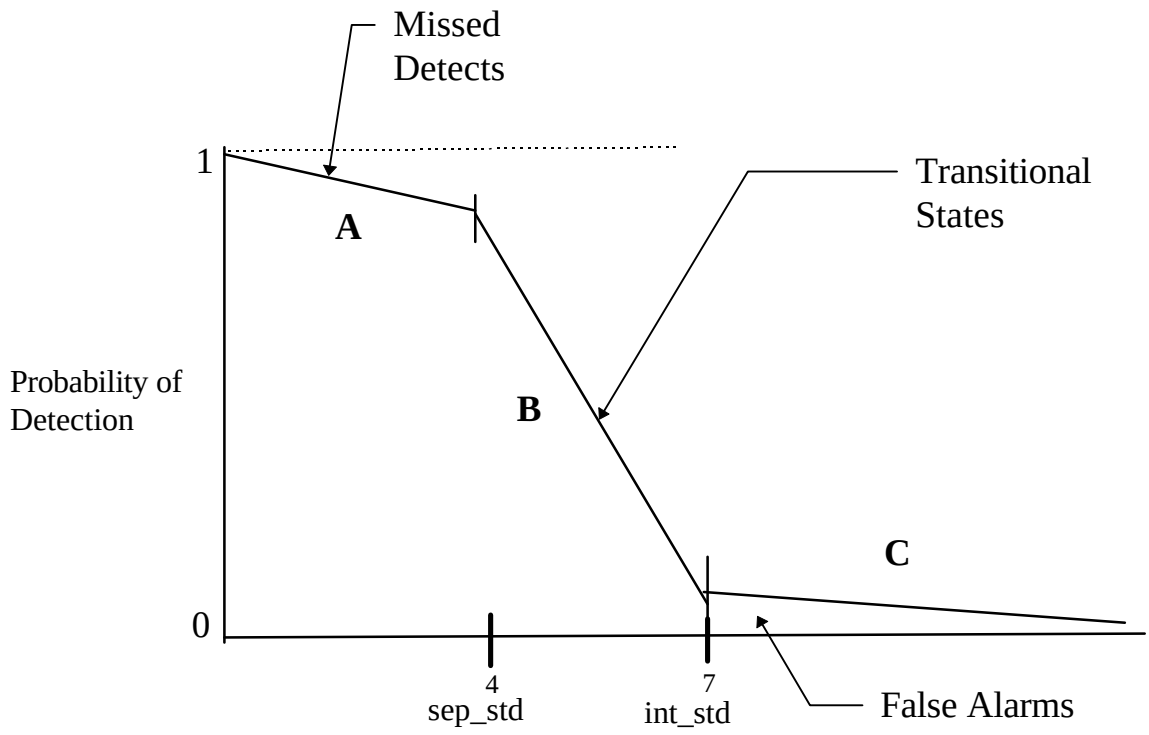

Figure A-4: Sketch of Conflict Probe Detection Performance

Truth_flag	= 0	If true cpa > Intervention standard (no alert needed)
	= 1	If true cpa <= Intervention standard, and true cpa > Separation standard
	= 2	If true cpa < Separation standard (alerting needed).

Then, the missed detects are those runs where truth_flag=2 and detect_flag = 0 or 1 (region **A**, Figure A-4), and the false alerts (region **C**, Figure A-4)are those where truth_flag=0 and detect_flag = 2. The other cases represent correct classifications or transitional cases (region **B**, Figure A-4) for conflict detection. The percentage of missed detects is found by counting the missed detects over many runs (typically 1500 to 2000 Monte Carlo runs) and dividing by the total number of runs where the truth_flag =2. Similarly, the percentage of false alerts is obtained by counting the number of false alerts and dividing by the number of cases where truth_flag = 0.

A more detailed picture of conflict probe performance can be presented as a histogram of conflict detection probability as sketched in Figure A-4, but this level of detail is not needed for most conflict probe studies.

In our studies, warning time is computed as the time from first alert until the separation is equal to the inner_cpa threshold. This time is computed when detect_flag=2 using

$$warn\_time = cpa\_tim\_o - \left(\left((inner\_cpa)^2 - (cpa\_o)^2 \right) / delv^2 \right)^{1/2}$$

where delv is an intermediate quantity representing the relative velocity between the ownship and the intruder in the CPA calculations in Section A.5.

A.7 Monte Carlo Performance Evaluations

In order to assess the accuracy levels required for the estimation of the probabilities of Missed Detection and False Alarm in the Conflict Probe study, the convergence of their average values after a number of Monte Carlo simulations was evaluated for a fixed threshold conflict probe logic concept configured with a separation standard of 3 nm, inner threshold of 3 nm, outer threshold (and outlier) of 5 nm, and a lookahead time of 20 min. Two basic approaches were taken: 1) the **running average** probabilities were computed for sets of n Monte Carlo simulations represented by an average over an ensemble of n runs. For example, Figures A-5 through A-8 show convergence for n=900 and n=1800 derived from a total number of N=6000 runs; 2) the **cumulative convergence** of the probabilities of Missed Detection and False Alarm is shown in Figures A-9 and A-10.

The **running average** method for the probability of **missed detection** shows the results of averaging over n=900 (Figure A-5). At this relatively low sample size, the convergence of the final value of average probability of missed detects is not robust as exemplified by the lack of data in some of the ensemble averages. As a general reference, however, the overall average value of missed detect probabilities over the total ensemble average is 0.94% indicating that even at this low ensemble sample size the average of the variations in the probability of missed detects is less than 1%. When the ensemble average is doubled to n=1800 (Figure A-6), the missed detect probabilities show significantly less variation, although the average of the total set of ensembles for this case is 0.95%, not significantly different from the n=900 results. It may be concluded that n=1800 is minimally adequate to predict a fairly robust value for the probability of missed detect performance of the conflict probe model.

Similarly, for the probability of **false alarms** compiled with the **running average** method, the statistical results are summarized in Figures A-7 and A-8 for the ensemble running averages of n=900 and n=1800, respectively. The average probability of false alarms for both cases was about 3% although the statistical variation of the ensemble averages is greater for the n=900 case in Figure A-7 as compared to the n=1800 case

shown in Figure A-8. Regardless of the variations, these results indicate that the rate of false alarms is estimated to a precision better than1% with n>=1800 samples.

The other method of evaluating the statistical convergence characteristics of the Monte Carlo simulation used the **cumulative convergence** method. The convergence statistics for the **missed detect** probability is shown in Figure A-9. The results indicate that a final estimated value of the probability of missed detects settles approximately at 1% after about n=1800 to n=2000 Monte Carlo simulations. This generally confirms the conclusions of the above running average mode of evaluation. Similarly, Figure A-10 shows the cumulative convergence of the probability of **false alarms**. The variation in the statistics begin to settle at an approximate final value of 1.8% after about n=2000 Monte Carlo simulations.

Given the above general findings on the statistical convergence characteristics for both missed detect and false alarm performance, the conflict probe studies were generally conducted with a minimum of 1800 Monte Carlo runs. In some cases, a greater number of cases were required to attain better robustness and convergence performance.

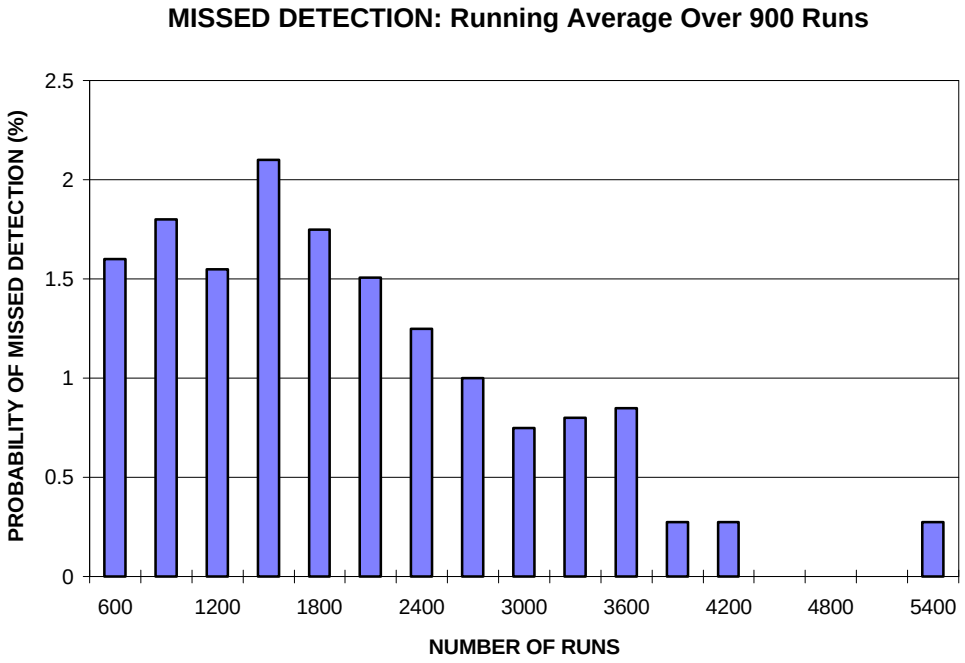

Figure A-5: Conflict Probe Missed Detection Statistics - 900 Sample Averages

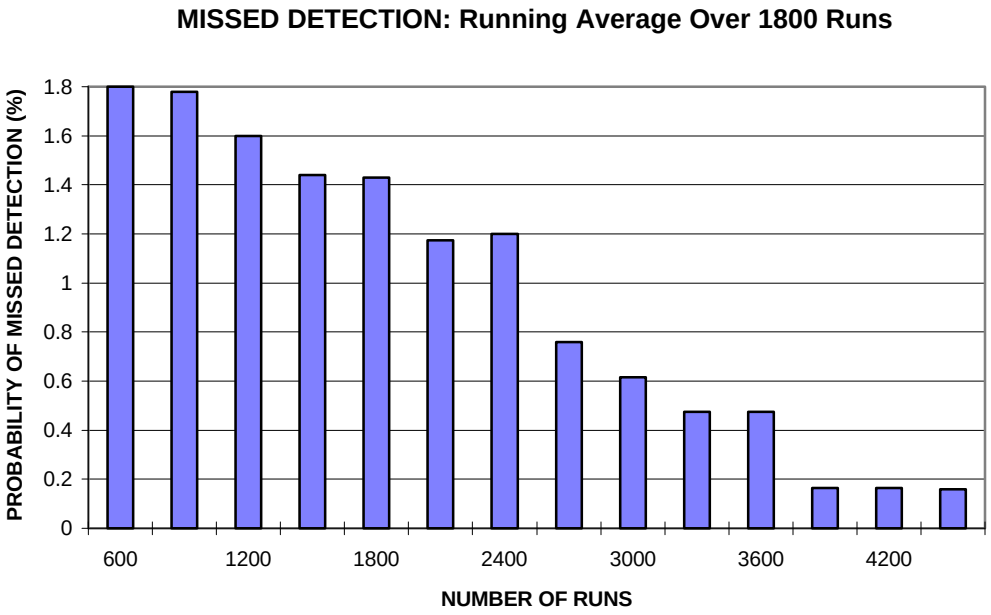

Figure A-6: Conflict Probe Missed Detection Statistics - 1800 Sample Averages

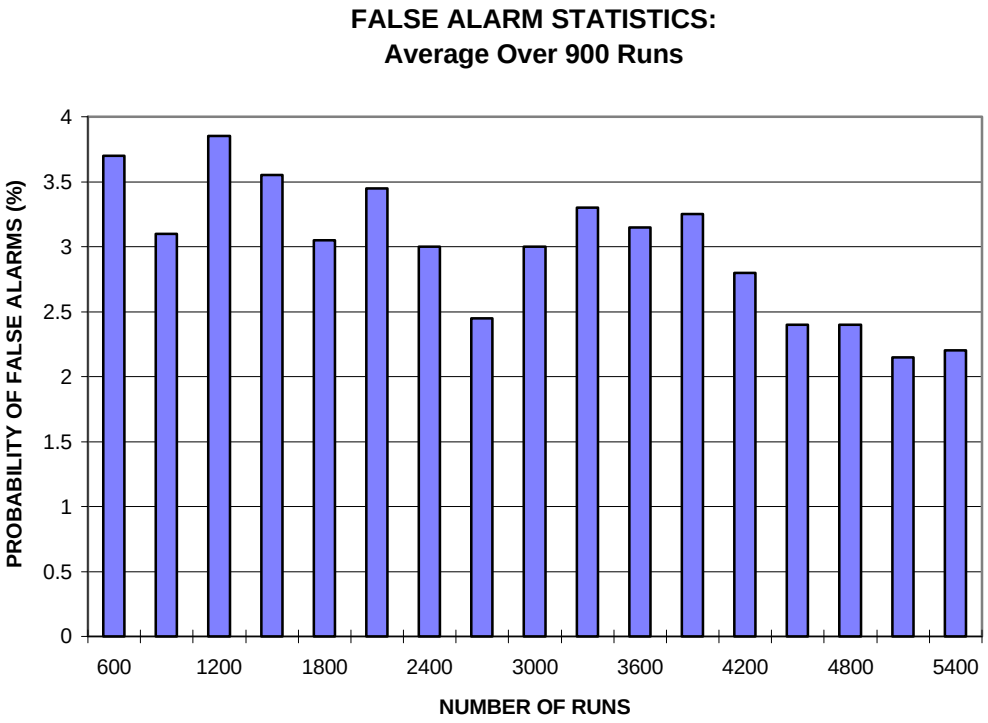

Figure A-7: Conflict Probe False Alarm Statistics - 900 Sample Averages

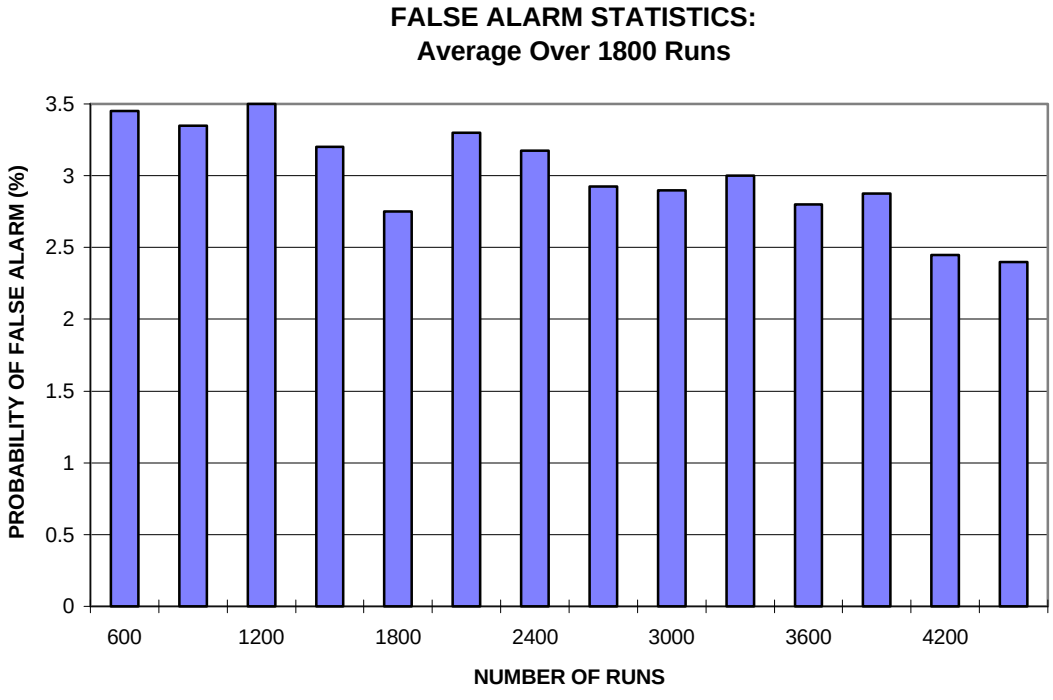

Figure A-8: Conflict Probe False Alarm Statistics - 1800 Sample Averages

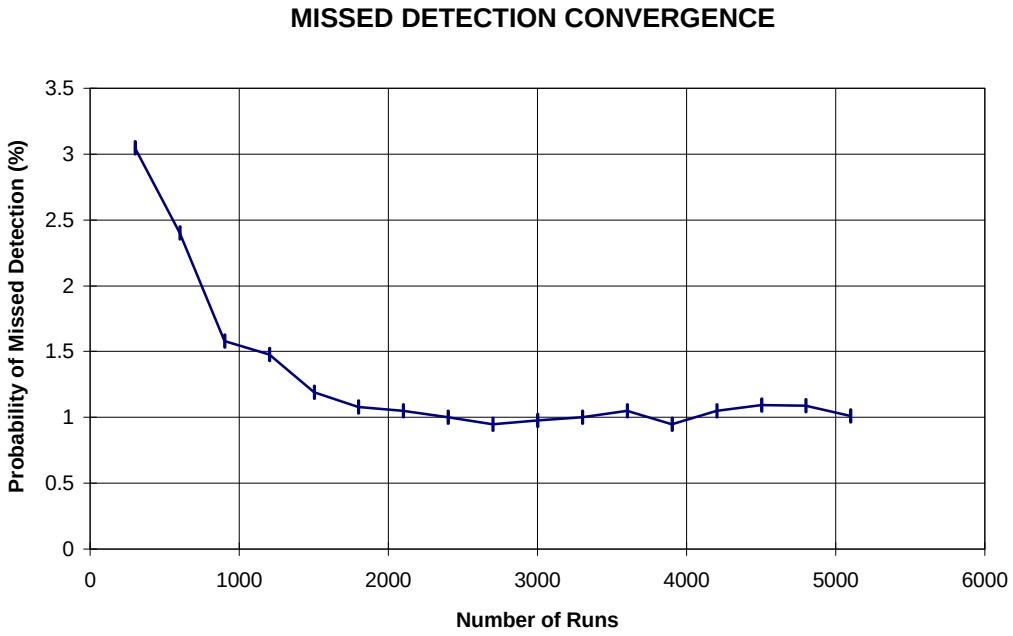

Figure A-9: Conflict Probe Missed Detection Convergence Statistics

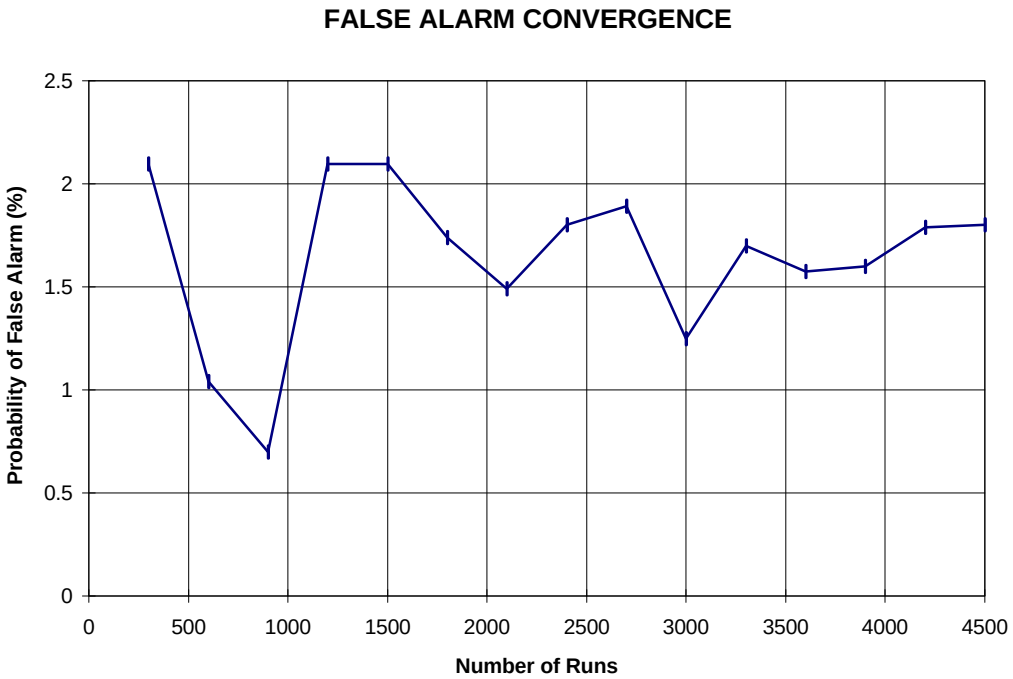

Figure A-10: Conflict Probe False Alarm Convergence Statistics

Appendix B: Conflict Probe Covariance Analysis

This section derives the math equations underlying the covariance based conflict probe.
(See Section 4.1 for an overview of the technical approach.) Section B.1 derives the longitudinal (along-track) covariance uncertainty for medium term path predictions. Section B.2 derives the two-dimensional covariance uncertainty for an intruder aircraft, relative to a reference or "ownship" aircraft path, explicitly using the equations in Section B.1. Section B.3 applies the results of Section B.2 to obtain dynamic equations for conflict detection and no-conflict decision thresholds, based on predicted path covariance uncertainty. Section B.4 derives an expression for predicted probability of loss-of-separation between two aircraft. This variable may be useful operationally, for planning conflict resolution tactics and for timing conflict resolutions, i.e. whether to act now to prevent a potential conflict, or to wait until the conflict situation becomes clearer. Section B.5 derives precise equations for predicting the start and end times for crossing / opposing and limited duration in-trail path conflicts.

B.1 Longitudinal Prediction Error Modeling - Cruise Flight

In this section we model the error dynamics for longitudinal flight predictions. Three error sources are modeled in our analysis:

* surveillance estimation error on along-track position and velocity states,
* wind - forecasting error, including the effect of horizontal wind shear,
* longitudinal speed-following Flight Technical Error (FTE).

This section provides a condensed derivation of covariance formulae for estimating longitudinal prediction uncertainty as a function of prediction time. In our studies, the speed following error terms were deleted, since the surveillance and wind forecasting errors typically dominate the steady state speed following errors. However, the speed following errors for manually flown flight can be on the order of three knots rms (Ref. 12), and should be included for completeness.

The basis of our error model are three differential equations which describe the evolution of prediction errors as a function of prediction time t. The first equation is a partition of the predicted ground speed x_dot = Vx (t) into several components:

$$Vx = Va + Wf(x) + Wx \qquad \text{(B.1 - 1)}$$

where

Vx = predicted ground speed at time t
Va = along-track true air speed at time t
Wf(x) = forecasted along-track wind at position x(t)
Wx = along-track wind forecast error

x (t) = predicted along-track path location at time t.

The assumed state space model for longitudinal speed control is given by

$$Va\_dot = -\lambda (Va - \underline{Va}) + \varepsilon \qquad \text{(B.1 - 2)}$$

where

λ = is the reciprocal of the time constant τ for speed control (τ is ~ 8 min for a Boeing 737 auto-throttle system)
$\underline{Va}$ = commanded (nominal) true air speed
σ_V = steady state speed following rms error (in nm/ min)
ε = random Gaussian white noise process with mean zero and covariance

$$E\, \varepsilon(t)\, \varepsilon(s) = 2\, \lambda\, \sigma_V^{\,2}\, \delta_{t,\,s} \quad . \qquad \text{(B.1 - 3)}$$

The forecasted along-track wind is modeled as the sum of the forecasted wind at the current position xo, and an estimated wind shear prediction term:

$$Wf(x(t)) = Wf(xo) + t\, Sf(xo) * Vo \qquad \text{(B.1 - 4)}$$

where

Sf (xo) = the estimated horizontal wind shear: δ Wf / δx
Vo = ground speed at the current time: Vo = Vx (0).

The error Wx in the forecasted wind is assumed a Gaussian random process with mean zero and distance autocorrelation function

$$E\, Wx(t)\, Wx(t+s) = \sigma_f^2 \exp(-D / Lf) \qquad \text{(B.1 - 5)}$$

where

σ_f = the rms error in the along-track wind forecast
D = the along-track distance between x(t) and x(t+s) ~ Vo*s
Lf = the distance constant for wind forecasting in nm.

(We note that the covariance function for wind forecasting is similar to that assumed for mean wind error in Section A.2, except for the constants σ_f and Lf. The rms error σ_f is nominally 6 knots for a one hour update, fine grid forecast, and the constant Lf is nominally in the 75 to 150 nm range (Ref. 17, 20).)

The last equation can be converted into a time based autocorrelation function using the approximation D ~ Vo*s. This yields

$$E\, Wx(t)\, Wx(t+s) = \sigma_f^2 \exp(-ao * s) \qquad \text{(B.1 - 6)}$$

with ao = Vo / Lf. This transformation enables us to express Wx (t) as a stationary process generated by a random differential equation

$$Wx\_dot = - ao * Wx + \eta \qquad \text{(B.1 - 7)}$$

where η is a white noise process with mean zero and covariance

$$E\ \eta(t)\ \eta(s) = 2\ ao\ \sigma_f^{\,2}\ \delta_{t,\,s} \ . \qquad \text{(B.1 - 8)}$$

We now obtain an explicit differential equation for x_dot by expanding (B.1 - 1) and using the definition of Vo:

$$x\_dot\ (t) = Va + (Wf(xo) + t*Sf(xo)\ Vo) + Wx(t)$$

$$= Vo*(1 + t*Sf(xo)) + (Wx(t) - Wx(0)) + (Va(t) - Va(0)) \qquad \text{(B.1 - 9)}$$

Now defining the speed error state $\delta Va = Va - \underline{Va}$, we can express our error model as a state space differential equation for (x , δVa , Wx):

$$x\_dot = 0 * x + \delta Va + Wx + g(t) \qquad \text{(B.1 - 10)}$$
$$\delta Va\_dot = - \lambda\ \delta Va + \varepsilon$$
$$Wx\_dot = - a\ Wx + \eta,$$

where $g(t) = Vo*(1 + t*Sf(xo)) - \delta Va(0) - Wx(0)$.

The state space model given by (B.1-10) can be solved explicitly using exponential functions and integrals of exponential functions. This yields the following equation for along-track position x(t):

$$x(t) = xo + Vo*(t + Sf(xo)*t\text{^}2/ 2) +$$
$$[(1 - exp(-\lambda\ t)) / \lambda - t]*\ \delta Va(0) + \int (1 - exp(-\lambda\ s))(\varepsilon\ (t-s)/ \lambda) ds$$
$$+ [(1 - exp(-ao\ t)) / ao - t]*Wx(0) + \int (1 - exp(-ao\ s))(\eta(t-s)/ ao) ds,$$

where the above integrals are defined over $0 <= s <= t$.

Subtracting the estimated position $x' (t) = xo' + Vo'*(t + Sf(xo)*t\text{^}2 /2)$, where (xo',Vo') denote current aircraft tracker estimates of position and speed, yields the following error equations for predicted position at time t:

$$\delta x(t) = \delta xo + \delta Vo*(t + Sf(xo)*t\text{^}2/ 2) + \qquad \text{(B.1 - 11)}$$
$$[(1 - exp(-\lambda\ t)) / \lambda - t]*\ \delta Va(0) + \int (1 - exp(-\lambda\ s))(\varepsilon\ (t-s)/ \lambda) ds$$
$$+ [(1 - exp(-ao\ t)) / ao - t]*Wx(0) + \int (1 - exp(-ao\ s))(\eta(t-s)/ ao) ds,$$

where (δxo, δVo) denotes current tracker errors in estimating (xo, Vo). For short term predictions, with $\lambda\ t << 1$ and $a\ t << 1$ we can ignore horizontal wind shear and

approximate the exponential terms with a first order Taylor expansion. This yields the simpler error expression

$$\delta x(t) = \delta xo + t*\delta Vo + \int s\,\varepsilon\,(t-s)\,ds + \int s\,\eta\,(t-s)\,ds \qquad \text{(B.1 - 12)}$$

Finally, the covariance error for longitudinal predictions is obtained by computing the expected value $Pxx(t) = E(\delta x(t))^2$. Under the assumption that the error terms are all independent random values except for the tracker errors, and using covariance equations (B.1 - 3) and (B.1 - 8) yields

$$Pxx(t) = (Sxx + 2\,e(t) * Sxv + e(t)^2 * Svv) + (\sigma_f / ao)^2 * G(ao\,t) + (\sigma_V / \lambda)^2 * G(\lambda\,t) \qquad \text{(B.1 - 13)}$$

where

$$e(t) = t + Sf(xo)*t\text{^}2/2 \qquad \text{(B.1 - 14)}$$

$$G(u) = (1 - u - \exp(-u))^2 + (2u - 3 + 4\exp(-u) - \exp(-2u)) \qquad \text{(B.1 - 15)}$$

Similarly, for short term predictions using (B.1-12) yields

$$Pxx(t) = (Sxx + 2t*Sxv + t\text{^}2*Svv) + 2(a\,\sigma_f^2 + \lambda\,\sigma_V^2) * t\text{^}3/3 . \qquad \text{(B.1 - 16)}$$

We note that the effective time constant for the wind errors = 1 / ao = Vo / Lf. Assuming a nominal speed Vo = 8 nm / min for a turbojet and Lf = 132 nm, we obtain a typical time constant of about 16 min. Consequently, equation (B.1 - 13) should be used for medium term predictions with t > 8 min, and (B.1 - 16) may be used for short term predictions, i.e. for t < 5 min.

B.2 Intruder Prediction Uncertainty Modeling

Intruder Path in Ownship Coordinates

We here adopt the notation and aircraft naming conventions used in Section A.5. The analysis of ownship and intruder prediction uncertainty is more easily accomplished by using a coordinate system moving with the ownship. The ownship coordinate system is defined with the origin at the ownship location, the x-axis aligned with the aircraft intended ground track, and the y-axis orthogonal with positive axis in the direction of the right wing. We here develop equations for the intruder path and path uncertainty, relative to the ownship . Figure B-1 illustrates the geometry for the intruder path in ownship coordinates.

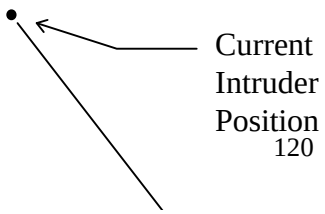

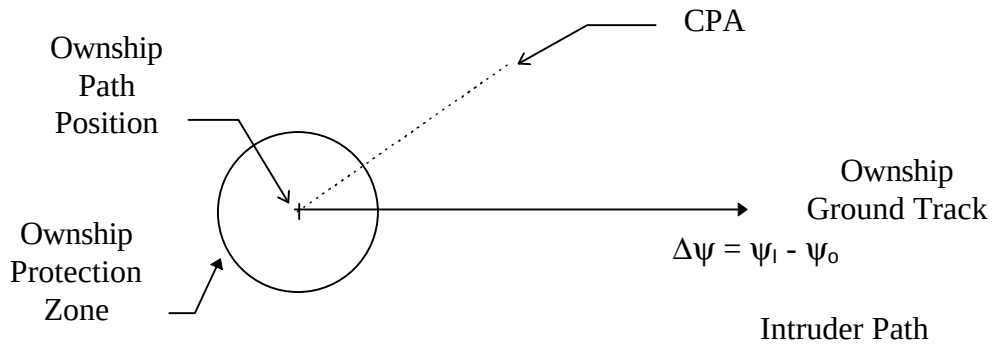

Figure B-1: Predicted Intruder path in Ownship Coordinates

Suppose we define primed coordinates as a rotation of the NED coordinates to align the x' axis along the ownship ground track. From equation A.5-2, the predicted position of the ownship at time Δt in the primed coordinates is obtained by rotating ($x_o(\Delta t)$, $y_o(\Delta t)$) by the ownship track angle ψ_o , i.e.

$$x'_o(\Delta t) = x_o \cos\psi_o + y_o \sin\psi_o + v_o e(\Delta t) \qquad \text{(B.2 -1)}$$

$$y'_o(\Delta t) = -x_o \sin\psi_o + y_o \cos\psi_o$$

where (x_o, y_o) denotes the ownship location at the current time, v_o denotes ownship ground speed, and $e(\Delta t)$ is defined by B.1 - 14, i.e.

$$e(\Delta t) = \Delta t + \Delta t^2 S_f / 2. \qquad \text{(B.2 -2)}$$

Similarly, the predicted position of the intruder at time Δt in coordinates rotated by the intruder track angle ψ_I is given by

$$X_I(\Delta t) = x_I \cos\psi_I + y_I \sin\psi_I + v_I e'(\Delta t) \qquad \text{(B.2 -3)}$$

$$Y_I(\Delta t) = -x_I \sin\psi_I + y_I \cos\psi_I$$

where (x_I, y_I) denotes the intruder location at the current time, v_I denotes intruder ground speed, and $e'(\Delta t)$ is defined by

$$e'(\Delta t) = \Delta t + \Delta t^2 S'_f / 2. \qquad \text{(B.2 -4)}$$

The intruder position in primed coordinates is then obtained by rotating the above equations by $\psi_o - \psi_I = -\Delta\psi$:

$$x'_I(\Delta t) = X_I(\Delta t) \cos \Delta\psi \; - Y_I(\Delta t) \sin \Delta\psi \qquad \text{(B.2 -5)}$$

$$y'_I(\Delta t) = X_I(\Delta t) \sin \Delta\psi + Y_I(\Delta t) \cos \Delta\psi$$

Consequently, the predicted intruder path in ownship coordinates is the difference between intruder and ownship paths in primed coordinates, i.e. from (B.2 -5) we find

$$\begin{bmatrix} \Delta x(\Delta t) \\ \Delta y(\Delta t) \end{bmatrix} = \begin{bmatrix} x'_I(\Delta t) - x'_o(\Delta t) \\ y'_I(\Delta t) - y'_o(\Delta t) \end{bmatrix}$$

$$= \begin{bmatrix} \cos \Delta\psi & - \sin \Delta\psi \\ \sin \Delta\psi & \cos \Delta\psi \end{bmatrix} \begin{bmatrix} X_I(\Delta t) \\ Y_I(\Delta t) \end{bmatrix} - \begin{bmatrix} x'_o(\Delta t) \\ y'_o(\Delta t) \end{bmatrix} \qquad \text{(B.2 -6)}$$

This is the fundamental equation needed for analysis of prediction uncertainty.

Error Equations for Intruder Prediction Uncertainty

Now from (B.2 -6) we obtain the following equation for relative intruder path error:

$$\begin{bmatrix} \delta x(\Delta t) \\ \delta y(\Delta t) \end{bmatrix} = \begin{bmatrix} \cos \Delta\psi & - \sin \Delta\psi \\ \sin \Delta\psi & \cos \Delta\psi \end{bmatrix} \begin{bmatrix} \delta X_I(\Delta t) \\ \delta Y_I(\Delta t) \end{bmatrix} - \begin{bmatrix} \delta x'_o(\Delta t) \\ \delta y'_o(\Delta t) \end{bmatrix} \qquad \text{(B.2 -7)}$$

where $\delta X_I(\Delta t)$, $\delta Y_I(\Delta t)$ denote the longitudinal and lateral prediction errors for the intruder path, and similarly $\delta x'_o(\Delta t)$, $\delta y'_o(\Delta t)$ denote the longitudinal and lateral prediction errors for the ownship path. From the derivation in Section B.1, the ownship prediction errors can be characterized by the following expressions:

$$\delta x'_o(\Delta t) = \delta x'_o + e(\Delta t) * \delta v'_o + \theta_o(\Delta t) \qquad \text{(B.2 -8)}$$

$$\delta y'_o(\Delta t) = \varepsilon_o(\Delta t) \qquad \text{(B.2 -9)}$$

where $(\delta x'_o , \delta v'_o)$ denotes ownship along-track position and velocity surveillance errors, $\theta_o(\Delta t)$ denotes the along-track wind forecasting error, and $\varepsilon_o(\Delta t)$ denotes the ownship lateral conformance error relative to the intended ground track. (For simplicity, we are ignoring other error sources such as longitudinal speed error.) The error sources are assumed to be independent random variables (except for cross-correlation between tracker position and velocity errors), with mean zero and variances given by

$$Po = E (\delta x'_o + e(\Delta t) * \delta v'_o)^2 = Sxx + 2\, e(\Delta t) * Sxv + e(\Delta t)^2 * Svv \qquad \text{(B.2-10)}$$

$$Qo = E (\theta_o(\Delta t))^2 = (\sigma_f / a_o)^2 * G(a_o \Delta t) \;, \quad a_o = v_o / Lf \qquad \text{(B.2-11)}$$

$$Ro = E (\varepsilon_o(\Delta t))^2 = (\sigma_y)^2 \qquad \text{(B.2-12)}$$

i.e. the longitudinal errors Po and Qo are functions of Δt and Ro is a constant.

Similarly, the intruder prediction errors can be characterized by the expression

$$\delta X_I(\Delta t) = \delta x_I + e'(\Delta t) * \delta v_I + \theta_I(\Delta t) \qquad \text{(B.2-13)}$$

$$\delta Y_I(\Delta t) = \varepsilon_I(\Delta t) \qquad \text{(B.2-14)}$$

where (δx_I , δv_I) denotes intruder along-track position and velocity surveillance errors, $\theta_I(\Delta t)$ denotes the along-track forecasting error, and $\varepsilon_I(\Delta t)$ denotes the intruder lateral conformance error relative to the intended ground track. The variances of the error components P_I, Q_I, R_I are given by equations analogous to (B.2-10) - (B.2-12).

The wind forecasting errors are assumed to be circular normal with independence between x and y component errors, and exponentially correlated errors between distant forecast points. Thus the random variables $\theta_o(\Delta t)$ and $\theta_I(\Delta t)$ are cross-correlated, complicating the estimation of prediction uncertainty. We can express the forecast error $\theta_I(\Delta t)$ in terms of x' and y' wind forecast errors in the primed coordinate system:

$$\theta_I(\Delta t) = \cos \Delta\psi * \theta_{XI}(\Delta t) + \sin \Delta\psi * \theta_{YI}(\Delta t) \qquad \text{(B.2-15)}$$

where $\theta_{XI}(\Delta t)$ and $\theta_{YI}(\Delta t)$ are independent random variables with mean zero and variance Q_I with

$$Q_I = (\sigma_f / a_I)^2 * G(a_I \Delta t) \ , \qquad a_I = v_I / Lf \qquad \text{(B.2-16)}$$

and the cross-correlation between $\theta_o(\Delta t)$ and $\theta_I(\Delta t)$ is given by

$$E\ \theta_o(\Delta t)^*\ \theta_I(\Delta t) = \cos \Delta\psi * J_{oI} \qquad \text{(B.2-17)}$$

$$J_{oI} = E\ \theta_o(\Delta t)^*\ \theta_{XI}(\Delta t).$$

The value of (B.2-15) - (B.2-17) is that the cross-correlation J_{oI} is bounded by the following inequalities:

$$0 <= J_{oI} <= (Qo^* Q_I)^{1/2} \ , \qquad \text{(B.2-18)}$$

where the cross-correlation $J_{oI}(\Delta t)$ can be shown to be non-negative since the x' axis wind forecasting errors at each point are exponentially correlated and positive. The upper bound is a well known property of cross-correlations, i.e. for any two random variables a and b we have $(E\ a^*b)^2 <= (E\ a^*a) * (E\ b^*b)$. The inequalities (B.2-18) are needed for obtaining an upper bound on intruder path covariance uncertainty.

Covariance Upper Bound for Relative Intruder Path Uncertainty

We now use equations (B.2-7) - (B.2-18) to derive an upper bound for the covariance uncertainty on the predicted intruder path in ownship coordinates. The covariance of interest is defined by

$$\mathbf{C} = \begin{bmatrix} Cxx & Cxy \\ Cxy & Cyy \end{bmatrix} = E\begin{bmatrix} \delta x(\Delta t) \end{bmatrix} * [\, \delta x(\Delta t), \delta y(\Delta t) \,] \qquad \text{(B.2-19)}$$
$$\begin{bmatrix} \delta y(\Delta t) \end{bmatrix}$$

Substituting (B.2-7) into (B.2-19) and expanding terms yields

$$\mathbf{C} = \mathbf{D} * COV\begin{bmatrix}\delta X_I(\Delta t)\\ \delta Y_I(\Delta t)\end{bmatrix} * \mathbf{D}^T + COV\begin{bmatrix}\delta x'_o(\Delta t)\\ \delta y'_o(\Delta t)\end{bmatrix} - \begin{bmatrix}2\cos\Delta\psi & \sin\Delta\psi \\ \sin\Delta\psi & 0\end{bmatrix} * E\,\theta_o(\Delta t) * \theta_I(\Delta t) \qquad \text{(B.2-20)}$$

where COV () denotes the covariance matrix of the input random vector, and **D** denotes the rotation matrix from intruder to ownship coordinates, i.e.

$$\mathbf{D} = \begin{bmatrix} \cos\Delta\psi & -\sin\Delta\psi \\ \sin\Delta\psi & \cos\Delta\psi \end{bmatrix}.$$

Using the expressions (B.2-13) and (B.2-14) for $\delta X_I(\Delta t)$ and $\delta Y_I(\Delta t)$ yields the covariance matrix

$$\mathbf{C_I} = COV\left(\begin{bmatrix}\delta X_I(\Delta t)\\ \delta Y_I(\Delta t)\end{bmatrix}\right) = \begin{bmatrix} P_I + Q_I & 0 \\ 0 & R_I \end{bmatrix}. \qquad \text{(B.2-21)}$$

Similarly, using the expressions (B.2-8) and (B.2-9) for $\delta x'_o(\Delta t)$ and $\delta y'_o(\Delta t)$ yields

$$\mathbf{C_o} = COV\left(\begin{bmatrix}\delta x'_o(\Delta t)\\ \delta Y_I(\Delta t)\end{bmatrix}\right) = \begin{bmatrix} P_o + Q_o & 0 \\ 0 & R_o \end{bmatrix}. \qquad \text{(B.2-22)}$$

Substituting (B.2-21) and (B.2-22) back into (B.2-20) and using (B.2-17) yields,

$$\mathbf{C} = \mathbf{D} * \mathbf{C_I} * \mathbf{D}^T + \mathbf{C_o} - \begin{bmatrix} 2\cos^2\Delta\psi & \sin\Delta\psi * \cos\Delta\psi \\ \sin\Delta\psi * \cos\Delta\psi & 0 \end{bmatrix} * J_{ol} \qquad \text{(B.2-23)}$$

The first two terms above are the covariance uncertainty of the intruder and the ownship, and the last term is due to wind forecast error cross correlation. The last term can be bounded using the inequalities in (B.2-18). We observe that the following matrix is non-negative, since the diagonal terms are positive and it's determinant is zero:

$$\begin{bmatrix} 2\cos^2\Delta\psi & \sin\Delta\psi * \cos\Delta\psi \\ \sin\Delta\psi * \cos\Delta\psi & \sin^2\Delta\psi / 2 \end{bmatrix} * J_{ol} \quad >= \quad \mathbf{0}$$

Consequently, we can add and subtract the lower right hand term above in (B.2-23) to obtain a covariance upper bound

$$\mathbf{C = D^* C_I^* D^T + C_o} - \begin{bmatrix} 2\cos^2\Delta\psi & \sin\Delta\psi^*\cos\Delta\psi \\ \sin\Delta\psi^*\cos\Delta\psi & \sin^2\Delta\psi/2 \end{bmatrix} * J_{ol} + \begin{bmatrix} 0 & 0 \\ 0 & \sin^2\Delta\psi/2 \end{bmatrix} * J_{ol}$$

$$\mathbf{<= D^* C_I^* D^T + C_o} + \begin{bmatrix} 0 & 0 \\ 0 & \sin^2\Delta\psi/2 \end{bmatrix} * J_{ol}$$

$$\mathbf{<= D^* C_I^* D^T + C_o} + \begin{bmatrix} 0 & 0 \\ 0 & \sin^2\Delta\psi/2 \end{bmatrix} * (Qo^* Q_I)^{1/2} \qquad \text{(B.2-24)}$$

Finally, expanding the matrix equation (B.2-24) into it's components yields the following upper bound on the covariance matrix for intruder prediction uncertainty:

$$Cxx = \cos^2\Delta\psi\,(P_I + Q_I) + \sin^2\Delta\psi * R_I + (P_o + Q_o) \qquad \text{(B.2-25)}$$
$$Cxy = \sin\Delta\psi * \cos\Delta\psi\,(P_I + Q_I - R_I)$$
$$Cyy = \sin^2\Delta\psi\,(P_I + Q_I + (Qo^* Q_I)^{1/2}/2) + \cos^2\Delta\psi * R_I + R_o$$

Although the derivation of (B.2-25) is lengthy, the calculation above is fairly simple to implement, and is only needed at the time of minimum approach, i.e. for $\Delta t = Tmin$.

Although an upper bound, the covariance approximation (B.2-25) is a fairly tight bound for crossing and opposing encounters. For in-trail encounters where the crossing angle is less than 20 degrees, and the relative velocity between conflicting aircraft is small, the above bound may be overly conservative. However, in this case the solution method for closest approach point and cpa time is not robust, and an alternative algorithm for slow overtake alerting (longitudinal conformance monitoring) is required.

B.3 Covariance Based Thresholding for Conflict Detection

The thresholding method for covariance based conflict detection requires solving for the critical point (δx^*, δy^*) on the predicted uncertainty ellipse at $\Delta t = Tmin$ such that the critical point maximizes the offset distance Runc from the relative intruder path. See Figure B-1, below. In the figure below, there is not a potential conflict if Rmin > Rsep + Runc, since the horizontal separation circle about the ownship does not intersect with the predicted intruder path uncertainty ellipse as the intruder transits the point of closest approach. We here derive analytic equations for covariance based thresholding.

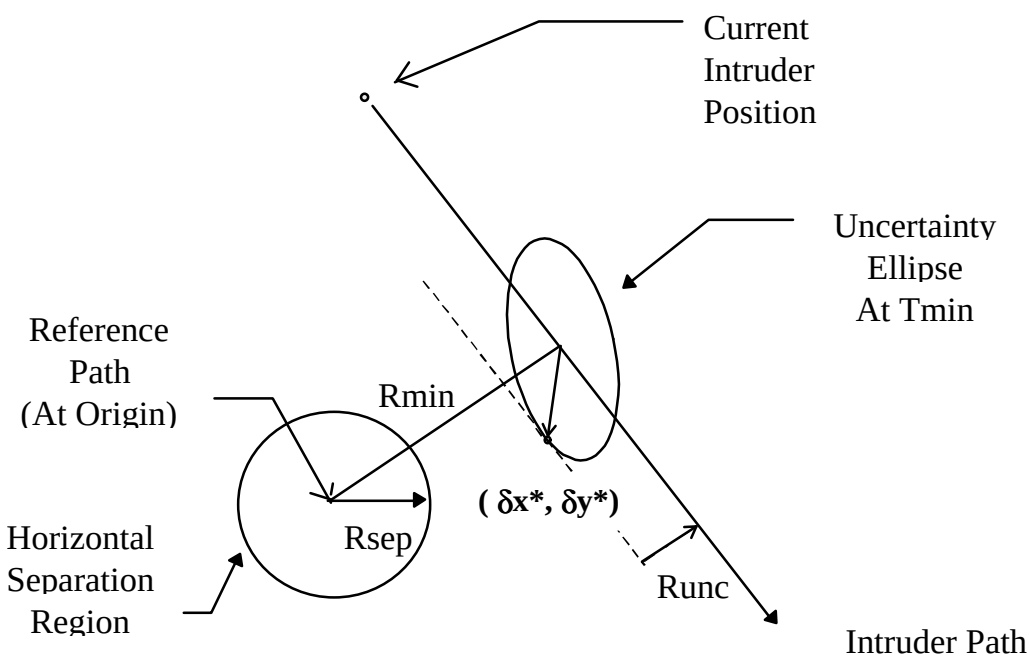

Figure B-2: Geometry for Covariance Based Conflict Detection

Let (v_x' , v_y') denote the relative velocity vector for the intruder path, and Cxx, Cxy, Cyy denote the covariance equations (B.2-25) evaluated at $\Delta t = Tmin$. Using the equations in section B.2 we find

$$v_x' = v_I \cos\Delta\psi\,(1 + Tmin^* S_f') - v_o(\,1 + Tmin^* S_f\,) \qquad \text{(B.3 - 1)}$$

$$v_y' = v_I \sin\Delta\psi\,(1 + Tmin^* S_f')$$

$$\Delta v = (\,(v_x')^2 + (v_y')^2\,)^{1/2}$$

The predicted uncertainty ellipse is defined by the locus of points (δx, δy) satisfying

$$(\,\delta x, \delta y)\begin{bmatrix} Cxx & Cxy \\ Cxy & Cyy \end{bmatrix}^{-1}\begin{bmatrix} \delta x \\ \delta y \end{bmatrix} = \rho^2 \qquad \text{(B.3 - 2)}$$

where ρ denotes the number of sigma units corresponding to a confidence level for the uncertainty ellipse, e.g. ρ = 2.45 for a 95% probability that the prediction errors are contained within the uncertainty ellipse. Expanding the indicated matrix operations above yields

$$Cyy\,\delta x^*\delta x - 2\,Cxy\,\delta x^*\delta y + Cxx\,\delta y^*\delta y = Det\,(C)\,^*\rho^2 \qquad \text{(B.3 - 3)}$$

$$Det\,(C\,) = Cxx^*Cyy - Cxy^*Cxy\,.$$

The critical point ($\delta x^*, \delta y^*$) is characterized as the point where the tangent line for the uncertainty ellipse has the same slope as the predicted intruder path, i.e.

$$\partial\, \delta y^* / \partial\, \delta x^* = v_y' / v_x' \qquad \text{(B.3 - 4)}$$

Differentiating (B.3 - 3) with respect to δx and substituting (B.3 -4) into the result yields the following expression for the critical point:

$$A\, \delta y^* + B\, \delta x^* = 0 \qquad \text{(B.3 - 5)}$$

$$A = Cxx\, v_y' - Cxy\, v_x'$$

$$B = Cyy\, v_x' - Cxy\, v_y' .$$

Equation (B.3 - 5) is valid with any values of the form

$$\delta x^* = A\, u \quad , \qquad \delta y^* = - B\, u \qquad \text{(B.3 - 6)}$$

where u is determined by substituting (B.3 - 6) back into (B.3 - 3), yielding

$$u = \rho^* (\text{Det}\, (C) / (Cyy * A^*A + 2\, Cxy * A^*B + Cxx * B^*B))^{1/2} \qquad \text{(B.3 - 7)}$$

There are two solutions for the critical point, since both the above vector and it's negative satisfy the above ellipse and tangency conditions.

The uncertainty distance Runc is obtained as the projection of ($\delta x^*, \delta y^*$) orthogonal to the intruder path. Since the vector (v_x' , v_y') lies along the intruder path, the vector $\mathbf{v}' = (v_y' , - v_x') / \Delta v$ is a unit vector orthogonal to the intruder path. Thus, Runc is given by the dot product

$$Runc = | (\delta x^*, \delta y^*) * \mathbf{v}' | = | (\delta x^* v_y' - \delta y^* v_x') | / \Delta v \qquad \text{(B.3 - 8)}$$

In practice, the threshold for conflict detection is based on an inner ellipse with $\rho = \rho_{in}$ (nominally $\rho_{in} = 0.8$), and the threshold for no-conflict decisions is based on an outer ellipse with $\rho = \rho_{out}$ (nominally $\rho_{out} = 2.8$), and the thresholds are given by

$$R\_inner = Rsep + \rho_{in} * Rsig \qquad \text{- conflict alerting thresholding}$$
$$R\_outer = Rsep + \rho_{out} * Rsig, \qquad \text{- no-conflict decision threshold}$$

where Rsig is given by substituting (B.3 - 5) into (B.3 - 8):

$$Rsig = u * | (A\, v_y' + B\, v_x') | / \Delta v \qquad \text{(B.3 - 9)}$$

and u is given by (B.3 - 7) with $\rho = 1$, i.e. Rsig is the one sigma uncertainty distance.

B.4 Predicted Loss-of-Separation Probability

One of the advantages of computing the predicted covariance matrix in (B.2-25) is that collision risk analysis and probability calculations become feasible as by-products of the conflict probe calculations, assuming that the intruder prediction errors (δx, δy) are bivariate normal with zero means and covariance matrix C. The probability of a loss-of-separation during a crossing encounter can be approximated by the probability that the difference δCpa between the estimated and true CPA falls into the Loss-of-Separation Region shown in Figure B-3. Since any point in the region described by

$$Rmin - Rsep <= \delta Cpa <= Rmin + Rsep$$

will fall will within the ownship protected region at some time during a close encounter, and the probability distribution of a deviation in δCpa is zero mean with standard deviation Rsig, this implies that the probability of loss-of-separation Ps during an encounter is approximately given by a one-dimensional normal distribution:

$$Ps = Prob (G1 <= N <= G2) = P_N (G2) - P_N (G1) \qquad (B.4 - 1)$$

where N is a normal random variable with mean zero and unit variance, $P_N (X)$ denotes the cumulative probability Prob (N <= X), and

$$G1 = (Rmin - Rsep) / Rsig \qquad (B.4 - 2)$$

$$G2 = (Rmin + Rsep) / Rsig.$$

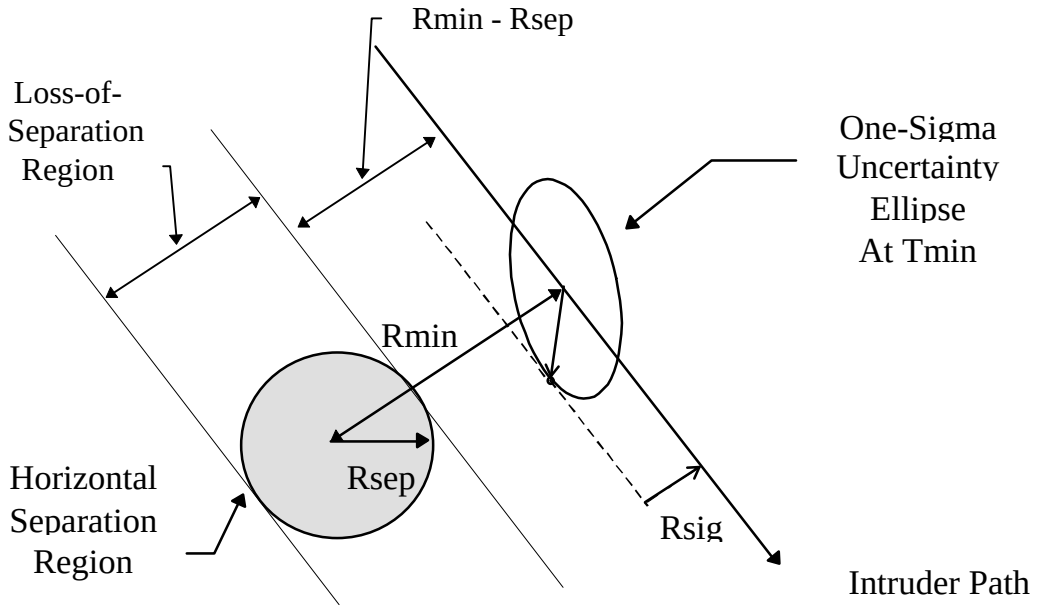

Figure B-3: Geometry for Loss-of-Separation Probability

In practice, since the estimates of Cpa distance can vary significantly from one probe update to the next, Rmin should be estimated using an average of Cpa estimates over several probe updates. The probability function P_N can be easily computed using either pre-stored tabular values, or an analytic approximation.

B.5 Predicted Conflict Entry and Exit Times

Once a potential conflict has been detected, it is important to estimate the time until the potential conflict begins, and the time until the potential conflict ends. Although we used a rough approximation for warning time in our Monte-Carlo studies, the equation used in Section A.6 may not be sufficiently accurate for medium term predictions in a 3-D conflict probe. In this section, we formulate the problem of estimating horizontal conflict entry and exit times, and show that the solution to this problem can be reduced to that of solving a simple quadratic equation for an equivalent, transformed problem.

Conflict Entry and Exit Time Problem Formulation

Conceptually, a potential conflict begins when the intruder path uncertainty ellipse first touches the ownship separation region, where the size of the uncertainty ellipse is sufficiently large. See Figure B-4. The size of the uncertainty ellipse and the value of ρ in (B.2-3) is determined such that the probability that prediction errors are contained within the upper half plane bounded by the tangent line in Figure B-4 is close to 1.0. For example, we may require that the probability of the intruder falling in the lower half plane be no greater than 1% at conflict entry time. The analysis in this case is similar to that in Section B.4, i.e. the probability that the intruder lies below the tangent line reduces to that for a one-dimensional normal distribution. Choosing ρ such that $P_N(\rho) = 0.99$, ensures that no more than 1% of the prediction errors will fall in the lower half-plane. In this case, we obtain $\rho = 2.33$ which is an adequate upper bound on the size of the uncertainty ellipse for determining conflict entry and exit times.

The conflict exit time is defined similarly, as the time when the separation circle and the uncertainty ellipse just touch at the end of an encounter. The size of the uncertainty ellipse is the same as for conflict entry, since the probability requirement for conflict exit is the same, e.g. less than 1% probability that the intruder position will fall in the half-plane containing the ownship separation circle.

Problem Transformation and Solution for Entry and Exit Times

The problem of finding the points of tangency of the uncertainty ellipse and the ownship separation circle, can be reduced to that of finding the intersection of the predicted intruder path with an expanded ellipse centered at the origin, with semi-axis lengths $\lambda_1 + Rsep$ and $\lambda_2 + Rsep$, where λ_1 and λ_2 are the semi-axes of the uncertainty ellipse, and the axes of the transformed ellipse are parallel to the uncertainty ellipse (Ref. 21, p. 27). Figure B-5 shows the geometry of the transformed problem.

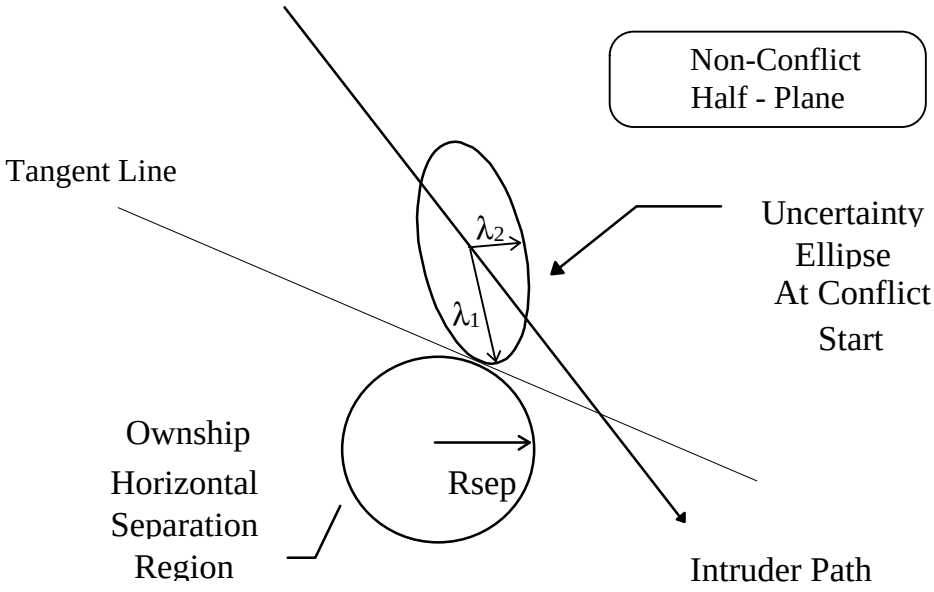

Figure B-4: Conflict Entry Time Geometry

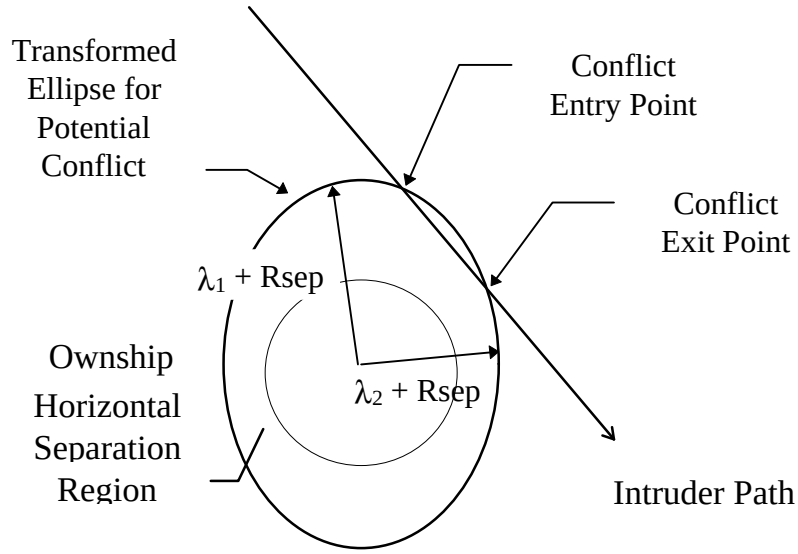

Figure B-5: Equivalent Geometry for Conflict Entry and Exit Times

The calculation procedure for conflict entry and exit times consists of three steps:
Step 1: Find the orientation angle and semi-axes of the uncertainty ellipse

Suppose θ denotes the orientation angle which diagonalizes the covariance matrix **C**(Tmin). Then the transformation of the covariance matrix from ownship coordinates to principal axes diagonalizing the covariance matrix satisfies the matrix equation

$$\begin{bmatrix} (\lambda_1)^2 & 0 \\ 0 & (\lambda_2)^2 \end{bmatrix} = \begin{bmatrix} \cos\theta & \sin\theta \\ -\sin\theta & \cos\theta \end{bmatrix} \begin{bmatrix} Cxx & Cxy \\ Cxy & Cyy \end{bmatrix} \begin{bmatrix} \cos\theta & -\sin\theta \\ \sin\theta & \cos\theta \end{bmatrix} \quad \text{(B.5 - 1)}$$

Expanding the indicated matrix operations yields

$$(\lambda_1)^2 = Cxx * \cos^2\theta + 2\,Cxy * \cos\theta * \sin\theta + Cyy * \sin^2\theta \quad \text{(B.5 - 2)}$$

$$(\lambda_2)^2 = Cxx * \sin^2\theta - 2\,Cxy * \cos\theta * \sin\theta + Cyy * \cos^2\theta \quad \text{(B.5 - 3)}$$

$$0 = Cxy * \cos^2\theta - (Cxx - Cyy) * \cos\theta * \sin\theta - Cyy * \sin^2\theta \quad \text{(B.5 - 4)}$$

Solving (B.5 -4) for θ yields

$$\tan 2\theta = 2\,Cxy / (Cxx - Cyy) ,$$

or equivalently,

$$\theta = \arctan (2\,Cxy / (Cxx - Cyy)) / 2 \quad . \quad \text{(B.5 - 5)}$$

The semi-axes λ_1 and λ_2 are obtained by taking the positive square roots of (B.5 -2), and (B.5 - 3), respectively, where θ is obtained from (B.5 -5).

<u>Step 2: Find the covariance matrix of the transformed problem</u>

Let **D** denote the covariance matrix of the transformed ellipse with orientation angle θ and semi-axes λ_1 + Rsep and λ_2 + Rsep. Then, the inverse transform to that in (B.5 -1) yields the transformed covariance matrix, i.e.

$$\begin{bmatrix} Dxx & Dxy \\ Dxy & Dyy \end{bmatrix} = \begin{bmatrix} \cos\theta & -\sin\theta \\ \sin\theta & \cos\theta \end{bmatrix} \begin{bmatrix} (\lambda_1+Rsep)^2 & 0 \\ 0 & (\lambda_2+Rsep)^2 \end{bmatrix} \begin{bmatrix} \cos\theta & \sin\theta \\ -\sin\theta & \cos\theta \end{bmatrix} .$$

Expanding the above matrix equation yields the component equations

$$Dxx = \cos^2\theta * (\lambda_1+Rsep)^2 + \sin^2\theta * (\lambda_2+Rsep)^2 \quad \text{(B.5 - 6)}$$

$$Dxy = \sin\theta * \cos\theta * ((\lambda_1+Rsep)^2 - (\lambda_2+Rsep)^2)$$

$$Dyy = \sin^2\theta * (\lambda_1+Rsep)^2 + \cos^2\theta * (\lambda_2+Rsep)^2$$

Step 3: Solve for Conflict Entry and Exit Times T1 and T2

In the vicinity of Tmin we can ignore the wind shear terms and express the intruder path in ownship coordinates using the approximate linear equation

$$\begin{bmatrix} \Delta x(t) \\ \Delta y(t) \end{bmatrix} = \begin{bmatrix} \Delta x' \\ \Delta y' \end{bmatrix} + \Delta t * \begin{bmatrix} v_x' \\ v_y' \end{bmatrix} \quad \text{(B.5 - 7)}$$

where $\Delta t = t - Tmin$, and the intruder position at Tmin is obtained by rotating (A.5 - 3) by the ownship angle ψ_o :

$$\begin{bmatrix} \Delta x' \\ \Delta y' \end{bmatrix} = \begin{bmatrix} \cos\psi_o & \sin\psi_o \\ -\sin\psi_o & \cos\psi_o \end{bmatrix} \begin{bmatrix} \Delta x(Tmin) \\ \Delta y(Tmin) \end{bmatrix} .$$

The transformed uncertainty ellipse consists of all pairs ($\Delta x, \Delta y$) such that

$$(\Delta x, \Delta y) \begin{bmatrix} Dxx & Dxy \\ Dxy & Dyy \end{bmatrix}^{-1} \begin{bmatrix} \Delta x \\ \Delta y \end{bmatrix} = 1 \quad \text{(B.5 - 8)}$$

Expanding the indicated matrix operations yields the scalar equation

$$Dyy * \Delta x * \Delta x - 2\, Dxy * \Delta x * \Delta y + Dxx * \Delta y * \Delta y = Det(D) \quad \text{(B.5 - 9)}$$

where $Det(D) = Dxx*Dyy - Dxy*Dxy$. Substituting (B.5 - 7) above yields a quadratic equation for Δt. Combining similar terms in Δt yields

$$a * \Delta t^2 + 2\, b * \Delta t + c = 0 \quad \text{(B.5 - 10)}$$

where

$$a = Dyy * (v_x')^2 - 2\, Dxy * v_x' * v_y' + Dxx * (v_y')^2 \quad \text{(B.5 - 11)}$$

$$b = Dyy * v_x' * \Delta x' - 2\, Dxy * (\Delta y' * v_x' + \Delta x' * v_y') + Dxx * \Delta y' * v_y'$$

$$c = Dyy * (\Delta x')^2 - 2\, Dxy * \Delta x' * \Delta y' + Dxx * (\Delta y')^2 - det(D) .$$

Consequently, solving the quadratic equation in (B.5 - 10) yields the following expressions for conflict entry and exit times:

$$T1 = Tmin - b/a - ((b/a)^2 - c/a)^{1/2} \quad \text{(B.5 - 12)}$$

$$T2 = Tmin - b/a + ((b/a)^2 - c/a)^{1/2} . \quad \text{(B.5 - 13)}$$

NOMENCLATURE

SYMBOL	EXCEL NAME	DEFINITION
cos(ψ)	costhe	cosine of crossing angle
cpa_o	cpa_o	Observed (estimated) distance at closest approach
cpa_tim_o	cpa_tim_o	Observed (estimated) time at closest approach
D1	Dist1	Distance from entry point to crossing fix (**ownship**)
D2	Dist2	Distance from entry point to crossing fix (**intruder**)
detect_flag	det_flag	Conflict detect status
Dmin	cpa	Distance at closest approach
dWli	dwli	Spatial derivative of along-track wind (wind shear) for **intruder**
dWxo	dwxo	Spatial derivative of along-track wind (wind shear) for **ownship**
Fore_const	Fore_const	Wind Forecasting Error (0.67 nm)
inner_cpa	inner_cpa	Conflict probe inner threshold
L	corr	Wind correlation constant: nominal value L=670 nm
Li_dot(t)	N/A	Along-track speed at time t from entry point for **intruder**
max_looktime	max_looktime	Maximum look-ahead time to crossing fix (min)
min_looktime	min_looktime	Minimum look-ahead time to crossing fix (min)
outer_cpa	outer_cpa	Conflict probe outer threshold
Rc	rang	Range at crossing time
Rcdot	rangdot	Range rate at crossing time
Ro	Ro	Relative distance (range) between ownship and intruder at entry
sep_std	sep_std	Separation standard

SYMBOL	EXCEL NAME	DEFINITION
sigy	sigy	Lateral conformance error
sin(ψ)	sinthe	sine of crossing angle
t	N/A	Time
Tc	cross-time	Mean time from entry to crossing fix
Tmin	cpa_tim	Time at closest approach
truth_flag	truth_flag	True cpa status
V1	V1bar	Mean ground speed for **ownship** including airspeed and mean wind
V2	V2bar	Mean ground speed for **intruder** including airspeed and mean wind
Wxc, Wyc	WXC, WYC	Vector wind uncertainty at the crossing fix
Wxi, Wyi	WXI, WYI	Vector wind uncertainty at the entry point for **intruder**
Wxo, Wyo	WXO, WYO	Vector wind uncertainty at the entry point for **ownship**
x_dot(t)	N/A	Along-track speed at time t from entry point for **ownship**
x1dist	x1dist	X coordinate distance at crossing time (**ownship**)
x1dot	x1dot	X coordinate velocity at crossing time (**ownship**)
x2dist	x2dist	X coordinate distance at crossing time (**intruder**)
x2dot	x2dot	X coordinate velocity at crossing time (**intruder**)
y1dist	y1dist	Y coordinate distance at crossing time (**ownship**)
y2dist	y2dist	Y coordinate distance at crossing time (**intruder**)
y2dot	y2dot	Y coordinate velocity at crossing time (**intruder**) Note: y1dot = 0.
yoff1	yoff1	Lateral offset value for each Monte Carlo run (**ownship**)
yoff2	yoff2	Lateral offset value for each Monte Carlo run (**intruder**)

SYMBOL	EXCEL NAME	DEFINITION
σ_s	sig_shear	Wind shear observation error (0.0005 nm)
σ_w	sigwnd	Wind uncertainty standard deviation Gaussian(o, σ_w), σ_w=25kts
σ_y	siglat	Lateral uncertainty (RNAV) Gaussian(0, σ_y), σ_y=0.5 nm
ψ	N/A	Crossing angle between ownship and intruder

REPORT DOCUMENTATION PAGE

Form Approved
OMB No. 0704-0188

1. AGENCY USE ONLY (*Leave blank*)	2. REPORT DATE	3. REPORT TYPE AND DATES COVERED
	January 1997	Contractor Report

4. TITLE AND SUBTITLE

Conflict Probe Concepts Analysis in Support of Free Flight

5. FUNDING NUMBERS

C NAS1-20267
WU 538-04-14-01

6. AUTHOR(S)

Anthony W. Warren; Robert W. Schwab; Timothy J. Geels; and Arek Shakarian

7. PERFORMING ORGANIZATION NAME(S) AND ADDRESS(ES)

Boeing Commercial Airplane Group
Seattle, Washington 98124-2207

8. PERFORMING ORGANIZATION REPORT NUMBER

9. SPONSORING / MONITORING AGENCY NAME(S) AND ADDRESS(ES)

National Aeronautics and Space Administration
Langley Research Center
Hampton, Virginia 23681-0001

10. SPONSORING / MONITORING AGENCY REPORT NUMBER

NASA CR-201623

11. SUPPLEMENTARY NOTES

Langley Technical Monitor: Sally C. Johnson

12a. DISTRIBUTION / AVAILABILITY STATEMENT

UNLIMITED - UNCLASSIFIED

SUBJECT CATEGORY: 04

12b. DISTRIBUTION CODE

13. ABSTRACT (*Maximum 200 words*)

This study develops an operational concept and requirements for en route Free Flight using a simulation of the Cleveland Air Route Traffic Control Center, and develops requirements for an automated conflict probe for use in the Air Traffic Control (ATC) Centers. In this paper, we present the results of simulation studies and summarize implementation concepts and infrastructure requirements to transition from the current air traffic control system to mature Free Flight. The transition path to Free Flight envisioned in this paper assumes an orderly development of communications, navigation, and surveillance (CNS) technologies based on results from our simulation studies. The main purpose of this study is to provide an overall context and methodology for evaluating airborne and ground-based requirements for cooperative development of the future ATC system.

14. SUBJECT TERMS

Free Flight
Air Traffic Control
Air Traffic Management

15. NUMBER OF PAGES

147

16. PRICE CODE

A07

17. SECURITY CLASSIFICATION OF REPORT	18. SECURITY CLASSIFICATION OF THIS PAGE	19. SECURITY CLASSIFICATION OF ABSTRACT	20. LIMITATION OF ABSTRACT
UNCLASSIFIED	UNCLASSIFIED	UNCLASSIFIED	UNLIMITED